SKB

# TECHNICAL REPORT 97-07

## A methodology to estimate earthquake effects on fractures intersecting canister holes

Paul La Pointe, Peter Wallmann,
Andrew Thomas, Sven Follin

Golder Associates Inc.

March 1997

**SVENSK KÄRNBRÄNSLEHANTERING AB**
*SWEDISH NUCLEAR FUEL AND WASTE MANAGEMENT CO*

P.O.BOX 5864 S-102 40 STOCKHOLM SWEDEN
PHONE +46 8 665 28 00
FAX +46 8 661 57 19

# A METHODOLOGY TO ESTIMATE EARTHQUAKE EFFECTS ON FRACTURES INTERSECTING CANISTER HOLES

*Paul La Pointe, Peter Wallmann, Andrew Thomas, Sven Follin*

**Golder Associates Inc.**

March 1997

# A METHODOLOGY TO ESTIMATE EARTHQUAKE EFFECTS ON FRACTURES INTERSECTING CANISTER HOLES

**Paul La Pointe**

**Peter Wallmann**

**Andrew Thomas**

**Sven Follin**

**Golder Associates Inc.**

**March 25, 1997**

Keywords: Earthquake, Fracture Displacement, Canister, Numerical Modeling, Literature Review

# ABSTRACT (ENGLISH)

A literature review and a preliminary numerical modeling study were carried out to develop and demonstrate a method for estimating displacements on fractures near to or intersecting canister emplacement holes. The method can be applied during preliminary evaluation of candidate sites prior to any detailed drilling or underground excavation, utilizing lineament maps and published regression relations between surface rupture trace length and earthquake magnitude, rupture area and displacements. The calculated displacements can be applied to lineament traces which are assumed to be faults and may be the sites for future earthquakes. Next, a discrete fracture model is created for secondary faulting and jointing in the vicinity of the repository. These secondary fractures may displace due to the earthquake on the primary faults. The three-dimensional numerical model assumes linear elasticity and linear elastic fracture mechanics which provides a conservative displacement estimate (actual values are likely to be less), while still preserving realistic three-dimensional fracture patterns.

Two series of numerical studies were undertaken to demonstrate how the methodology could be implemented and how the results could be applied to questions regarding site selection and performance assessment. The first series of simulations illustrates how earthquake damage to a hypothetical repository for a specified location could be estimated. The geological parameters for this model are based on published values for Äspö.

Results from 100 realizations suggest that the maximum shear displacement along secondary fractures due to an earthquake of magnitude 6.1 occurring along a strike-slip fault 2 km from a hypothetical repository is about one millimeter. This small amount of displacement is consistent with findings reported in the literature for earthquake damage to underground openings. A maximum displacement of 1 mm implies that at least 100 earthquakes of magnitude 6.1 would be required to produce a cumulative displacement of 0.1 m, which is the threshold for possible canister hole damage. It would be necessary to estimate recurrence rates for earthquakes in the region of interest in order to determine whether there might be a sufficient number of earthquakes within the regulatory time frame to cause more than 0.1 m of cumulative displacement. Estimation of earthquake recurrence rates for Sweden was not within the scope of the present study.

A second series of numerical studies examined the displacements induced by earthquakes varying in magnitude from 6.0 to 8.2 as a function of how close the earthquake was in relation to the repository, including the incorporation of uncertainty in the model. These simulations assumed that the earthquake occurred as a result of reverse-slip or strikes-slip on a steeply dipping fault. These mechanisms are consistent with literature which has

suggested that great earthquakes have occurred in Sweden due to de-glaciation during the past 10,000 years. Results from the numerical modeling suggest that induced maximum displacements vary from millimeters to tenths of meters.

A review of the literature demonstrates that there are quantitative relations between surface rupture length, subsurface rupture length, rupture width, rupture area, earthquake magnitude, and average and maximum fault displacement for different types of faults. These regression equations do not appear to differ based on geographic location or tectonic setting. Many of these relations, such as the relation between surface rupture length and displacement, are power law functions, suggesting a fractal scaling behavior. The relation is different for the displacement along the secondary fractures, as calculated by the numerical model. Analysis of the displacements along secondary fractures due to a remote earthquake show a relation between fracture size (as described by the fracture radius) and induced displacement that is approximately linear, although there is some variability which may be due to fracture orientation and distance from the earthquake source.

# SAMMANFATTNING (ABSTRACT, SWEDISH)

Denna rapport presenterar en metod för att uppskatta förskjutningsbelopp (skjuvrörelser) i bergsprickor i närheten av ett djupförvar. Metoden är baserad på litteraturstudier och numerisk modellering. Litteraturuppgifterna utgörs av regressionssamband mellan sprickzonslängd och jordbävningsmagnitud samt mellan sprickzonsarea och förskjutningsbelopp. Metoden kan användas i ett tidigt skede av en platsundersökning för att uppskatta skjuvrörelser i ett regionalt lineament i händelse av en jordbävning i detsamma. Den numeriska modellen kan därefter användas för att beräkna inducerade skjuvrörelser i förekommande bergstrukturer av mindre storlek i närheten av ett tänkt djupförvar. Den använda numeriska modellen är tredimensionell och förutsätter linjär elasticitet och sprickpropagering. Modellen ger realistiska sprickmönster och elastictetsantagandet ger konservativa förskjutningsbelopp, dvs. de inducerade skjuvrörelser som simuleras är sannolikt större än i de som bedöms förekomma i verkligheten.

Två serier med Monte-Carlo simuleringar har utförts med den numeriska modellen i syfte att demonstrera hur metoden skulle kunna tillämpas vid platsvalsprocesser och säkerhetsredovisningar.

Den första serien behandlar frågan hur man kan uppskatta påverkan på ett djupförvar på ett givet avstånd från en förkastning. Ett hundra realiseringar av en jordbävning med magnituden 6.1 på Richterskalan har använts för att uppskatta inducerade förskjutningsbelopp i mindre bergstrukturer i närheten av ett djupförvar. I denna fall är förkastningen, där jordbävningen tänkts ske, beläget på ett horisontellt avstånd av 2 km från djupförvaret. De mindre bergstrukturerna bygger på data från Äspö med omnejd. Utfallet av Monte-Carlo simuleringen ger ett maximalt förskjutningsbelopp i de mindre bergstrukturerna på ca 1 mm. Denna ringa skjuvrörelse stämmer väl överens med rapporterade erfarenheter vad gäller skador från jordbävningar i underjordsanläggningar. En maximal förskjutning av 1 mm innebär att det förmodligen krävs åtminstone 100 *samverkande* jordbävningar med magnituden 6.1 för att uppnå en sammanlagd förskjutning på 100 mm. (Gränsvärdet för förskjutning i en spricka, som skär igenom ett kapselhål, är i denna rapport antagen till 100 mm.) För att man ska kunna beräkna den sammantagna effekten av alla jordbävningar, som kan tänkas förekomma under ett djupförvars driftstid, erfordras uppgifter om frekvensen för olika magnituder.

Det andra serien med simuleringar behandlar det s.k. respektavståndet vid kraftiga jordbävningar (6.0 till 8.2 på Richterskalan). Simuleringarna antar

att förkastningen, där jordbävningen sker, är brantstående och att jordbävningen orsakas av en "reverse-slip" eller en "strike-slip" förskjutning. Sådana typer av förskjutningar är koncistenta med de litteraturuppgifter som anser att postglaciala jordbävningar har ägt rum i Sverige. Resultatet indikerar att de inducerade förskjutningarna ligger i intervallet millimetrar till tiotals metrar beroende på magnitud och avstånd.

Litteraturstudierna visar att det finns kvantifierbara samband mellan spricklängder i markytan, spricklängder på djupet, sprickvidd, sprickarea, jordbävningsmagnitud och uppmätta förskjutningsbelopp (medelvärde och maximum) för olika typer av sprickzoner och förkastningar. De samband som redovisas verkar vara oberoende av geografiskt läge och tektonisk miljö. Flera av sambanden verkar dessutom vara av typen $y = a\,x^b$ , vilket skulle kunna tolkas som tecken på ett fraktalt beteende. En analys av de simulerade förskjutningarna i den använda numeriska modellen ger ett tämligen linjärt samband mellan inducerad förskjutning och sprickradie. Den variation som kan observeras i de numeriska resultaten skulle kunna bero på skillnader i sprickorientering och skillnader i avstånd till jordbävningsstrukturen.

# TABLE OF CONTENTS

# LIST OF FIGURES

# LIST OF TABLES

# 1. INTRODUCTION

## 1.1 PROJECT GOALS

The goal of this project is to develop and demonstrate a methodology for estimating earthquake effects on high-level nuclear waste repositories in terms of earthquake-induced fracture movements. For the purposes of this study, the threshold for canister damage due to fault slip for the KBS-3 concept was chosen to be 0.1 m (Ericsson, 1996, personal comm.). The KBS-3 concept consists of canisters emplaced in vertical deposition holes (diameter approximately 1.8 m and depth approximately 6 m) surrounded by bentonite clay. The method developed in this project is designed for a generic evaluation of earthquake effects. Nonetheless, the methodology can be adapted to assess earthquake risk after a site has been selected and additional data have been obtained from boreholes, detailed geological mapping or underground excavations.

As part of the study, an extensive literature review was carried out to determine what types of damage due to fractures have been observed in underground excavations, mines and boreholes due to earthquakes. This review served two purposes: to qualitatively verify that the methodology is predicting the observed subsurface fracture behavior; and to obtain boundary conditions for a numerical model used to predict secondary fracture movements.

## 1.2 TASK DESCRIPTIONS

There were two main tasks in this study:

- Task 1 - Literature Review
- Task 2 - Numerical Modeling

In addition to providing insight into what types of damage might occur in an underground repository, the literature review in Task 1 was also focused on determining how surface geological data could be used to develop a numerical modeling strategy, and how to quantitatively estimate boundary conditions for the numerical models.

Task 2 describes the numerical model, the modeling strategy, and the model results.

## 1.3 REPORT OVERVIEW

The report is divided by task. Section 2 describes the literature review of Task 1 and the conclusions regarding damage and modeling strategy. Section 3 describes the numerical code used in Task 2. Section 4 describes the input data and the modeling results. Section 5 reports the conclusions and limitations of this study. The report also includes three appendices that list the code verification, the publications that were reviewed as part of Task 1, and a discussion of the material properties used in modeling.

## 1.4 LIMITATIONS

This study has several limitations. First, the numerical modeling assumes linear elasticity and linearly elastic fracture mechanics. Dynamic effects were ignored. The linear elasticity assumption should be conservative, in that all of the earthquake energy is dissipated in slip along existing fractures, rather than in plastic or ductile rock deformation, thus maximizing estimated displacements.

The numerical study has also focused on the estimated displacements due to a single earthquake event. Evidence for earthquake magnitudes comes from one of two sources; *paleoseismic* studies, which infer magnitudes from geological evidence relating to displacement and rupture length; and *historical evidence*, in which magnitudes are directly calculated from seismographic records or from eyewitness reports of movements or damage. Of the two, historical evidence is the most reliable. The maximum historical earthquake in Sweden is probably on the order of 5.0 or less (SKBF/KBS, 1983). Earthquake design criterion in the United States, where historical records cover only the last few hundred years at most, use a qualitative rule that the maximum credible earthquake is approximately one order of magnitude greater than the maximum historical earthquake. This guideline is an attempt to include larger earthquakes that may have occurred at a recurrence interval larger than the historical observation period. In Sweden, the period of observation covers a considerably larger historical period, perhaps one thousand years. The much longer time span available in Sweden would suggest that this rule would be overly conservative. However, it is useful to evaluate what type of repository damage might occur for an earthquake with a moment magnitude on the order of 6.0, which is approximately one order of magnitude greater than the maximum historical earthquake.

Some paleoseismic studies (Arvidsson, 1996; Johnston, 1996) suggest that earthquakes of a much greater magnitude may have occurred in Sweden due to the isostatic readjustment of the Fennoscandian Shield as the ice sheets retreated approximately 9000 years ago. Evidence for earthquakes due to glacial unloading has also been found elsewhere (Thorson, 1996). While current studies are not definitive, some researchers have postulated a magnitude 8.2 earthquake in Sweden due to glacial unloading. Although the

existence of such earthquakes may be controversial, it is beyond the scope of the present study to resolve the issue. However, the possible impact of such earthquakes can be estimated.

The modeling study has attempted to evaluate three parameters: earthquake magnitude; distance between the fault on which the earthquake occurs and the repository; and the induced displacements on existing fractures that intersect canister holes. The goal of the modeling is to use a series of simplifying, conservative assumptions to determine how close a repository might be located to an earthquake as a function of earthquake magnitude. The key design parameter is the amount of displacement that occurs on fractures intersecting canister holes as a result of the earthquake. Although the displacement boundary conditions correspond to single earthquakes, the combined net displacement due to many earthquakes was not calculated. Without a much greater study of earthquake recurrence rates for a particular part of Sweden, which is outside the scope of the present study, it is not possible to estimate the total net slip over the period of regulatory interest.

A final limitation of the present study is its focus on mechanical effects. The influence of an earthquake on the local hydrology was not evaluated. The reasons for this were two-fold: hydrological effects may be a greater concern during repository construction and pre-closure operation, rather than during the post-closure period; and the numerical modeling code used does not have the ability to include pore-pressure effects.

# 2. TASK 1 - LITERATURE REVIEW

## 2.1 DATABASE SEARCH

The primary source of data was from a search of relevant public literature databases. The database search was conducted by Golder Associates Inc. (GAI) Corporate Library in Seattle, Washington. Six data bases were selected to be searched for information. The data bases are listed in Table 2-1 with a brief description of their sources.

**Table 2-1 Databases Searched for Literature Review**

| Database Name | Description |
|---|---|
| EI Compendex Plus | A database of worldwide engineering and technical literature including articles from journals, transactions and special publications of technical societies and proceedings of conferences |
| GeoArchive | A geoscience data base that references serials, books, doctoral dissertations and technical reports in fields including geology, geophysics, engineering geology and geoscience. |
| GEOBASE | Worldwide database covering geology, geography, ecology and related topics including conference proceedings, reports and theses |
| GeoRef | Geological and geophysics database including publications from the 20 professional geological and earth science group members of the American Geological Institute |
| National Technical Information Service | Database providing access to the results of government sponsored research, development, analyses and engineering from the US, Japan, Germany, France and the UK. |
| Pascal | A multidisciplinary database of international literature covering many topics including civil engineering and earth sciences |

The search was conducted using key words and phrases. The database entries were searched using the following key words:

- *Earthquake*
- *Seismic*
- *Rock*
- *Fracture*
- *Crack*
- *Propagation*

The final key word search was narrowed to two categories:

1. References containing the words of *earthquake* or *seismic* and the word *rock* within three words of *fracture* or *crack* and those with the phrase *crack propagation*

2. References containing the words *earthquake* or *seismic* and the word *rock* within three words of *fracture* or *crack* but without the phrase *crack propagation*

There were 20 reference items obtained in the first category and 330 items in the second category. The references and abstracts were manually reviewed and the relevant references retained. The majority of these references were obtained by the GAI Corporate Library and used as required for this report.

In addition to the above search, an additional search of the 6 databases was undertaken for the author, S. Hsiung, who has written a number of papers which appeared relevant to the topic. Approximately 50 reference items were found which were reviewed for relevance and obtained where possible for use in this report. Approximately 20 additional references referred to in the reviewed publications were obtained and reviewed. A complete citation of all literature reviewed is contained in Appendix B.

## 2.2 MOVEMENT OF FRACTURES, AND DAMAGE TO UNDERGROUND OPENINGS DUE TO EARTHQUAKES

Studies of seismic effects on underground openings may be divided into three categories: rock bursts; underground explosions; and true earthquakes. Rock bursts are a common occurrence in many underground mines, particularly those that are deep or are in rock that has high in-situ stress. While most rock bursts are triggered by a combination of the in-situ stress state and mining activities, earthquakes can also trigger rock bursts. Rock bursts have been well-studied, and there is much literature on them. Underground explosions include conventional blasting, but more importantly, underground nuclear weapons testing, in which energy yields are much more substantial. There is some literature concerning underground nuclear testing at the Nevada Test Site (NTS) that is publicly available. The most relevant literature remains the studies of natural earthquakes, since explosions create motions that are essentially a single compressive pulse of short duration, unlike the cyclic loading that may last several seconds imposed by a natural earthquake. Rock becomes weaker under prolonged cyclic loading, and thus natural earthquakes may impact underground openings differently than rock bursts or explosions.

Kana and others (1991) have synthesized much of the literature concerning rock bursts worldwide and also nuclear weapons testing at the NTS. Their approach was to relate damage to ground motions, either to peak acceleration or to peak particle velocity. Damage was classified as to the dominant mechanism:

- Fault slip
- Rock mass failure
- Shaking

Of these, fault slip is the most damaging. Shaking, on the other hand, typically leads to spalling and cracking of the tunnels or drifts. This type of damage can be reduced by lining the tunnel. Rock mass failure can also be reduced through bolting or other types of support and reinforcement.

There are many studies having to do with damage to surface or near-surface structures and earthquake motions, but these are not as relevant to subsurface damage due to the difference in the type of waves that are propagated. More appropriate information comes from studies in deep hardrock mines. Some of the most comprehensive data come from studies in the South African gold mines, which are among the deepest in the world and where quantitative studies have been carried out. One such study is that of Wagner (1984). Results from his study are reproduced in Table 2-2. His results include earthquake events up to magnitude 5, and distances from the earthquake source from 10 m to 750 m. Damage appears to be related to shaking and spalling, rather than to fault slippage at the opening. Empirical studies of damage as well as laboratory and numerical studies (Dowding and Rozen, 1978; Barton and Hansteen, 1979; Lenhardt, 1988) suggest that peak velocities greater than 20 to 60 cm/sec lead to major damage in the subsurface (Figure 2-1b).

McGarr and others (1981) developed a regression relation between peak particle velocity, earthquake magnitude and distance between an underground opening and the earthquake source from field studies. The equation developed is shown below:

$$\log(v) = 3.95 + 0.57M - \log(R) \qquad \text{Equation 2-1}$$

where v is the peak particle velocity in cm/sec
M is the earthquake magnitude
R is the distance between source and opening in cm

Using these parameters for repository design in Sweden, and assuming a minimum damage threshold velocity of 20 cm/sec, it is possible to calculate the minimum distance between an earthquake and the repository as a function of magnitude. Figure 2-2 shows this relation. A magnitude 6 earthquake would need to be about 15 km away, while a magnitude 8.2 earthquake would have to be more than 210 km away.

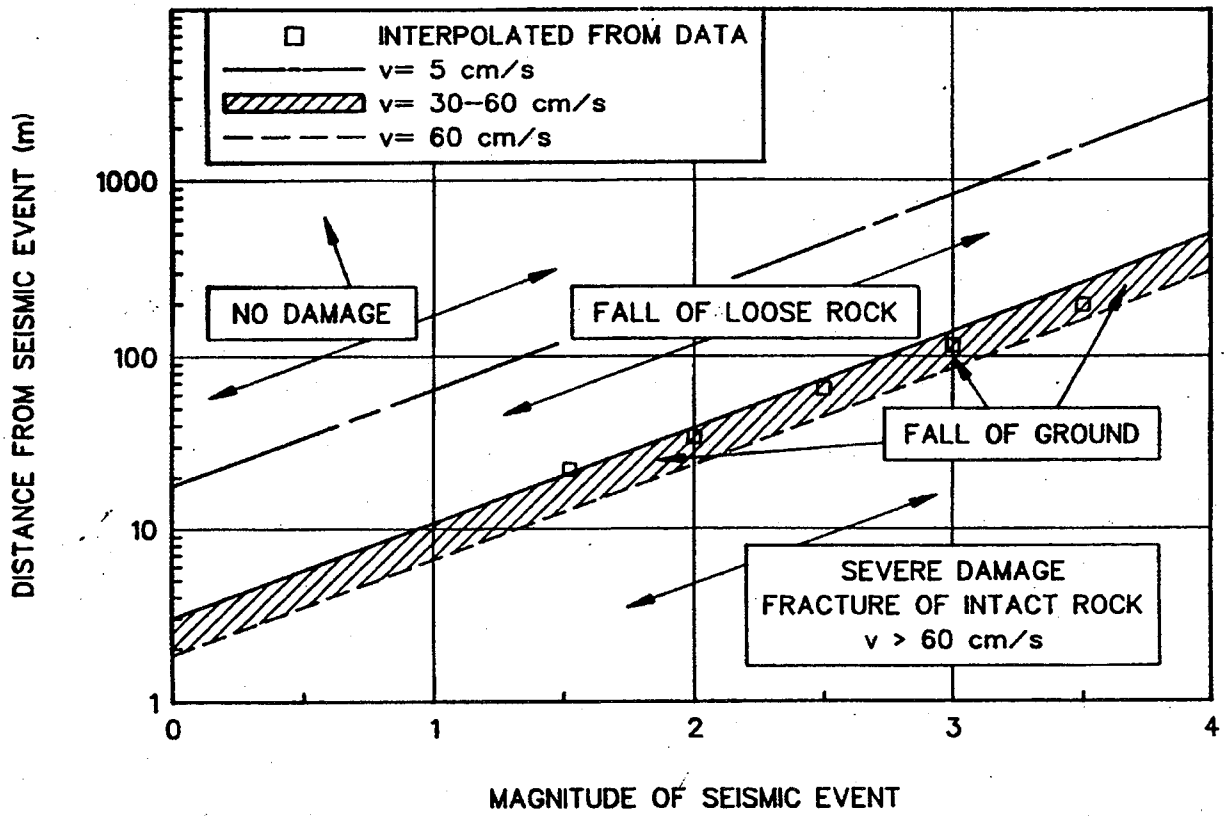


REFERENCE: Critical Assessment of Seismic and Geomechanics Literature Related to a High-Level Nuclear Waste Underground Repository, page 51. (From Lenhardt, 1988)

FIGURE **2.1**
**DAMAGE IN TERMS OF PEAK GROUND VELOCITY (v)**

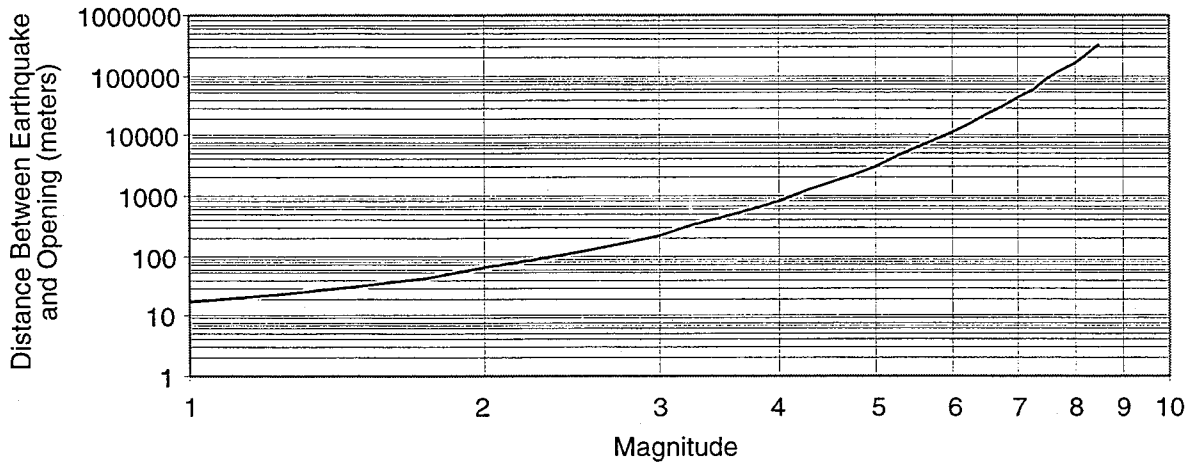


FIGURE **2-2**
**CRITICAL DISTANCE FOR EXCEEDING PEAK VELOCITY THRESHOLD**

Table 2-2 Summary of Rockburst Damage to Underground Excavation

| Mining District | Magnitude of Event | Distance of Damaged Areas from Source of Event (m) | Nature of Damage | Estimated Peak Velocity |
|---|---|---|---|---|
| Klerksdorp | 4.4 | 200 m | Faces within 100 m from source completely closed. Extensive damage to sidewalls of tunnels. | at 200 m, $\bar{v}$ = 2 m/s<br>at 100 m, $\bar{v}$ = 3.5 m/s |
| Klerksdorp | 5.0 | up to 750 m | Faces within 250 m from source completely closed. Stope faces up to 750 m from source showed appreciable damage. | at 750 m, $\bar{v}$ = 0.9 m/s<br>at 250 m, $\bar{v}$ = 2.6 m/s |
| Klerksdorp | 3.9 | 100 m | Extensive sidewall damage in tunnels. | at 100 m, $\bar{v}$ = 1.7 m/s |
| Klerksdorp | 2.7 | ±100 m | 40 m of stope face damaged. 90 m from event extensive roof falls in tunnel. | at 100 m, $\bar{v}$ = 0.4 m/s<br>at 50 m, $\bar{v}$ = 1 m/s |
| Klerksdorp | 1.1 | ±10 m | Stope travelling way collapsed. | at 10 m, $\bar{v}$ = 0.4 m/s |
| Carletonville | 4.0 | ±100 m | Total closure of stope for a distance of 100 m either side of focus of event. Follow-on tunnels not affected. | at 100 m, $\bar{v}$ = 1.7 m/s<br>at 50 m, $\bar{v}$ = 3.5 m/s |
| East Rand | 2.9 | ±50 m | Stope face completely closed for a distance of 30 m and extensive falls for another 10 m. Cross-cut to stope collapsed but post developed footwall tunnels undamaged. | at 50 m, $\bar{v}$ = 0.26 m/s<br>at 15 m, $\bar{v}$ = 1.2 m/s |
| Central Rand | 2.0 | ±50 m | Main haulage almost completely closed over a distance of 20 m and showing appreciable damage for over a total distance of 90 m. | at 50 m, $\bar{v}$ = 0.26 m/s<br>at 10 m, $\bar{v}$ = 1.2 m/s |

REFERENCE: Critical Assessment of Seismic and Geomechanics Literature Related to a High-Level Nuclear Waste Underground Repository, page 50. (From Wagner, 1984)

There are many simplifications that have gone into this equation. As a result, it should be taken as a general guideline, not a design tool. For example, Voegele (1993) studied earthquake damage to an underground missile tunnel at the Nevada Test Site (NTS) due to a magnitude 5.6 earthquake occurring along a fault approximately 2 km away. This earthquake should have produced major damage for a 20 cm/sec velocity threshold according to Equation 2-1, and would likely have produced major damage at a 60 cm/sec threshold. However, direct observation of the tunnel after the earthquake revealed that "No evidence of damage that could be related to seismic accelerations or displacements could be found in the tunnel" (Voegele, 1993, p. 185).

Also, this equation clearly overestimates the amount of damage that underground openings experienced in the 1964 Alaskan earthquake (Richter Magnitude 8.5). A 20 cm/sec threshold velocity for an 8.5 earthquake suggests that mines within 312 km should have experienced major damage. However, the U. S. Geological Survey (Pratt and others, 1978) determined that although surface damage was extreme, there was no significant damage to mines or tunnels.

Raney (1988) also provides a comprehensive summary of reported effects of earthquakes greater than magnitude 6.0 in the western U. S. on mines and other underground openings. His detailed reports of each earthquake include all documented or anecdotal damage reports, and effects on hydrology. His report concludes that natural or induced seismic events have produced little damage to underground openings outside the immediate epicentral area. Within the epicentral area, damage due to shaking, spalling, rock falls and water influx are possible. The greatest damage takes place when fault movement occurs along faults that intersect the opening.

These studies are for "conventional" damage to mines or other underground openings. For example, primary fault movement can lead to secondary collapse of timbering or flooding, which can have disastrous consequences for a mining operation. These types of damage may be relevant during the excavation and pre-closure phase of the repository, but are not directly applicable to assessing post-closure canister damage or damage to the canister emplacement hole. The major damage mechanism is induced slip along pre-existing joints and secondary faults due to an earthquake. The literature review uncovered no systematic studies of fault slippage induced by a remote earthquake in mines as a function of earthquake magnitude, epicentral distance, or fault size. However, there are several studies that examine the relation among earthquake parameters on the earthquake fault itself. This is the subject of Section 2.3.

## 2.3 ASSIGNING BOUNDARY CONDITIONS TO NUMERICAL MODELS BASED ON RECONNAISSANCE SURFACE GEOLOGY

The goal of the literature review was to establish relations between mappable surface expressions of faults and earthquake parameters, such as magnitude and displacement. Because earthquakes occur due to a variety of geological mechanisms, the review also considered whether any derived relations were earthquake type-specific or rock type-specific. The best data concerning the relation among earthquake parameters can be found in a series of papers by Coppersmith and his colleagues (Schwartz and Coppersmith, 1986; Coppersmith and Youngs, 1992, Wells and Coppersmith, 1994).

Wells and Coppersmith (1994) assembled a world-wide database of 244 well-documented crustal earthquakes for which parameters having to do with magnitude, surface rupture length, subsurface rupture length and width, and displacements were reliably known. The database was derived from a larger dataset of 421 earthquakes greater than magnitude 4.5. Smaller crustal earthquakes and those associated with subduction zones, plate interfaces and those within oceanic slabs were excluded. All earthquakes were classified in terms of their sense of slip (strike-slip (left-lateral or right-lateral), oblique (dominantly strike-slip), oblique (dominantly reverses-slip or normal-slip), reverse-slip, and normal-slip). They were also classified in terms of whether they occurred in a compressional, extensional or transitional environment, and also whether they occurred at plate margins or within stable continental crust. A series of key figures and regression equations from their work are reproduced below (Figure 2-3).

The relevant relations required for obtaining numerical quantities for the modeling described in Section 4 are the functional relations between magnitude and the surface rupture length, displacement and subsurface rupture area (Figure 2-4).

Wells and Coppersmith (1994) concluded that slip-type is insignificant at the 95% significance level for the regressions between surface rupture length (SRL) and magnitude (M), and between subsurface rupture length (RLD). For rupture area (RA) versus M and downdip rupture width (RW) versus M, strike-slip and normal are the same at 95%, but reverse faults are significantly different. They conclude that the fault-specific regression coefficients should be used for reverse fault problems, but that all other types of faults may be lumped together.

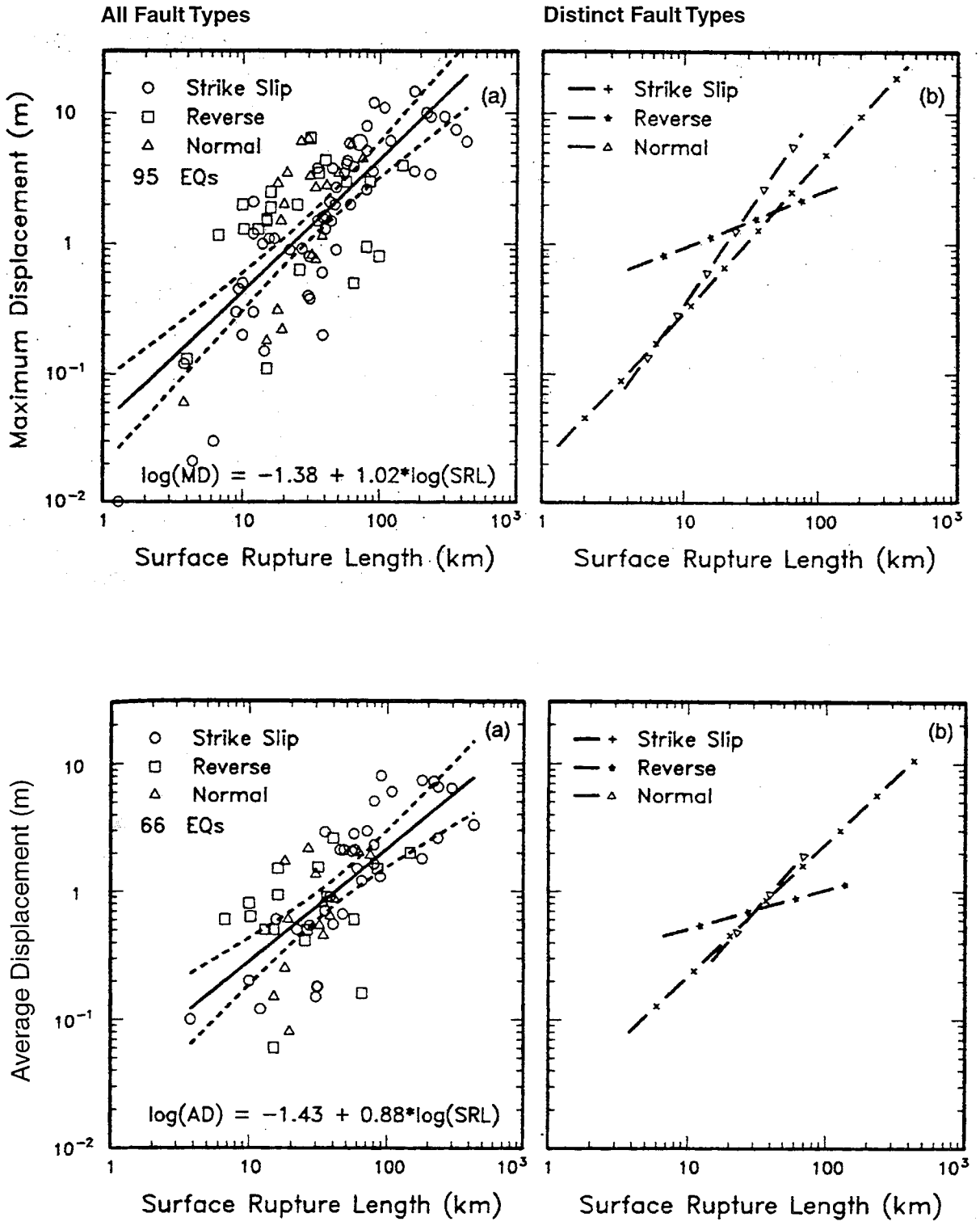


REFERENCE: New Empirical Relationships among Magnitude, Rupture Length, Rupture Width, Rupture Area, and Surface Displacement (Donald L. Wells and Kevin J. Coppersmith) Bulletin of the Seismological Society of America, Vol. 84, pp. 974-1002, August 1994.

FIGURE **2-3a**
**DISPLACEMENT VS. SURFACE RUPTURE LENGTH**

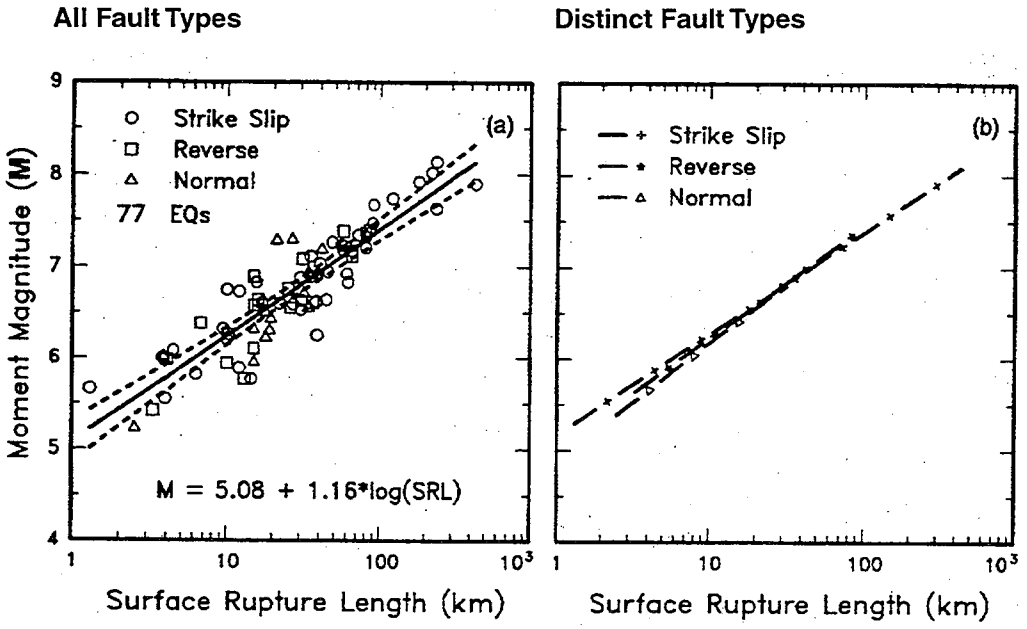


REFERENCE: New Empirical Relationships among Magnitude, Rupture Length, Rupture Width, Rupture Area, and Surface Displacement (Donald L. Wells and Kevin J. Coppersmith) Bulletin of the Seismological Society of America, Vol. 84, pp. 974-1002, August 1994.

FIGURE **2-3b**
**MOMENT MAGNITUDE VS. SURFACE RUPTURE LENGTH**

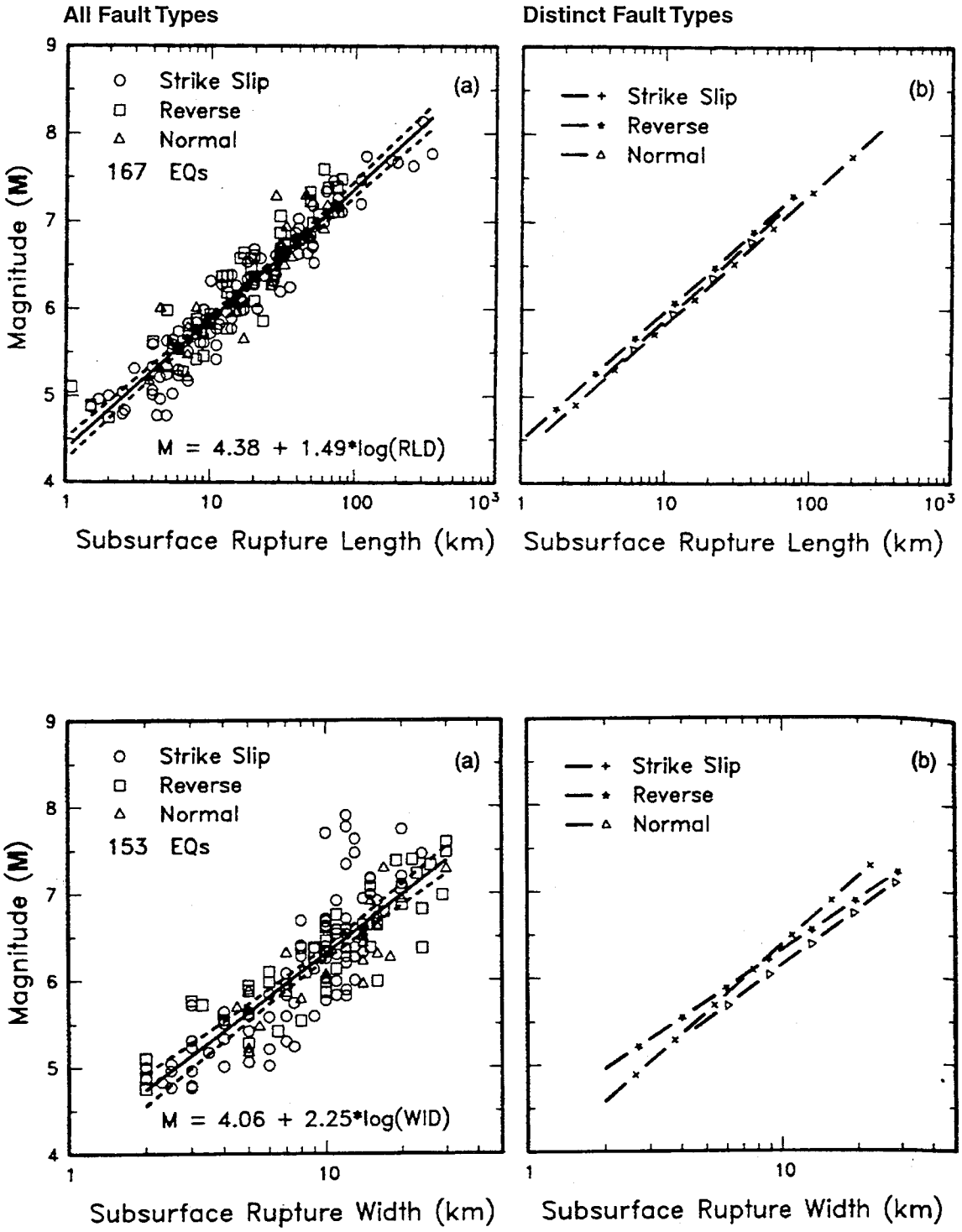


REFERENCE: New Empirical Relationships among Magnitude, Rupture Length, Rupture Width, Rupture Area, and Surface Displacement (Donald L. Wells and Kevin J. Coppersmith) Bulletin of the Seismological Society of America, Vol. 84, pp. 974-1002, August 1994.

FIGURE **2-3c**

**MOMENT MAGNITUDE VS. SUBSURFACE RUPTURE LENGTH AND WIDTH**

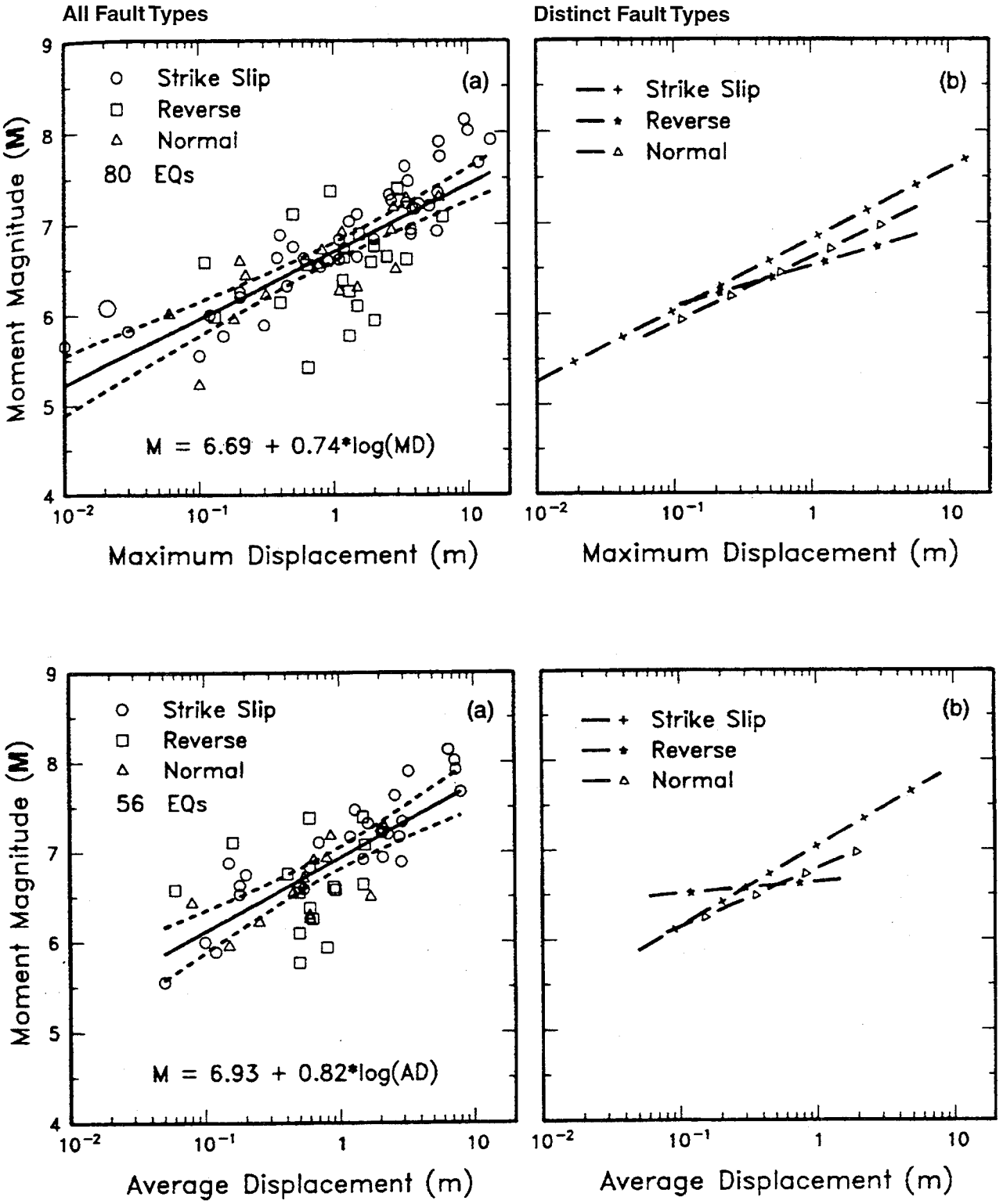


REFERENCE: New Empirical Relationships among Magnitude, Rupture Length, Rupture Width, Rupture Area, and Surface Displacement (Donald L. Wells and Kevin J. Coppersmith) Bulletin of the Seismological Society of America, Vol. 84, pp. 974-1002, August 1994.

FIGURE **2-3d**
**MOMENT MAGNITUDE VS. MAXIMUM AND AVERAGE DISPLACEMENT**

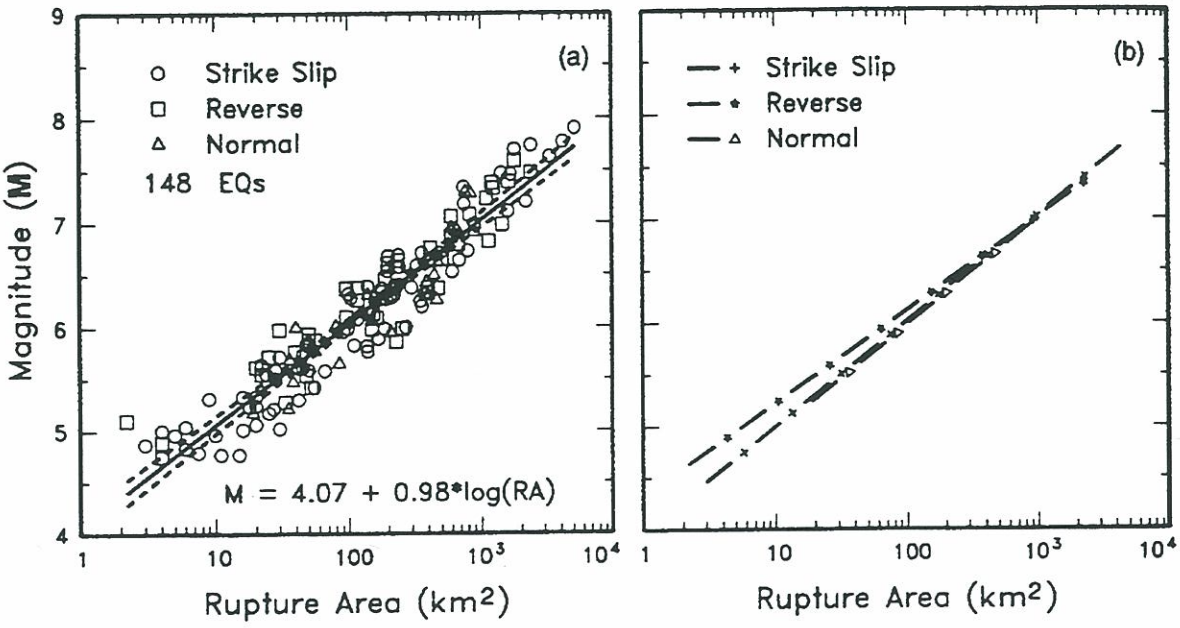


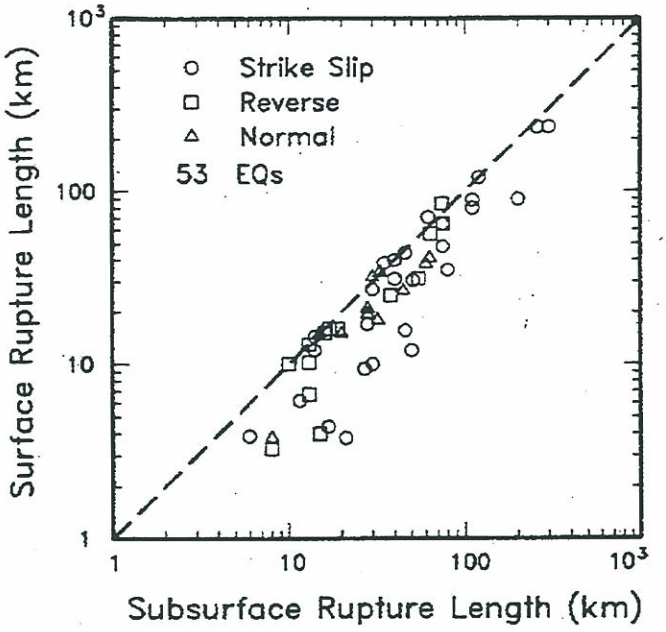


REFERENCE: New Empirical Relationships among Magnitude, Rupture Length, Rupture Width, Rupture Area, and Surface Displacement (Donald L. Wells and Kevin J. Coppersmith) Bulletin of the Seismological Society of America, Vol. 84, pp. 974-1002, August 1994.

FIGURE **2-3e**

**MAGNITUDE VS. RUPTURE AREA AND SURFACE RUPTURE LENGTH VS. SUBSURFACE RUPTURE LENGTH**

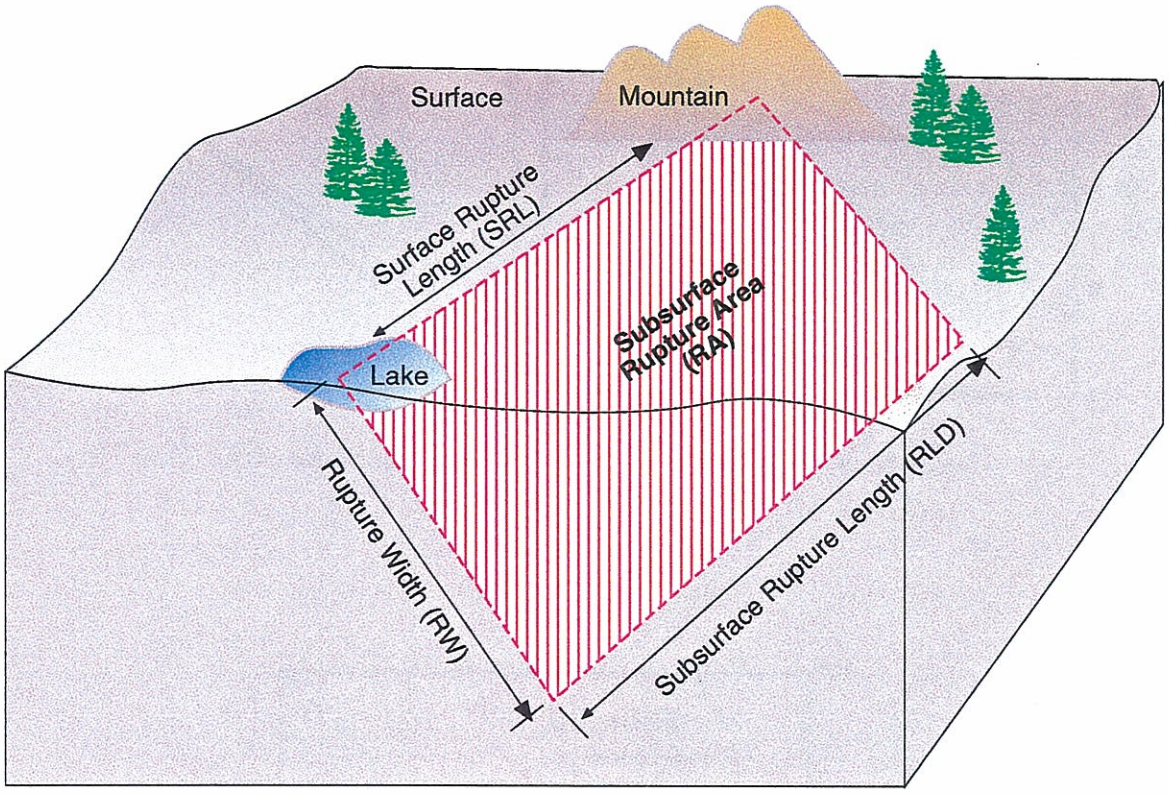


| Key Parameters: | Use: |
|---|---|
| SRL vs. M | Estimate M from SRL |
| Displacement vs. M | Estimate Displacement from M |
| RW vs. M<br>RLD vs. M | Determine fault length and width as a function of M |

Where:

M = 2/3 log $M_0$ - 10.7 (Hanks and Kanamori, 1970)
$M_0$ = $\mu$ x D x RA
$\mu$ = shear modulus
D = average displacement
RA = rupture area

FIGURE **2-4**
**KEY EARTHQUAKE PARAMETERS**

Although previous work (for example, Slemmons and others, 1989) suggests that compressional versus extensional tectonic settings may affect the relations between rupture length relationships, Wells and Coppersmith (1994) found no difference at the 95% significance level for any of their regressions. They conclude that their relations are independent of tectonic setting and geographical location.

One limitation of their regressions are that they are all based on earthquakes larger than 4.5, and in some instances, larger than 6.0. For example, surface rupture length is difficult to determine for earthquakes less than 6.0. For this reason, extrapolation of the regression relations to earthquakes smaller than 6.0 may not be accurate, and certainly extrapolation of any of the regression relations to earthquakes smaller than 4.5 entails substantial uncertainty.

These regression relations indicate what earthquake magnitude is associated with a maximum surface displacement of 0.1 m. From Table 2-3b, the regression equation for all faults is:

$$M = 6.69 + 0.74 \log(MD) \qquad \text{Equation 2-2}$$

where MD is the maximum displacement in meters, and M is the moment magnitude. This equation suggests that an earthquake on the order of magnitude 5.95 is required to produce a maximum displacement of 0.1 m. Using the equation to relate surface rupture length to MD (Table 2-3c):

$$\text{Log(SRL)} = 1.43 + 0.56 \text{ Log(MD)} \qquad \text{Equation 2-3}$$

where SRL is the surface rupture length in kilometers, the corresponding surface rupture length is found to be 7.4 km, based on all fault types. The SRL for strike-slip faults is about 7.1 km, while for normal-slip and reverse-slip faults the SRL would be 10.2 km. This appears to be much greater than mapped fault trace segments as inferred from lineament maps in the Äspö area. Such large faults should be easy to detect during a reconnaissance siting program and avoided.

It is important to consider whether these regression relations are valid for Sweden, or whether Swedish earthquakes differ in some way from those in Wells and Coppersmith's (1994) database. If so, then these regression equations cannot be used to determine conservative modeling parameters.

There is some evidence that displacements may be greater for the smaller (magnitude < 5.0) earthquakes in Sweden than would be predicted by Wells and Coppersmith's (1994) relations. For example, Slunga (1991) reports that the magnitude 4.5 Skövde earthquake had a peak displacement of about 300 mm. The regression relation for strike-slip earthquakes in Table 2-3b implies that a magnitude 4.5 earthquake would have a maximum surface displacement of about 4 mm, nearly two orders of magnitude less. There could be several possible explanations for this discrepancy. These include:

## Table 2-3a

Regressions of Rupture Length, Rupture Width, Rupture Area, and Moment Magnitude (M)

| Equation* | Slip Type† | Number of Events | Coefficients and Standard Errors | | Standard Deviation | Correlation Coefficient | Magnitude Range | Length/Width Range (km) |
|---|---|---|---|---|---|---|---|---|
| | | | $a$(sa) | $b$(sb) | $s$ | $r$ | | |
| $M = a + b * \log (SRL)$ | SS | 43 | 5.16(0.13) | 1.12(0.08) | 0.28 | 0.91 | 5.6 to 8.1 | 1.3 to 432 |
| | R | 19 | 5.00(0.22) | 1.22(0.16) | 0.28 | 0.88 | 5.4 to 7.4 | 3.3 to 85 |
| | N | 15 | 4.86(0.34) | 1.32(0.26) | 0.34 | 0.81 | 5.2 to 7.3 | 2.5 to 41 |
| | All | 77 | 5.08(0.10) | 1.16(0.07) | 0.28 | 0.89 | 5.2 to 8.1 | 1.3 to 432 |
| $\log (SRL) = a + b * M$ | SS | 43 | −3.55(0.37) | 0.74(0.05) | 0.23 | 0.91 | 5.6 to 8.1 | 1.3 to 432 |
| | R | 19 | −2.86(0.55) | 0.63(0.08) | 0.20 | 0.88 | 5.4 to 7.4 | 3.3 to 85 |
| | N | 15 | −2.01(0.65) | 0.50(0.10) | 0.21 | 0.81 | 5.2 to 7.3 | 2.5 to 41 |
| | All | 77 | −3.22(0.27) | 0.69(0.04) | 0.22 | 0.89 | 5.2 to 8.1 | 1.3 to 432 |
| $M = a + b * \log (RLD)$ | SS | 93 | 4.33(0.06) | 1.49(0.05) | 0.24 | 0.96 | 4.8 to 8.1 | 1.5 to 350 |
| | R | 50 | 4.49(0.11) | 1.49(0.09) | 0.26 | 0.93 | 4.8 to 7.6 | 1.1 to 80 |
| | N | 24 | 4.34(0.23) | 1.54(0.18) | 0.31 | 0.88 | 5.2 to 7.3 | 3.8 to 63 |
| | All | 167 | 4.38(0.06) | 1.49(0.04) | 0.26 | 0.94 | 4.8 to 8.1 | 1.1 to 350 |
| $\log (RLD) = a + b * M$ | SS | 93 | −2.57(0.12) | 0.62(0.02) | 0.15 | 0.96 | 4.8 to 8.1 | 1.5 to 350 |
| | R | 50 | −2.42(0.21) | 0.58(0.03) | 0.16 | 0.93 | 4.8 to 7.6 | 1.1 to 80 |
| | N | 24 | −1.88(0.37) | 0.50(0.06) | 0.17 | 0.88 | 5.2 to 7.3 | 3.8 to 63 |
| | All | 167 | −2.44(0.11) | 0.59(0.02) | 0.16 | 0.94 | 4.8 to 8.1 | 1.1 to 350 |
| $M = a + b * \log (RW)$ | SS | 87 | 3.80(0.17) | 2.59(0.18) | 0.45 | 0.84 | 4.8 to 8.1 | 1.5 to 350 |
| | R | 43 | 4.37(0.16) | 1.95(0.15) | 0.32 | 0.90 | 4.8 to 7.6 | 1.1 to 80 |
| | N | 23 | 4.04(0.29) | 2.11(0.28) | 0.31 | 0.86 | 5.2 to 7.3 | 3.8 to 63 |
| | All | 153 | 4.06(0.11) | 2.25(0.12) | 0.41 | 0.84 | 4.8 to 8.1 | 1.1 to 350 |
| $\log (RW) = a + b * M$ | SS | 87 | −0.76(0.12) | 0.27(0.02) | 0.14 | 0.84 | 4.8 to 8.1 | 1.5 to 350 |
| | R | 43 | −1.61(0.20) | 0.41(0.03) | 0.15 | 0.90 | 4.8 to 7.6 | 1.1 to 80 |
| | N | 23 | −1.14(0.28) | 0.35(0.05) | 0.12 | 0.86 | 5.2 to 7.3 | 3.8 to 63 |
| | All | 153 | −1.01(0.10) | 0.32(0.02) | 0.15 | 0.84 | 4.8 to 8.1 | 1.1 to 350 |
| $M = a + b * \log (RA)$ | SS | 83 | 3.98(0.07) | 1.02(0.03) | 0.23 | 0.96 | 4.8 to 7.9 | 3 to 5,184 |
| | R | 43 | 4.33(0.12) | 0.90(0.05) | 0.25 | 0.94 | 4.8 to 7.6 | 2.2 to 2,400 |
| | N | 22 | 3.93(0.23) | 1.02(0.10) | 0.25 | 0.92 | 5.2 to 7.3 | 19 to 900 |
| | All | 148 | 4.07(0.06) | 0.98(0.03) | 0.24 | 0.95 | 4.8 to 7.9 | 2.2 to 5,184 |
| $\log (RA) = a + b * M$ | SS | 83 | −3.42(0.18) | 0.90(0.03) | 0.22 | 0.96 | 4.8 to 7.9 | 3 to 5,184 |
| | R | 43 | −3.99(0.36) | 0.98(0.06) | 0.26 | 0.94 | 4.8 to 7.6 | 2.2 to 2,400 |
| | N | 22 | −2.87(0.50) | 0.82(0.08) | 0.22 | 0.92 | 5.2 to 7.3 | 19 to 900 |
| | All | 148 | −3.49(0.16) | 0.91(0.03) | 0.24 | 0.95 | 4.8 to 7.9 | 2.2 to 5,184 |

*SRL—surface rupture length (km); RLD—subsurface rupture length (km); RW—downdip rupture width (km), RA—rupture area (km$^2$).
†SS—strike slip; R—reverse; N—normal.

REFERENCE: New Empirical Relationships among Magnitude, Rupture Length, Rupture Width, Rupture Area, and Surface Displacement (Donald L. Wells and Kevin J. Coppersmith) Bulletin of the Seismological Society of America, Vol. 84, pp. 974-1002, August 1994.

## Table 2-3b

Regressions of Displacement and Moment Magnitude (M)

| Equation* | Slip Type† | Number of Events | Coefficients and Standard Errors a(sa) | Coefficients and Standard Errors b(sb) | Standard Deviation s | Correlation Coefficient r | Magnitude Range | Displacement Range (km) |
|---|---|---|---|---|---|---|---|---|
| M = a + b * log (MD) | SS | 43 | 6.81(0.05) | 0.78(0.06) | 0.29 | 0.90 | 5.6 to 8.1 | 0.01 to 14.6 |
| | {R‡ | *21* | *6.52(0.11)* | *0.44(0.26)* | *0.52* | *0.36* | *5.4 to 7.4* | *0.11 to 6.5}* |
| | N | 16 | 6.61(0.09) | 0.71(0.15) | 0.34 | 0.80 | 5.2 to 7.3 | 0.06 to 6.1 |
| | All | 80 | 6.69(0.04) | 0.74(0.07) | 0.40 | 0.78 | 5.2 to 8.1 | 0.01 to 14.6 |
| log (MD) = a + b * M | SS | 43 | −7.03(0.55) | 1.03(0.08) | 0.34 | 0.90 | 5.6 to 8.1 | 0.01 to 14.6 |
| | {R | *21* | *−1.84(1.14)* | *0.29(0.17)* | *0.42* | *0.36* | *5.4 to 7.4* | *0.11 to 6.5}* |
| | N | 16 | −5.90(1.18) | 0.89(0.18) | 0.38 | 0.80 | 5.2 to 7.3 | 0.06 to 6.1 |
| | All | 80 | −5.46(0.51) | 0.82(0.08) | 0.42 | 0.78 | 5.2 to 8.1 | 0.01 to 14.6 |
| M = a + b * log (AD) | SS | 29 | 7.04(0.05) | 0.89(0.09) | 0.28 | 0.89 | 5.6 to 8.1 | 0.05 to 8.0 |
| | {R | *15* | *6.64(0.16)* | *0.13(0.36)* | *0.50* | *0.10* | *5.8 to 7.4* | *0.06 to 1.5}* |
| | N | 12 | 6.78(0.12) | 0.65(0.25) | 0.33 | 0.64 | 6.0 to 7.3 | 0.08 to 2.1 |
| | All | 56 | 6.93(0.05) | 0.82(0.10) | 0.39 | 0.75 | 5.6 to 8.1 | 0.05 to 8.0 |
| log (AD) = a + b * M | SS | 29 | −6.32(0.61) | 0.90(0.09) | 0.28 | 0.89 | 5.6 to 8.1 | 0.05 to 8.0 |
| | {R | *15* | *−0.74(1.40)* | *0.08(0.21)* | *0.38* | *0.10* | *5.8 to 7.4* | *0.06 to 1.5}* |
| | N | 12 | −4.45(1.59) | 0.63(0.24) | 0.33 | 0.64 | 6.0 to 7.3 | 0.08 to 2.1 |
| | All | 56 | −4.80(0.57) | 0.69(0.08) | 0.36 | 0.75 | 5.6 to 8.1 | 0.05 to 8.0 |

*MD—maximum displacement (m); AD—average displacement (M).
†SS—strike slip; R—reverse; N—normal.
‡Regressions for reverse-slip relationships shown in italics and brackets are not significant at a 95% probability level.

## Table 2-3c

Regressions of Surface Rupture Length and Displacement

| Equation* | Slip Type§ | Number of Events | Coefficients and Standard Errors a(sa) | Coefficients and Standard Errors b(sb) | Standard Deviation s | Correlation Coefficient r | Displacement Range (m) | Rupture Length Range (km) |
|---|---|---|---|---|---|---|---|---|
| log (MD) = a + b * log (SRL) | SS | 55 | −1.69(0.16) | 1.16(0.09) | 0.36 | 0.86 | 0.01 to 14.6 | 1.3 to 432 |
| | {R‡ | *21* | *−0.44(0.34)* | *0.42(0.23)* | *0.43* | *0.38* | *0.11 to 6.5* | *4 to 148}* |
| | N | 19 | −1.98(0.50) | 1.51(0.35) | 0.41 | 0.73 | 0.06 to 6.4 | 3.8 to 75 |
| | All | 95 | −1.38(0.15) | 1.02(0.09) | 0.41 | 0.75 | 0.01 to 14.6 | 1.3 to 432 |
| log (SRL) = a + b * log (MD) | SS | 55 | 1.49(0.04) | 0.64(0.05) | 0.27 | 0.86 | 0.01 to 14.6 | 1.3 to 432 |
| | {R | *21* | *1.36(0.09)* | *0.35(0.19)* | *0.39* | *0.38* | *0.11 to 6.5* | *4 to 148}* |
| | N | 19 | 1.36(0.05) | 0.35(0.08) | 0.20 | 0.73 | 0.06 to 6.4 | 3.8 to 75 |
| | All | 95 | 1.43(0.03) | 0.56(0.05) | 0.31 | 0.75 | 0.01 to 14.6 | 1.3 to 432 |
| log (AD) = a + b * log (SRL) | SS | 35 | −1.70(0.23) | 1.04(0.13) | 0.32 | 0.82 | 0.10 to 8.0 | 3.8 to 432 |
| | {R | *17* | *−0.60(0.39)* | *0.31(0.27)* | *0.40* | *0.28* | *0.06 to 2.6* | *6.7 to 148}* |
| | N | 14 | −1.99(0.72) | 1.24(0.49) | 0.37 | 0.59 | 0.08 to 2.1 | 15 to 75 |
| | All | 66 | −1.43(0.18) | 0.88(0.11) | 0.36 | 0.71 | 0.06 to 8.0 | 3.8 to 432 |
| log (SRL) = a + b * log (AD) | SS | 35 | 1.68(0.04) | 0.65(0.08) | 0.26 | 0.82 | 0.10 to 8.0 | 3.8 to 432 |
| | {R | *17* | *1.45(0.10)* | *0.26(0.23)* | *0.36* | *0.28* | *0.06 to 2.6* | *6.7 to 148}* |
| | N | 14 | 1.52(0.05) | 0.28(0.11) | 0.17 | 0.59 | 0.08 to 2.1 | 15 to 75 |
| | All | 66 | 1.61(0.04) | 0.57(0.07) | 0.29 | 0.71 | 0.06 to 8.0 | 3.8 to 432 |

*SRL—surface rupture length (km); MD—maximum displacement (m); AD—average displacement (m).
§SS—strike slip; R—reverse; N—normal.
‡Regressions for reverse-slip relationships shown in italics and brackets are not significant at a 95% probability level.

REFERENCE: New Empirical Relationships among Magnitude, Rupture Length, Rupture Width, Rupture Area, and Surface Displacement (Donald L. Wells and Kevin J. Coppersmith) Bulletin of the Seismological Society of America, Vol. 84, pp. 974-1002, August 1994.

- Swedish faults have a lower shear stiffness than other faults worldwide;
- Small faults are less stiff than large faults;
- Maximum surface displacements are less than subsurface displacements;
- The observed 300 mm subsurface displacement at Skövde is not anomalous; rather, it is within the normal range of subsurface displacements of 4.5 moment magnitude earthquakes.

Each of these possible explanations is discussed below.

The first hypothesis is that earthquakes in Sweden differ from the earthquakes in the Wells and Coppersmith (1994) database. There are problems with this explanation, however. To a first-order approximation, earthquake moment is equal to the product of fault slip, shear stiffness and rupture area, as shown in Figure 2-4. This implies that the faults along which earthquakes take place in Sweden are one- to two orders of magnitude less stiff. It is not obvious why Swedish fault zones, which have developed in crystalline rocks of higher shear stiffness than most other rock types, should be significantly less stiff than fault zones in the rest of the world.

The second possibility has to do with extrapolating results from large earthquakes to earthquakes of smaller magnitude. Wells and Coppersmith's (1994) regression relations between displacement and magnitude are based on earthquakes with moment magnitudes greater than 5.2, as shown in Table 2-3b. If these larger earthquakes occurred on effectively stiffer faults, then extrapolation to smaller, presumably less stiff faults, might produce an underestimate of slip. However, a large amount of evidence from both the field and the laboratory suggests that effective stiffness *decreases* with fracture size, leading to larger displacements. This can also be seen in the regression coefficients shown in Tables 2-3a and 2-3b for strike-slip and normal faults (the regression coefficients for reverse faults are not considered statistically significant by Wells and Coppersmith). Combining equations for rupture area (RA) as a function of magnitude, and maximum displacement (MD) as a function of magnitude, shows that:

$MD \propto RA^{1.14}$ for strike-slip faults Equation 2-4
$MD \propto RA^{1.09}$ for normal faults

The fact that the exponent for both these cases is greater than 1.0 implies that, for the same energy release, proportionately larger maximum displacements occur on faults of greater size. This means that larger faults behave as if they were less stiff than small faults. Therefore, extrapolation of the regression relations to smaller faults should *overestimate* maximum displacements, not underestimate them.

The third explanation for the larger displacement for the Skövde earthquake is that the 300 mm represents the peak subsurface slip, while Wells and Coppersmith's (1994) regression relations are for average and maximum surface displacement.

The displacement along a fracture is not uniform. At the edges of the fracture, the displacement is zero, so there is a general decrease in the displacement magnitude away from the initial rupture point towards the edges. Since most large earthquakes have focal depths kilometers or even tens of kilometers below the surface, it might seem logical that surface displacements are significantly less than subsurface displacements.

Wells and Coppersmith (1994) evaluated the relation between surface and subsurface displacements for earthquakes in their database. As expected, they found that subsurface displacements were up to ten times greater than average surface displacements, with a mode of 1.32. However, they also found that maximum surface displacements exceeded subsurface displacements. They reported that the mode of subsurface to maximum surface displacement was 0.76. This led them to conclude that:

> "...average subsurface displacement is more than average surface displacement and less than maximum surface displacement. Furthermore, for these earthquakes, most slip on the fault plane at seismogenic depths is manifested at the surface." (Wells and Coppersmith, 1994; pg. 987).

Also, local irregularities in fault geometry or material properties can concentrate strain along the fault, leading to higher-than-average local displacement or deformation (Withjack and others, 1995).

The preceeding discussion has focused on possible geological explanations for the difference between the reported 300 m peak subsurface slip and the much lower maximum surface slip predicted by the regression equations. There is also a simple statistical explanation that reconciles the Skövde earthquake with Wells and Coppersmith's work: the 300 mm displacement may be greater than the mean estimated slip, but is well within the actual data values in Wells and Coppersmith's database. This hypothesis was tested by computing the subsurface slip from the raw data in Wells and Coppersmith's earthquake database.

Although they do not report values for subsurface displacement, Wells and Coppersmith (1994) list values for earthquake moment, rupture area and shear stiffness. These three values can be used to calculate subsurface displacement according to the equation in Figure 2-4.

The results of nonlinear regression to compute the relation between subsurface displacement (SD) and moment magnitude are shown in Figure 2-5. Table 2-4 summarizes the nonlinear regression results:

**Table 2-4 Results of Nonlinear Regression of Subsurface Displacement vs. Magnitude**

| Fault Type | C | D |
|---|---|---|
| Strike Slip | -2.95 | 0.47 |
| Normal | -7.01 | 1.05 |
| Reverse | -4.21 | 0.64 |

where $SD = C*M^D$

Figure 2-5 shows that normal faults have a different relation between magnitude and slip from strike-slip and reverse faults. The figure also shows that the subsurface displacements for strike-slip and reverse faults are similar for very large (> 7.0) earthquakes, but differ for smaller earthquakes. In the range of magnitude 4.0 to 5.0, strike-slip earthquakes have the greatest subsurface displacement.

Figure 2-5 shows that the mean predicted subsurface magnitude for a 4.5 magnitude earthquake is about 150 mm. Within the range of 4.5 to 5.0, there are strike-slip earthquakes in the database that have estimated subsurface displacements of approximately 300 mm.

This suggests that the Skövde earthquake is within the normal range of subsurface displacements for strike-slip and reverse faults in Wells and Coppersmith's (1994) database, even if it is greater than the mean values.

This implies that the regression relations established by Wells and Coppersmith (1994) are consistent with the historical earthquake record in Sweden. It also illustrates that the maximum surface displacement calculated from the regression relations may tend to underestimate subsurface displacements for smaller earthquakes in Sweden, and that the nonlinear regression relations shown in Table 2-4 might be better for assigning boundary conditions for earthquakes in this magnitude range in order to provide conservative results.

It is interesting to note that the regression equation for SRL and displacement are in the form of power laws, suggesting a fractal scaling behavior. Numerous studies over the past decade have examined earthquakes from a fractal perspective, as summarized in Turcotte (1992). Two of the fractal aspects of earthquakes are of interest in assessing repository performance: the relation between fault size (or trace length) and displacement; and the recurrence rate as a function of magnitude. However, the fractal analyses of fault size vs. displacement are probably of limited use for numerical modeling input, except as limiting values.

For example, Walsh and Watterson (1987, 1989, 1992) showed that total fault displacement had a power law relation to fault length. They found an exponent on the order of 1.6 obtained by studying normal faults in coal,

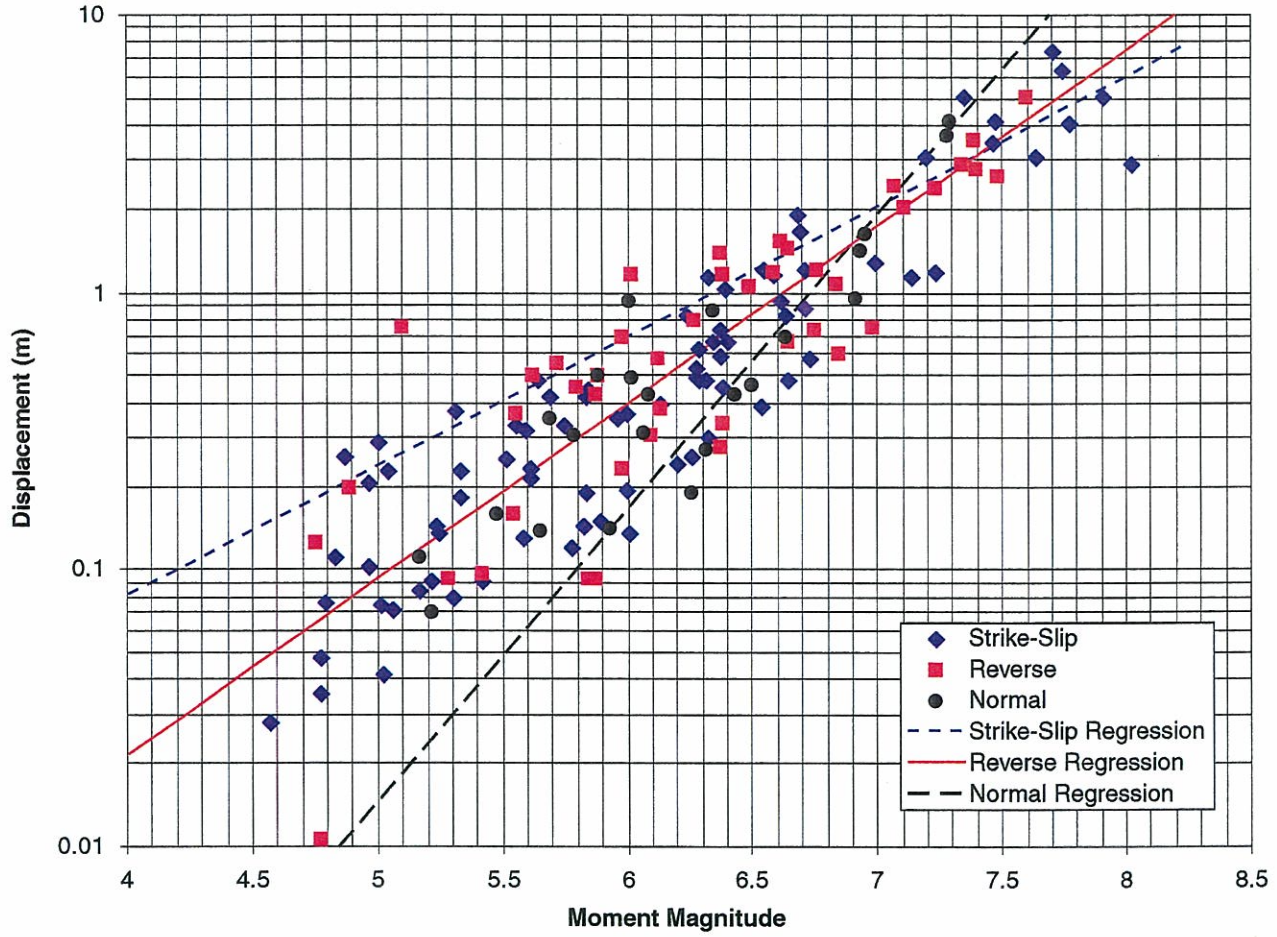


FIGURE **2-5**
**RELATION BETWEEN MOMENT MAGNITUDE AND MAXIMUM SUBSURFACE FAULT SLIP**

which is similar to the exponent of 1.51 found for normal faults for the regression between SRL and MD. However, Walsh and Watterson studied total net displacement, and total fracture length, not the lengths or slip pertaining to individual ruptures. Major faults in many places in the world have been active over periods of millions or even tens of millions of years, so that the net slip observed may have taken place over a considerably longer time period than is of regulatory interest. Moreover, cumulative slip and net slip are not necessarily equal. For net slip to equal cumulative slip, all individual slip vectors must be parallel. However, studies of faulting demonstrate that faults are re-activated during as new tectonic or geologic events occur. For example, the faults described by Arvidsson (1996) originally may have been strike-slip, and then subjected to reverse-slip during de-glaciation. Without knowing the period of time over which active faulting has occurred, and marshaling geological data to conclude that net slip and cumulative slip are similar, the published fractal studies cannot be reliably used for estimating potential cumulative displacement as a function of fault size.

In addition, while there appear to be various types of power-law correlations among the rupture area and other parameters, such as moment and displacement, there are no studies to show how total surface trace lengths relate to individual earthquake displacements.

Thus, the key to using fractal studies of total displacement vs. total fault length is to know the recurrence rates for the faults of interest and whether net observable slip is approximately equal to cumulative slip. Unfortunately, recurrence rates can vary widely. They must be determined for particular fault systems, and it is unlikely that recurrence rates for faults in the western U. S. or in the coal fields of the U. K. are relevant to recurrence rates in southern Sweden.

# 3. NUMERICAL MODEL DESCRIPTION

## 3.1 CODE DESCRIPTION

Ideally, a numerical code should be able to model the seismic response of realistic three-dimensional fracture networks, taking into account the complex rheology of fractured rock masses, the dynamics of seismic wave propagation, and fracture growth. However, no numerical codes that can model all of these effects exist at present. Each has its limitations. Kana and others (1991) describe the strengths and limitations of numerical codes that have been used to model various aspects of earthquakes.

To be useful, the numerical model should capture the most important effects, and ignore less important ones, while still providing useful decision-making information. The three-dimensional fracture geometry is a first-order effect, and the types of geometric simplifications found in finite difference, finite element and distinct element codes are probably not sufficiently realistic for the current project. The rheology of the model, can be simplified, but this must be done with the knowledge of how it relates to results that might be obtained with more realistic rheologies. Thus, the models should have two characteristics:

1. They should be based on realistic three-dimensional fracture geometry representative of the fracturing in Sweden, and

2. The simplifications made in the model should lead to bounding results

The long-term mechanical response of the earth's crust can be well-approximated by a visco-elastic rheology. For this reason, clay is often used to model crustal tectonic processes that lead to development of faults and joints (for example, Withjack and others, 1995), while numerical models employ visco-elastic rheology (Islam and others, 1991) to match the clay models. However, the numerical models that have been used to study the generation and structural evolution of faults typically require simplifications that make them less useful for studying repository problems. In particular, they are often 2D finite element or finite difference models, and cannot include hundreds of fractures. In general, it is very difficult to simulate the discrete behavior of discontinuities in a large 3D rock volume with a continuum numerical method such as finite elements or finite differences. For these reasons, a Displacement Discontinuity formulation may be more useful, since it can model the explicit tractions and displacements of fractures in three dimensions.

POLY3D (Thomas, 1993) is a fully three-dimensional displacement discontinuity code designed to study fracture mechanics problems. Its polygonal element formulation makes it well-suited to model irregular, curved faults and joints without creating gaps or numerical problems (Figure 3-1). It is formulated for a linearly elastic material. Although a visco-elastic material would be more realistic for long term crustal processes, a linearly elastic material provides a worst-case bound on the stresses and displacements developed on existing fractures due to imposed tractions or displacements on the model boundary. In effect, all deformation produces stress or displacement of fractures in the rock mass; none of it is dissipated in viscous or plastic rock deformation.

For this reason, POLY3D is used for this demonstration project. The calculated displacements and stresses are likely to be greater than would actually occur in the rock, and thus provide a worst-case bound.

## 3.2 VERIFICATION

The POLY3D code was first verified for use in the current project by comparing its solutions for two problems. These two verification test cases represent the types of fracture interactions expected in this application.

Verification results are presented and discussed in Appendix A. The first test case compared POLY3D results to an analytical solution for line displacements in an infinite medium. Agreement was excellent. The second test case consisted of intersecting fractures, in which superimposed displacement fields for individual fractures were compared to a simulation containing all of the fractures simulated at the same time. The superposed solutions showed excellent agreement with the simulation containing all of the fractures. These simple test cases showed that POLY3D correctly calculates the displacements on intersecting fractures due to displacement boundary conditions in three dimensions.

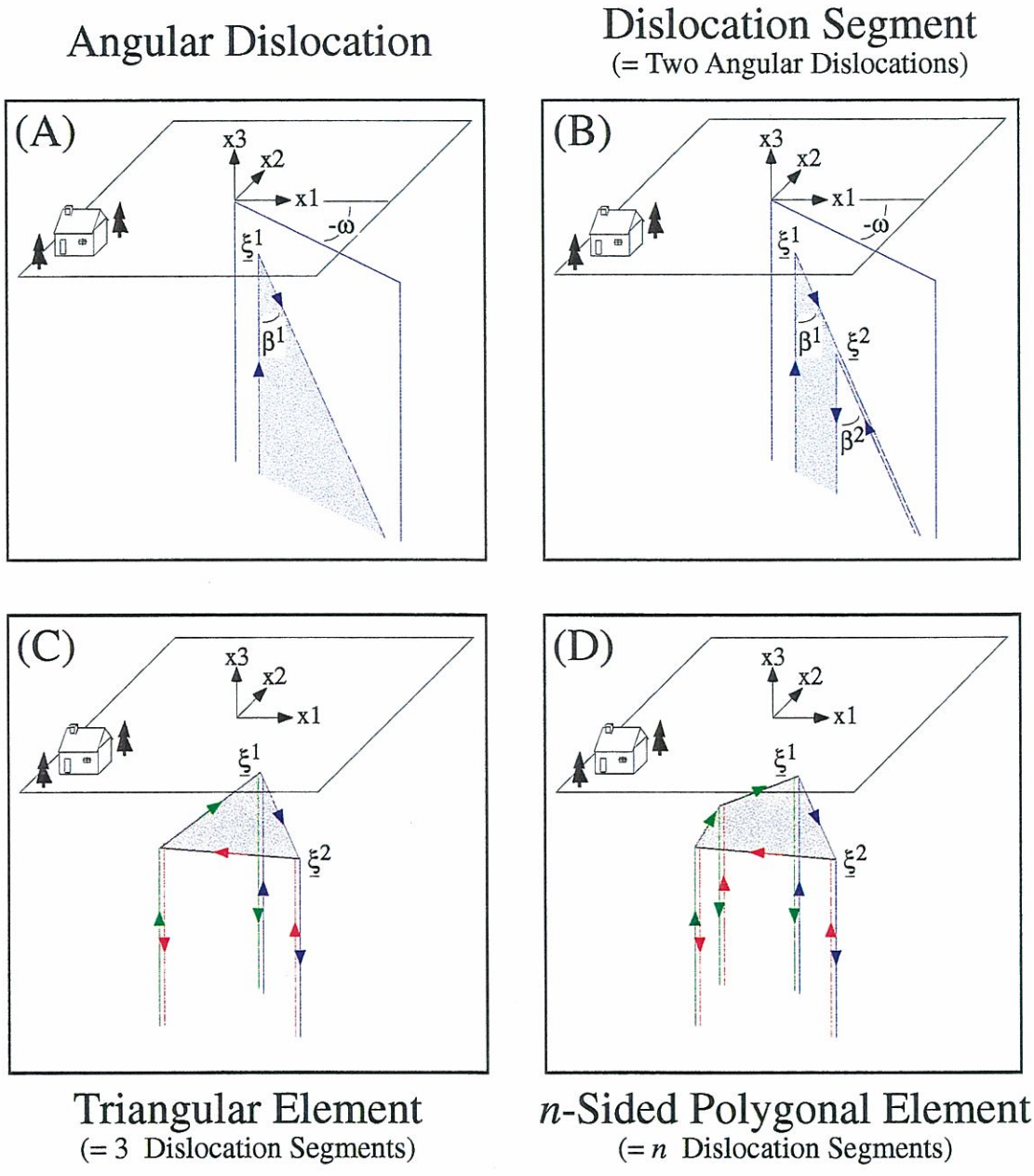


**(A) The angular dislocation of Comninou & Dundurs (1975) lies in a vertical plane with one leg perpendicular to the free surface. Two angular dislocations with identical Burgers vector, b, can be superposed to yield a single dislocation segment (B), which can in turn be superposed to yield a polygonal elements (C) & (D) of arbitrary orientation (Jeyakumaran et al., 1992).**

FIGURE **3-1**
**FORMULATION OF POLY 3D**

# 4. BOUNDARY CONDITIONS AND MODEL GEOLOGY

Two sets of numerical simulations were carried out. The first set was focused on the effects of a maximum credible earthquake based on historical earthquake records and the regression relations established by Wells and Coppersmith (1994). The modeling parameters are based on the geology of the Äspö area. The goal of these simulations is to illustrate how displacements can be calculated for a selected site, and to evaluate scaling relations between several important earthquake parameters. The second set of simulations provide a rough estimate of the minimum distance that an earthquake can occur away from a repository without exceeding 0.1 m average displacement on fractures intersecting canister holes. Earthquakes with magnitudes varying from 6.0 to 8.2 were considered. This series of simulations also illustrates how data and model uncertainty can be incorporated into estimates to provide more useful results for performance assessment or probabilistic analysis.

## 4.1 ÄSPÖ EXAMPLE

### 4.1.1 Boundary Conditions

The boundary conditions chosen for the first numerical modeling series reflect a worst-case scenario in several respects. First, historical earthquakes in Sweden do not appear to have been greater than Richter magnitude 5.0 (SKBF/KBS (1983), Vol. II, 8:30-8:37). Moreover, "No reports have been found of damage underground, in mines and tunnels, despite the fact that mining has been conducted in the country for many hundreds of years" (SKBF/KBS (1983), pg. 8:30). The existing seismicity is postulated to occur either due to fault movements associated with glacial unloading (SKBF/KBS (1983), 8:24), or due to plate tectonic processes. Muir-Wood (1993). Analysis of fault movements reported by Tirén and others (1987; pg. 38) suggests that the tectonic events that have caused the most recent slippage produce primarily strike-slip motions.

Block boundaries have been inferred through lineament and geophysical analyses for the Äspö area, as described in Tirén and others, (1987), Tirén and Beckholmen (1988), Nisca and Triumf (1989), Stranfors and Ericsson (1993), and Muir-Wood (1993). While potentially any of the mapped lineaments could serve as the epicenter of a future earthquake, many studies (for example, Wells and Coppersmith, 1994) demonstrate that moment magnitude is strongly correlated with surface rupture length. Thus, a worst-

case earthquake should occur on the fault with the longest possible surface rupture length.

Based upon 2D modeling results (Stephansson and others, 1979), it appears likely that future tectonically-induced earthquakes, or those due to glacial unloading, would arise from re-adjustment of existing crustal blocks in response to plate or isostatic movements, rather than from the creation of new, large-scale faults. This means that existing block boundaries should serve as the foci of future earthquakes.

Surface rupture length is not always identical to mapped trace length. For example, some of the fault may be buried, beneath a body of water, or poorly expressed as a geomorphologic feature. In these cases, the subsurface rupture length may be greater than the surface trace length. On the other hand, the current fault trace may be the result of several earthquake events; each earthquake event may have only ruptured a segment of the mapped fault trace. In this common case, the surface rupture length is commonly less than the mapped total length.

Determination of the rupture segments that correspond to distinct earthquake events is difficult for earthquakes of magnitude less than 6.0 in many cases (Darragh and Bolt, 1987; Wells and Coppersmith, 1994). Wells and Coppersmith (1994) suggest that the true surface rupture length for these smaller-magnitude earthquakes may be best approximated by combining several discontinuous mapped traces that are co-aligned. Knuepfer (1989), who studied strike-slip faults, suggests that the following criteria can be used to define the endpoints of a single rupture:

- Geometric properties, such as fault bends; release structures (double bends, step-overs, splays); and fault trace gaps, discontinuities or steps
- Structural features, such as branches and intersections with faults and folds; and terminations of faults against other cross-cutting structures
- Geological features, such as basin margins; and changes in bedrock geology relating to changes in rock rheology
- Behavioral changes, such as changes in complexity of fault traces; change in sense of slip; change in the mechanics of slip; the recency of prior ruptures on the same segment; and in the die-out of fault traces

A detailed evaluation of the lineaments in the Äspö area to determine the rupture lengths is beyond the scope of the present study. In order to provide a worst-case bounding earthquake, the lineament map prepared by Tirén and Beckholmen (1988), reproduced as Figure 4-1, was used as a basis for determining the maximum credible surface rupture length. It is possible that many of these lineaments do not correspond to faults. Also, the faults that do correspond to lineaments may not have been seismically active in the past. The trace selected has been highlighted in Figure 4-1. It was selected for the reason that it was the largest mapped unbroken lineament trace in the

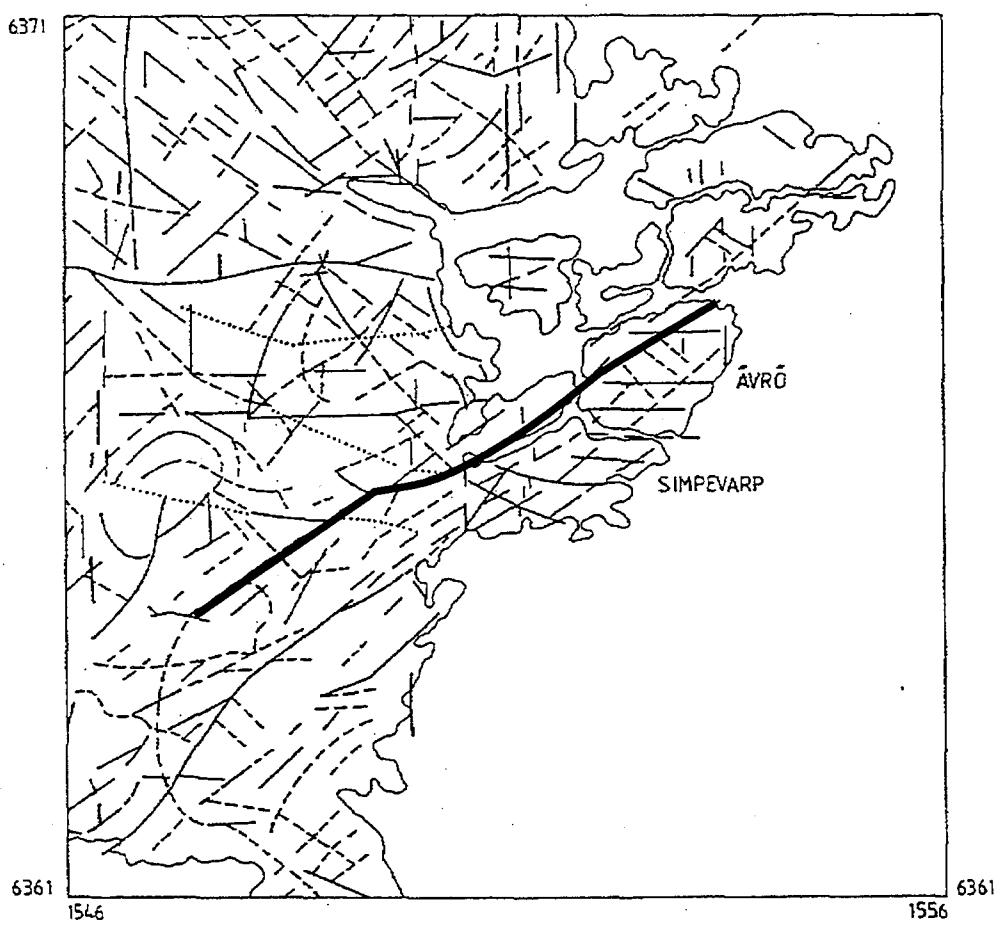


LINEAMENT MAP BASED ON DIGITAL TERRAIN MODELS: RESIDUAL ELEVATION, EDGE TEXTURE AND LINE TEXTURE MAPS

ÄVRÖ-SIMPEVARP AREA
MAP SHEET 6 G SE and 6 H SW

—— Local lineaments well defined

– – – Local lineaments visible

—— Narrow and sharp structures fractures / faults

..... Narrow passages floored with sediments

0 5km

PROJECT SKB-SBL

SWEDISH GEOLOGICAL
DIVISION OF ENGINEERING
GEOLOGY, UPPSALA 1987

FIGURE **4-1**
**LINEAMENT MAP FOR ÄVRÖ-SIMPEVARP AREA (FROM TIRÉN AND BECK HOLMEN, 1988)**

region. This implies that if it were a seismically active fault it should have the largest earthquake moment, as indicated by the regression relations in Table 2-3a.

Note that Knuepfer's (1989) criteria would probably suggest that this trace length consists of three distinct ruptures of about 2 km each. However, for the purposes of this study, this trace has been assumed to reflect a single rupture event. If so, it is the largest surface rupture event in the lineament map. This mapped surface rupture length is approximately 7 km.

Published graphs and rigorous regression analyses, as described in Section 2.3, suggest that a surface rupture length of 7 km corresponds to an earthquake moment magnitude of 6.1. This is considerably larger than any known historical earthquake in Sweden. This also corresponds to a maximum displacement of 0.2 m, and an average displacement of 0.15 m. For comparison, a magnitude 4.0 earthquake would have a maximum displacement of 1.23 mm, although the regression analyses were not based upon any earthquakes of such low magnitudes, so there is much less confidence in the 1.23 mm value than there is for the 6.1 magnitude earthquake. A 2 km surface rupture length for a strike-slip fault corresponds to an earthquake of magnitude 5.5, which appears reasonable for historical earthquakes in Sweden, and may more accurately reflect the true surface rupture lengths for the area around Äspö.

Earthquake depth cannot be directly inferred from the lineament maps. Earthquakes associated with strike-slip tectonic processes can be deep and large. McClure (1981) provides evidence that the most damaging tectonic earthquakes are those that occur below 900 m in depth. From the regression relations in Table 2-3, the subsurface down-dip rupture length should be about 8 km. For the purposes of this exercise, the epicenter for the earthquake is taken to be about 4 km below the surface, since the regression relations in Table 2-3 suggest that the subsurface rupture zone should be 16 km in horizontal extent and 8 km deep. Empirical data from Coopersmith (1991) and dePolo (1991) would suggest that magnitude 6.0 and greater events nucleate at depths greater than 7 km. Locating the rupture at this depth, however, increases the distance between seismic dislocation and the repository. Thus, an epicentral depth of 4 km is likely to be conservative.

The rock units found at Äspö consist of several lithologies. In general, they are granitic crystalline rocks which share in common high stiffness (E, or Young's Modulus), high strength and high fracture toughness. Young's modulus for intact rock is, according to Pusch (1996) on the order of 4e4 to 1e6 MPa. In the same report Pusch uses a $\nu$ (Poisson's ratio) = 0.2-0.3. Rhén and others (1996) have summarized the mechanical properties of the major rock units at Äspö. They found that the mean value for Young's Modulus ranged from 73 GPa for Äspö diorite to 78 GPa for greenstone. The Småland (Ävrö) granite and the Äspö diorite make up the majority of the rock found at Äspö, and they have a combined average E of about 73.5

GPa with a standard deviation of about 4.5 GPa. Mean values for Poisson's Ratio for these four rock units varies from 0.23 to 0.24.

A high value of E will lead to greater displacements due to an applied stress than will a low value of E. Thus, high values of E are conservative. Likewise, a higher value of Poisson's Ratio will lead to greater lateral deformation to an applied stress than a lower value of Poisson's Ratio. This means that high values of Poisson's Ratio are conservative. The results reported in this section assume values for E and Poisson's Ratio that are slightly more conservative than the mean: E = 75 GPa and Poisson's Ratio = 0.25. The results reported in Section 4.2 assume a value of E of 75,000 MPa, and a $\nu$ of 0.25.

Table 4-1 summarizes the boundary conditions used for the numerical modeling.

### 4.1.2 Repository

The repository layout is as described in Dershowitz and others (1996; Figure 2-7), reproduced as Figure 4-2. In these simulations, the repository is located 2 km from the lineament/fault on which the magnitude 6.1 earthquake takes place. The repository is centered at a depth 500 m below the surface.

## 4.2 RESULTS

In the first series of simulations, one hundred realizations were run. In these realizations, the location, geometry and properties of the secondary faults and joints were varied. The fault on which the earthquake occurs, and the repository itself, remained unchanged. The performance of a repository during an earthquake is expressed in terms of fracture displacements. In particular, the slip parallel to the fracture surface is of greater concern than fracture dilation.

POLY3D computes the displacements at the center of each fracture due to imposed displacements on the fault on which the earthquake occurs. Pollard and Segall (1987) have shown, through linear elastic fracture mechanics that the maximum shear displacement occurs at the fracture center, decreasing towards the fracture edges. Thus, the displacements computed through the POLY3D code are worst-case values.

Of the 100 realizations, 3 failed for numerical reasons. The results summarized in the remaining sections are derived from the 97 successful realizations.

### 4.2.1 Maximum Shear Displacements

Figures 4-3 and 4-4 summarize the maximum shear displacements induced on existing secondary faults and joints by the earthquake on the 7 km fault during a magnitude 6.1 event. Figure 4-3 shows that the mean maximum displacement is between 0.1 and 1 mm. The maximum is less than 1 cm. Figure 4-4 shows the cumulative probability for maximum shear displacement. In both Figures, the results for all fractures, as well as for those that intersect canister holes, are shown. There is no appreciable difference.

### 4.2.2 Relation Between Fracture Size and Maximum Shear Displacement

Figure 4-5 is a plot relating fracture size and maximum shear displacement. Size is represented by a surrogate variable, the crack half-length, which is a parameter widely used in fracture mechanics. The fracture half-length in this case is defined as the radius of a circle that has the same area as the fracture. The plot shows that there is a relation between the fracture area and the maximum shear displacement:

$$\text{Radius (m)} = 1.68 + 26526 * \text{Displacement (m)} \qquad \text{Equation 4-1}$$

The regression coefficients are given in Table 4-2. Note that the regression is significant to an $R^2$ of 0.62

**Table 4-2 Regression of Fault Radius on Fault Displacement for Secondary Faults.**

| | Coefficients | Standard Error | Regression Significance ($R^2$) |
|---|---|---|---|
| Intercept | 1.683597 | 0.067499 | 0.621349 |
| X Variable | 26525.96 | 210.2548 | |

This suggests that there is a relation between fracture size and maximum shear displacement in the simulations. The variability may be due to fracture orientation and distance from the earthquake source, although this was not rigorously investigated. This scaling behavior is non-fractal, unlike the scaling behavior in the literature for primary faults. In general, the regression substantiates the statement that smaller fractures have smaller shear displacements, and that the relation is linear with fracture half-length. This relation cannot be compared to field evidence.

**Table 4-1 Model Boundary Conditions and Material Properties**

| Parameter | Value | Source | Comments |
|---|---|---|---|
| Selection of Class 1 Feature for Earthquake | not applicable | Largest mapped surface lineament in Äspö area, Fig. 3-11, Tirén and others (1987). | Worst-case value corresponding to Magnitude 6.1 Earthquake |
| Earthquake Focal Depth | from 0 to 8 km below surface, occurring over entire fault | Shallower than depth for most destructive earthquakes, Coopersmith (1991), dePolo (1991) | Worst-case value, since closer proximity to repository leads to greater displacements and stresses |
| Earthquake Mechanism | Tectonic, strike-slip | Tirén and others (1987) | Regression equations not substantially different for other mechanisms. |
| Fault Slip | 0.15 m | Estimated from Table 1, assuming strike-slip motion. | Average displacement for a single rupture event. |
| Earthquake Fault Orientation | Strike: 240<br>Dip: 90 | Lineament map, Tirén and others (1987) for strike; dip assumed based on analogy to other faults. | |
| Young's Modulus | 75,000 MPa | Representative value for typical intact rocks found in Sweden (Pusch, 1996) | Use of a purely linear elastic code with a high value of E maximizes stresses and displacements on other fractures and faults for a given earthquake. |
| Repository Distance from Primary Fault | 2 km | | |
| Poisson's Ratio | 0.25 | Representative value for typical intact rocks found in Sweden (Pusch, 1996) | |
| Secondary (lower order) faults and large joints | Current DFN models for Äspö | La Pointe and others (1995) and Follin and Hermansson (1996) | Based on detailed analyses of fracturing at Äspö. |
| Mechanical Properties of Secondary Faults | Frictionless | | Worst-case bound; accounts for pore-pressure reduction of fracture resistance to sliding |

Additional discussion of the mechanical properties of fracture zones in crystalline rock may be found in Appendix B.

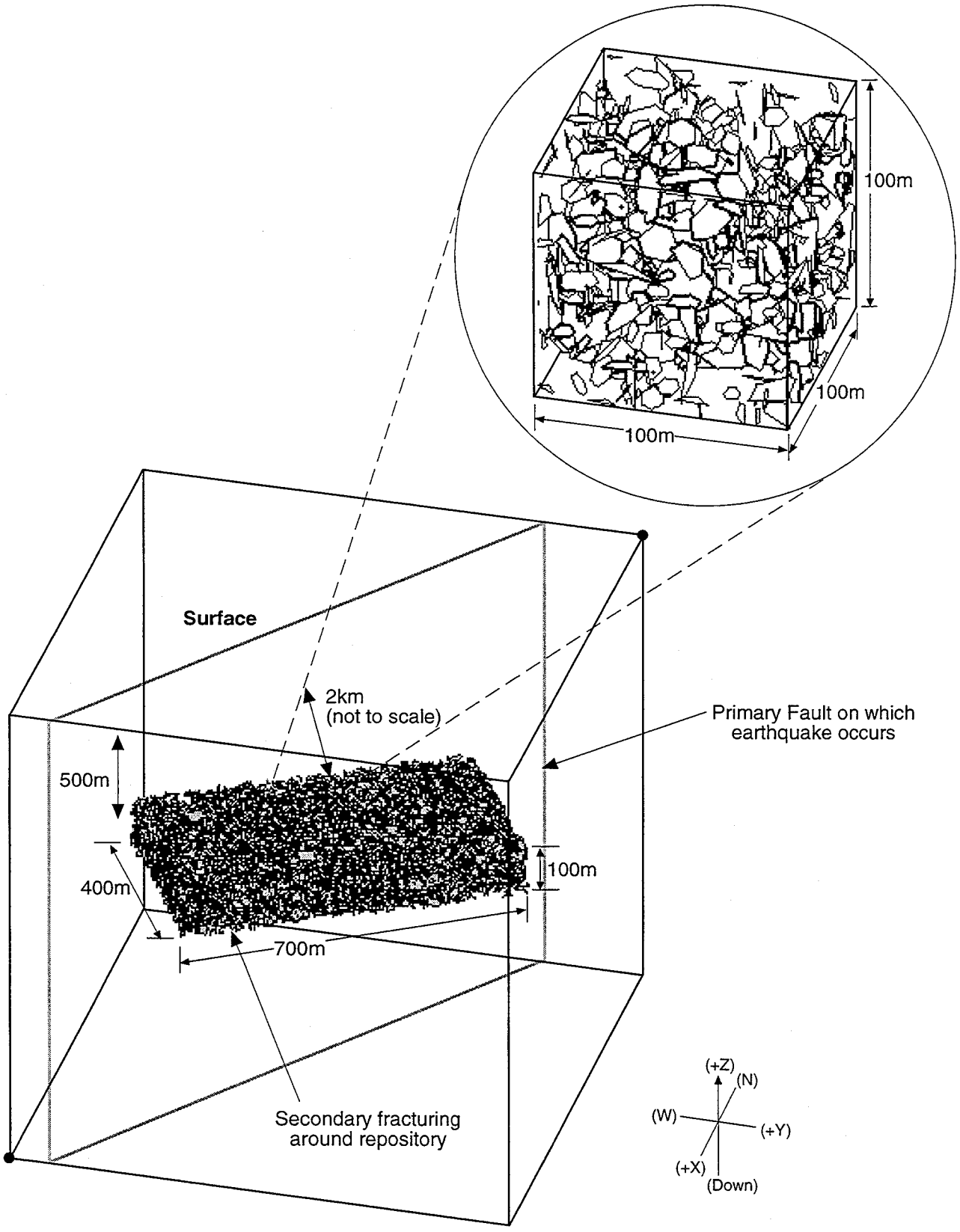


FIGURE **4-2**
**POLY 3-D FRACTURE MODEL**

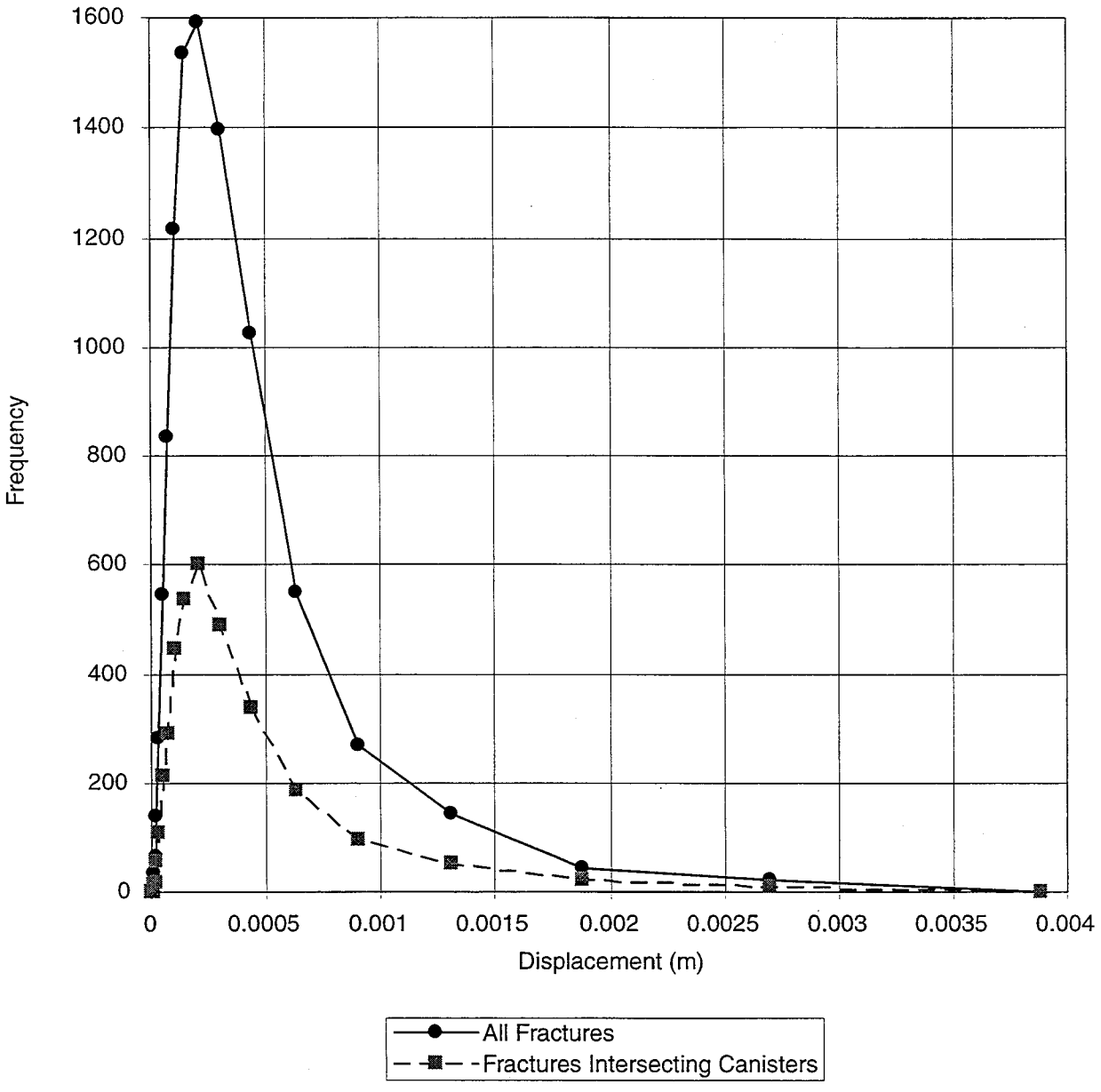


FIGURE **4-3**
**HISTOGRAM OF MAXIMUM SHEAR DISPLACEMENTS**

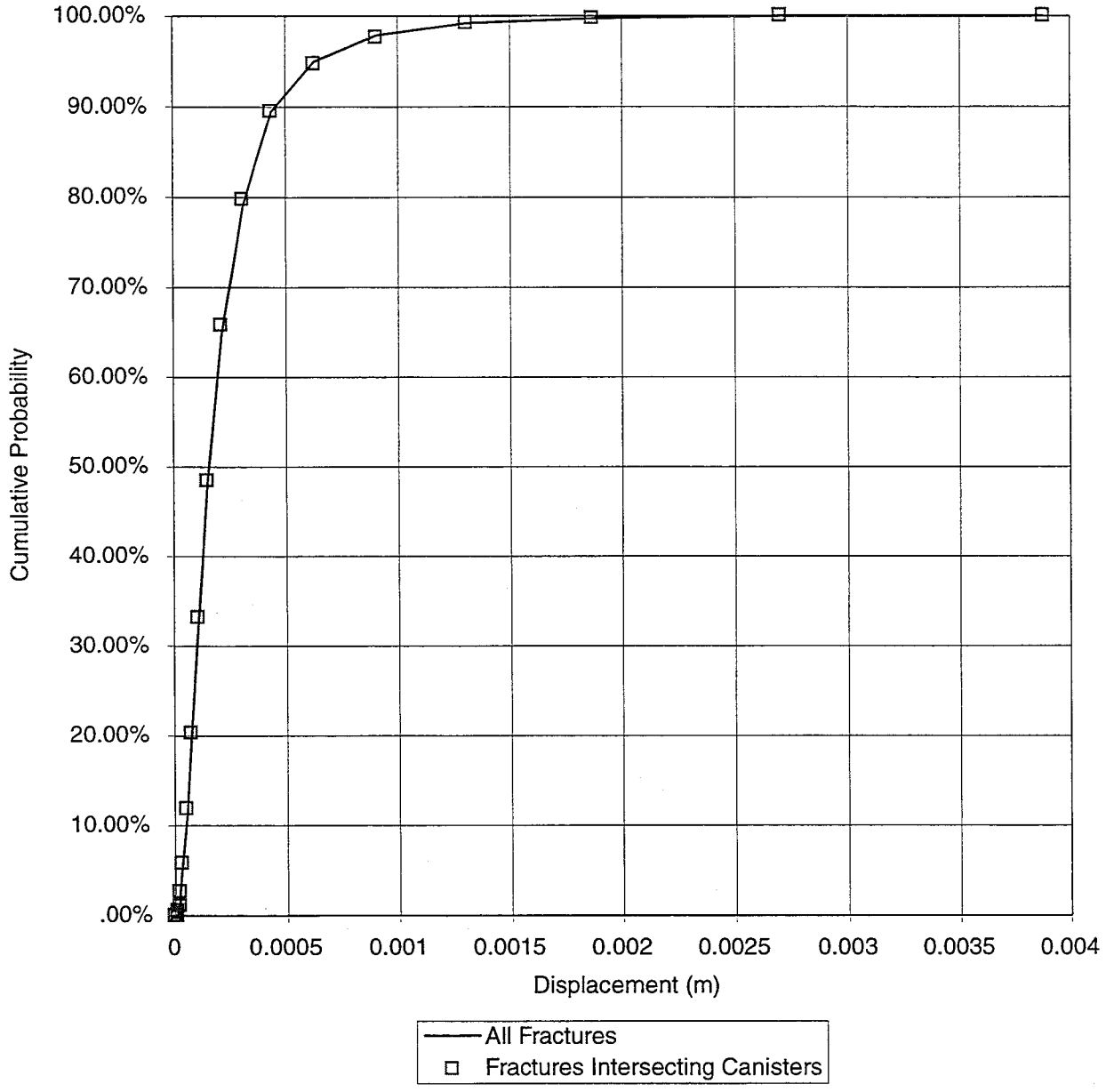


FIGURE **4-4**
**CUMULATIVE PROBABILITY OF MAXIMUM SHEAR DISPLACEMENTS**

There may be several reasons why the scaling appears to be linear rather than fractal. While rock breakage mechanisms, such as those that give rise to earthquakes, have been shown to produce fractal properties under some conditions, the movement induced on secondary faults is not the same process. The reason that the relation appears to be linear may be due to the linearly elastic fracture mechanics assumptions underpinning POLY3D. Pollard and Segall (1987) have shown that the displacements induced at a crack midpoint are a linear function of the stresses applied to the crack and the crack half-length (Equation 4-2).

$$\begin{Bmatrix} U_1 \\ U_2 \\ U_3 \end{Bmatrix} = \begin{Bmatrix} \Delta\sigma_I \\ \Delta\sigma_{II} \\ \dfrac{\Delta\sigma_{III}}{(1-\nu)} \end{Bmatrix} \frac{(1-\nu)\alpha}{\mu} \qquad \text{Equation 4-2}$$

where: $U_i$ is the displacement in local crack coordinates
$\Delta\sigma_i$ are the stress components in the mode$_i$ directions
$\mu$ = shear modules
$\nu$ = Poisson's Ratio
$\alpha$ = crack half-length

Since applied stress may not vary much among the fractures intersecting canisters as they are all approximately 2 km from the earthquake, the calculated displacements would be dominantly a linear function of fracture radius, since the applied stress variability would vary much less.

## 4.3 MAGNITUDE-THRESHOLD DISTANCE ESTIMATES

The second series of simulations was carried out to estimate how far from an earthquake a repository needs to be such that displacements on the fractures near the repository are less than 0.1 m and to illustrate how uncertainty can be incorporated. No specific repository design was assumed in these simulations. Rather, fractures were generated in a box extending from 200 m to 600 m below the surface. The box measured 1.5 km by 1.0 km in horizontal extent. The long dimension was taken to be parallel to the fault on which the earthquake occurred. The dimensions of this box were based upon the typical dimensions of hypothetical repositories.

In order to estimate the threshold distance for 0.1 m displacement, a series of numerical calculations were made for different earthquake magnitudes and different distances from the fault to the repository. For each magnitude, the subsurface rupture length, width and fault displacement were calculated from the equations given in Table 2-3. These values are shown in Table 4-3 below. The displacements are based on mean maximum surface displacement regression relations.

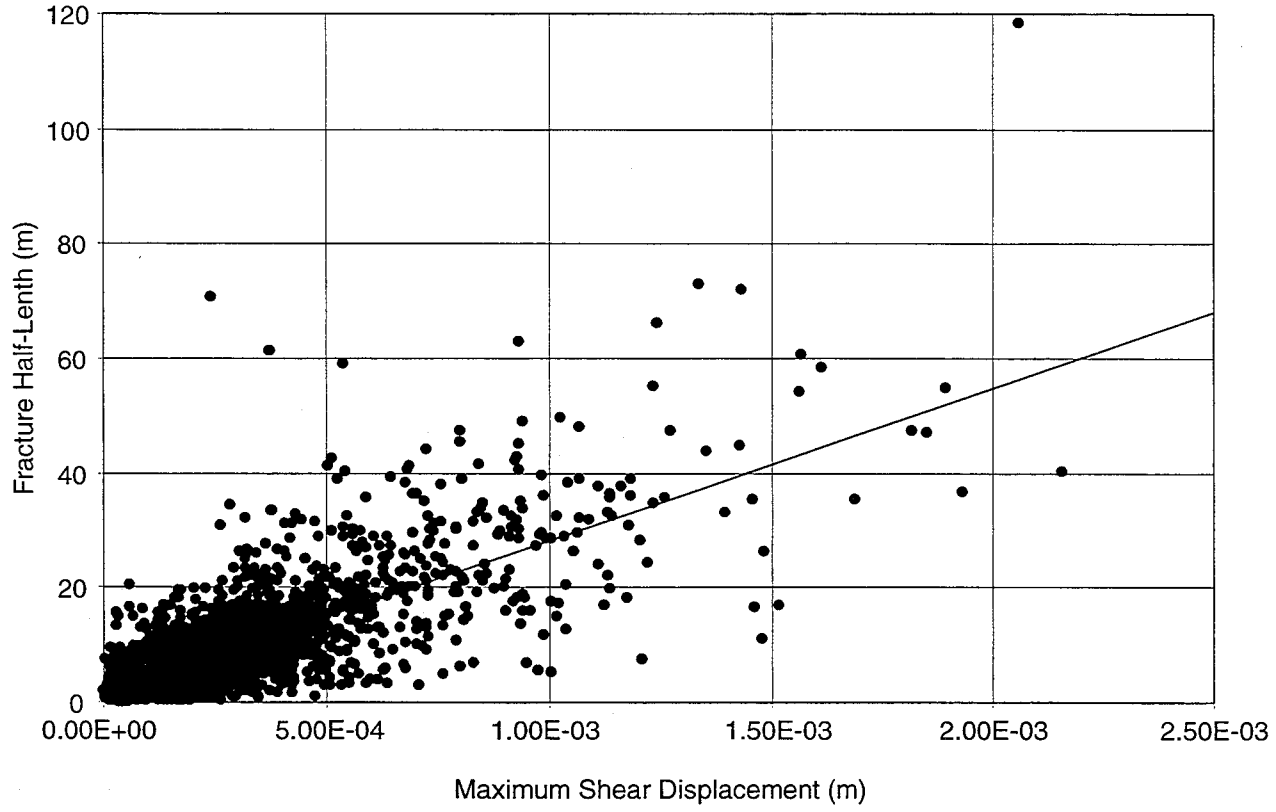


FIGURE **4-5**
**MAXIMUM DISPLACEMENT vs. FRACTURE HALF-LENGTH**

To obtain initial estimates of the threshold distance, simulations were run for each earthquake magnitude for a wide range of different distances. Distance was measured from the edge of the repository to the nearest point on the fault on which the earthquake took place (Figure 4-6). Distances considered in this scoping phase range from 50 m to 20 km. For each distance and magnitude, 10 fracture model realizations were simulated. These simulations focused on the conjectured re-activation of existing faults due to glacial unloading (Arvidsson, 1996). In this model, the stress relief due to the removal of the Fennoscandian ice sheets led to isostatic rebound and reverse-slip re-activation of existing faults.

**Table 4-1 Fault Geometry and Mean Displacements Used for Earthquake Simulations**

| Magnitude | Displacement (meters) | Horizontal Length (kilometers) | Depth (kilometers) |
|---|---|---|---|
| 6.0 | 0.12 | 14.13 | 7.24 |
| 6.5 | 0.34 | 28.84 | 9.89 |
| 7.0 | 0.95 | 58.88 | 13.49 |
| 7.5 | 2.69 | 120.23 | 18.41 |
| 8.0 | 7.59 | 245.47 | 25.12 |
| 8.2 | 11.48 | 326.59 | 28.44 |

Reverse faults are typically of two types: re-activated normal faults or primary low-angle thrust faults. The mechanism postulated by Arvidsson (1996) is that existing steeply-dipping faults were re-activated due to de-glaciation. In the modeling studies reported in this section, the earthquake is assumed to occur along a nearly vertical fault.

In a scenario in which an existing fault that ruptures to the surface is re-activated as a reverse fault, the hanging wall will move upwards at the surface relative to the footwall. The surface of the earth behaves as a boundary free of normal stress. When slippage along a steeply-dipping fault occurs, the ability of the blocks on either side of the fault to move reduces elastic deformation. Such a scenario is modeled as an *infinite half-space*. A more conservative case is to model the earthquake as a dislocation within an *infinite space*. In this case, there is no free surface devoid of normal and shear stress representing the earth's surface. This increases the magnitude of the stress and strain fields in the model in the region near to a hypothetical repository.

While the infinite half-space scenario might seem to be more geologically realistic, as the earth's surface is a boundary free of normal stress, it neglects the dynamic process of earthquake generation. An earthquake which initiates several kilometers below the surface generates a rupture that propagates upwards and outwards from the focal point. This rupture evolves through time. At early times, the rupture is far below the repository. In

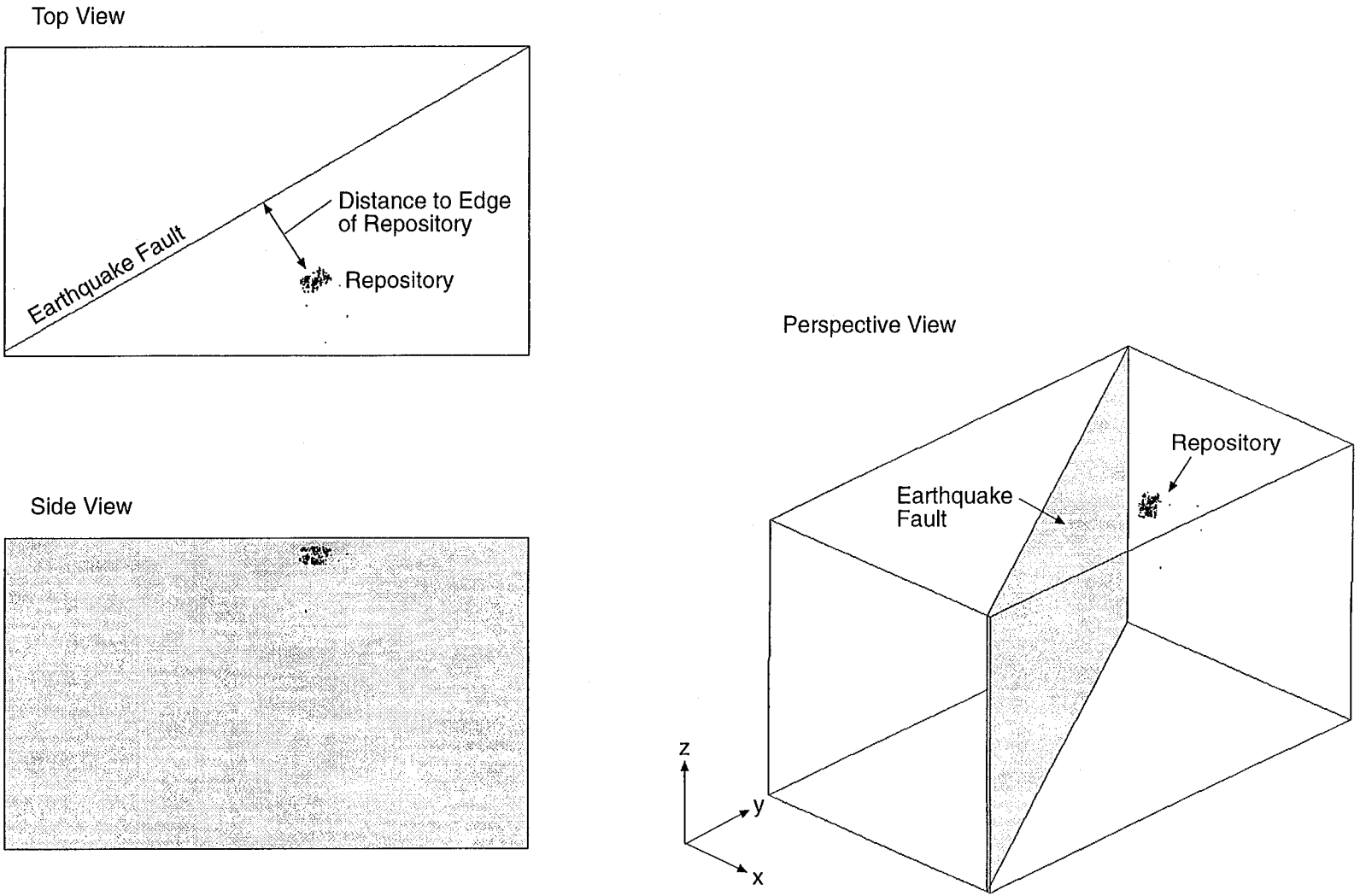


FIGURE **4-6**
**POLY3D MODELING SETUP FOR DISTANCE-DISPLACEMENT SIMULATIONS**

time, the dislocation front propagates upwards. Studies of the stress field generated by a propagating crack show that the maximum shear and normal stresses occur near the crack tip. Thus, in a dynamic situation, the maximum slip induced by the earthquake occurs as the propagating rupture reaches the vicinity of the repository. In order to simulate this effect with a static simulation, a second set of simulations were carried out. In these simulations, the earthquake dislocation front is located a few hundred meters above the depth of the repository. There is no free surface. This approximates the situation where the repository is located near the fracture tip. The results which follow illustrate the possible displacements for the two static approximations to the more realistic geological and dynamic processes.

Figures 4-7 and 4-8 show the mean and maximum displacements induced on fractures as a result of earthquakes of differing magnitudes for the worst-case infinite space scenario. Induced displacements are generally on the order of millimeters to tenths of meters for distances less than 100 m. The maximum induced displacements for the conservative infinite space simulations (Figure 4-7) suggest that an earthquake up to magnitude 8.2 occurring at distances greater than about 1000 meters from the repository will not lead to displacements greater than 0.1 m. Average displacements (Figure 4-8) are approximately one-tenth the maximum displacements. The infinite half-space simulations show smaller induced displacements, as expected. In these simulations, all combinations of earthquake magnitude and repository distance produce displacements less than 0.01 m.

In addition, the displacements appear to scale linearly with slip magnitude on the earthquake fault (Figure 4-9), rather than with the product of slip magnitude and rupture area. The reason for this may be that fault displacements distant from the repository horizon have little effect; thus, the induced displacements are more a function of the average fault slip that occurs during an earthquake than the rupture area of the fault.

## 4.4 INCORPORATION OF UNCERTAINTY

Uncertainty can come from a variety of sources. It is convenient from a computational standpoint to separate uncertainty into *model* or *conceptual* uncertainty and *data* uncertainty. Model uncertainty arises when alternative geological interpretations are consistent with known geology. An example of this is the question of whether to use regression relations for maximum surface displacement as a function of magnitude or subsurface displacement as a function of magnitude for providing conservative model input. The regression predictions predict greater subsurface displacements than maximum surface displacements for smaller earthquakes, while predicting greater maximum surface displacements than subsurface displacements for the largest earthquakes. Thus it is useful to consider *both* types of displacements in assigning boundary conditions to the numerical model. Because the maximum surface displacements were considered in the

previous section, the subsurface displacements are considered in this section in order to incorporate *model* uncertainty.

The other type of uncertainty arises from the data itself. Regression equations are an idealization of the relation between magnitude and displacement. As a result, predictions made using regression relations have a degree of uncertainty. Wells and Coppersmith (1994) quantify this uncertainty by calculating the 95% confidence interval. A similar relation was calculated as part of this study for the regression between magnitude and subsurface displacement, and used as the basis for the Monte Carlo simulations described in the remainder of this chapter.

Due to the time constraints of this project, only ten Monte Carlo realizations were generated for each earthquake magnitude. These realizations are shown in Figure 4-10. For an actual performance assessment calculation, it would be necessary to run at least an order of magnitude more realizations for each earthquake magnitude.

Figures 4-11a-f summarize the induced fault slip as a function of earthquake magnitude and distance. The figures illustrate two trends. First, the variability in maximum fracture offset appears to be a function only of earthquake magnitude, not the distance from the fault on which the earthquake takes place. Secondly, the variability increases with earthquake magnitude. The variability for magnitude 6.0 earthquakes is about a half-order of magnitude. This increases to somewhat over an order of magnitude for magnitude 8.2 earthquakes. These figures suggest that the relation between distance and maximum induced slip is not well-approximated by a simple functional relation, although this may be due to the fact that only ten realizations were used to compute the mean of the results.

Figure 4-12 summarizes the relation between the subsurface slip on the earthquake fault and the maximum induced slip on the repository fractures. This graph shows that the relation is well-characterized by a power law, as in the previous simulations, even after uncertainty has been incorporated.

## 4.5 DISCUSSION OF RESULTS

The results obtained by considering alternative conceptual models for fault boundary conditions, and incorporating data variability by means of regression uncertainty, illustrate how it is possible to provide probabilistic information on the possible slip along fractures intersecting canisters due to an earthquake at a distance from the repository. Considering only the mean values, the numerical simulations show that earthquakes whose slip is based upon the maximum surface displacement are very similar to the simulations based on the subsurface slip. For example, the simulations based on maximum surface slip (Figure 4-7) shows that earthquakes with magnitudes 7.0 or less do not exceed the 0.1 m slip threshold for the distance range

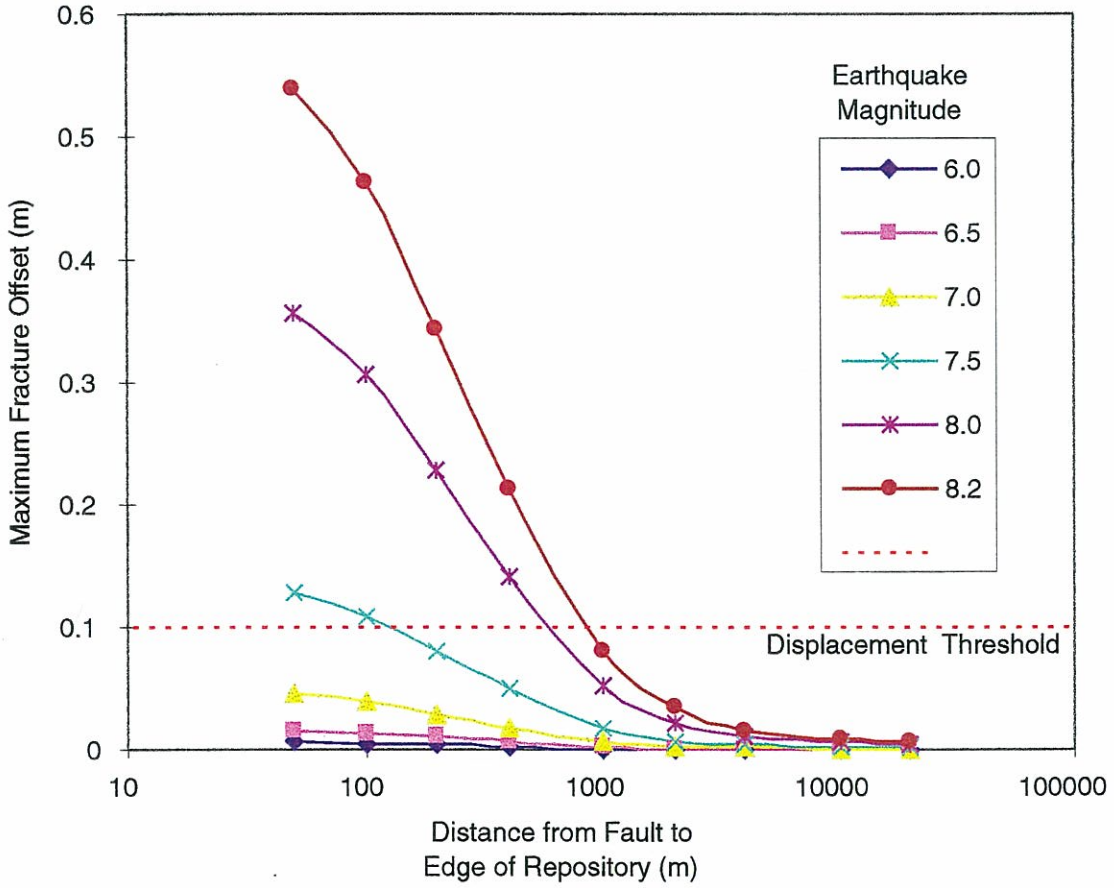


FIGURE **4-7**
**MAXIMUM REPOSITORY FRACTURE OFFSETS RESULTS FROM EARTHQUAKES OF MAG 6.0 TO 8.2**

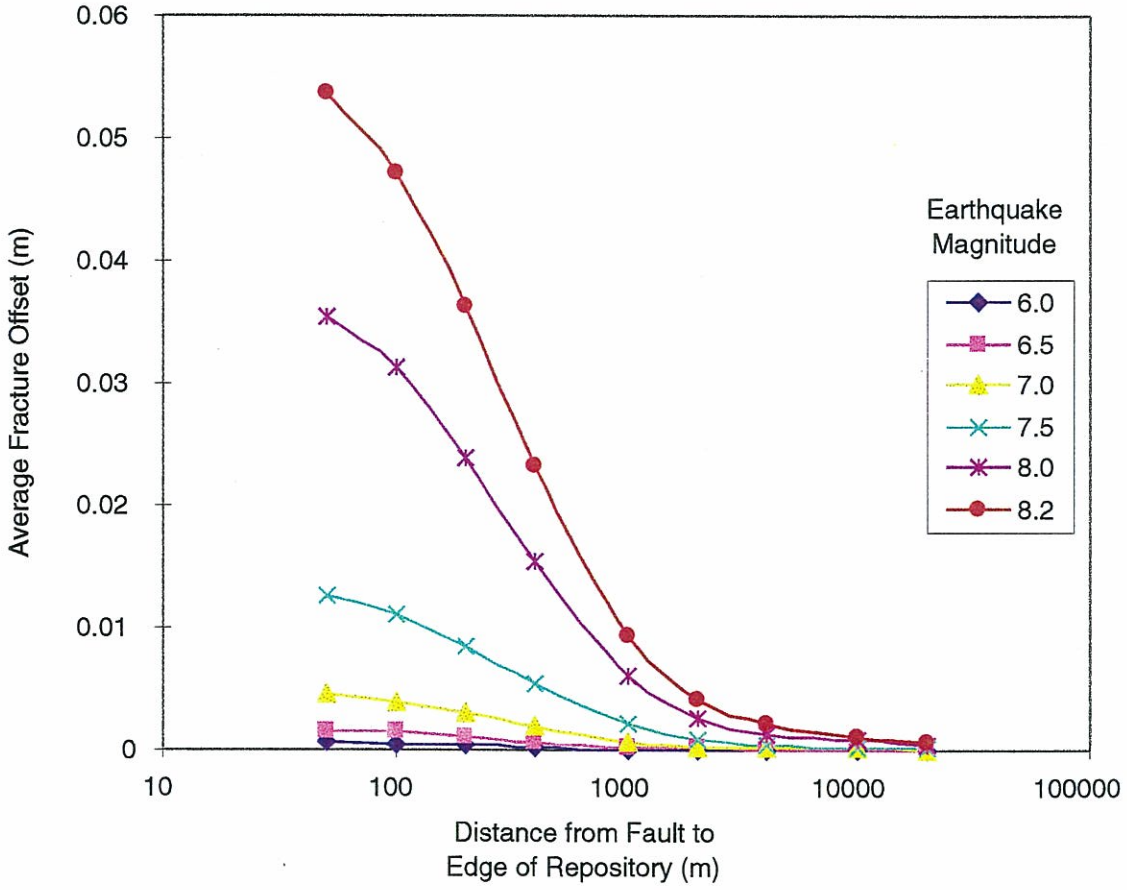


FIGURE **4-8**
**AVERAGE REPOSITORY FRACTURE OFFSETS RESULTING FORM EARTHQUAKES OF MAG 6.0 TO 8.2**

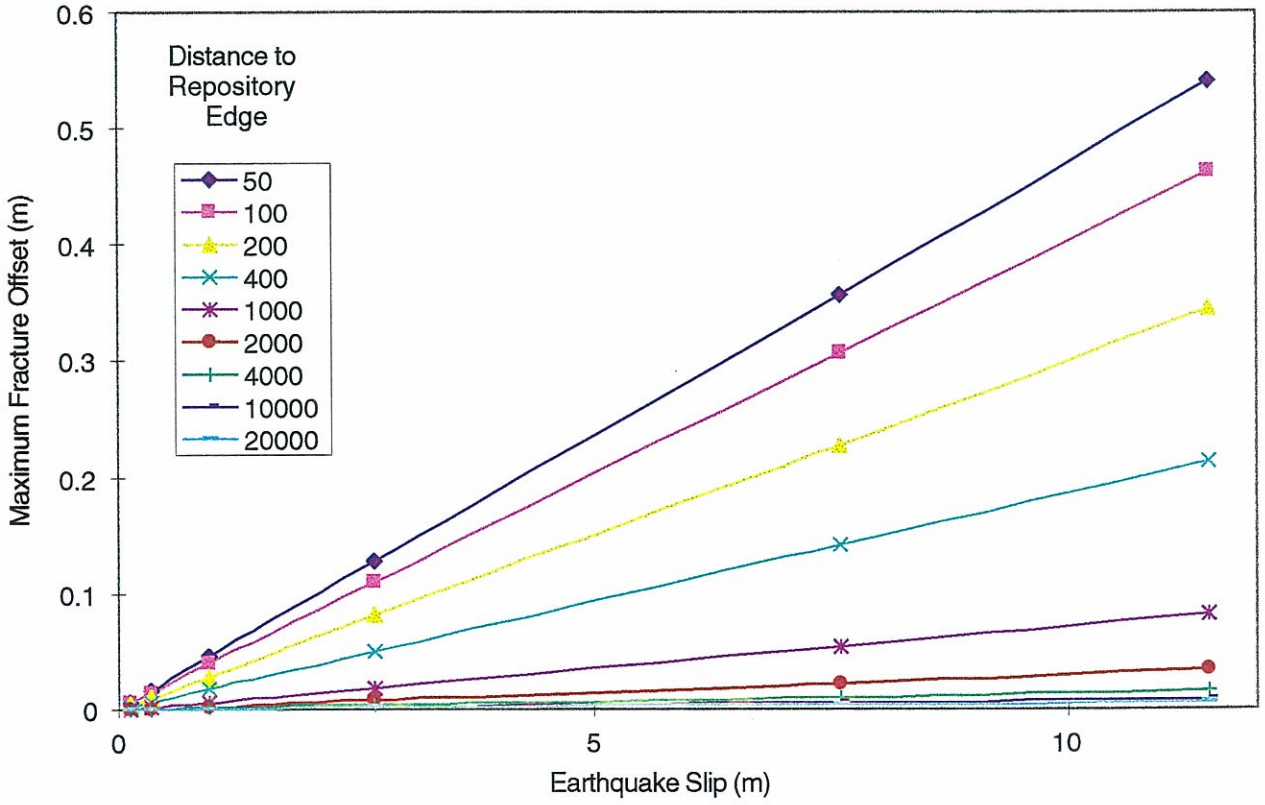


FIGURE **4-9**

**MAXIMUM REPOSITORY FRACTURE OFFSETS RESULTING FROM EARTHQUAKES ON FAULTS 50 TO 20,000m FROM THE EDGE OF THE REPOSITORY**

considered. A magnitude 7.5 event at a distance of slightly greater than 100 m exceeds the 0.1 m threshold. Figures 4-11a-c also show that the mean displacement for models based on the subsurface slip is less than 0.1 m, although the slip magnitudes are somewhat greater, as expected. Figure 4-11d shows that a magnitude 7.5 earthquake exceeds the threshold at about 100 m. For a magnitude 8.2 earthquake, Figure 4-11f shows that the threshold is exceeded at a distance of 900 m, while Figure 4-7 shows a similar result. Thus, the results suggest that both conceptual models lead to similar conclusions regarding how close a repository can be located to an earthquake using the 0.1 m threshold.

The simulations summarized in Figure 4-11 contain additional information that can be used to calculate the probability that an earthquake located a particular distance from the repository will produce unacceptable displacements. The results show that magnitude 7.0 earthquakes could produce displacements greater than 0.1 m within 300 m of the repository. For magnitude 8.2 earthquakes (Figure 4-11f), unacceptable displacements may occur for earthquakes closer than 3 km. Such probabilistic information can be used as part of performance assessment calculations, or to aid in the development of site selection criteria.

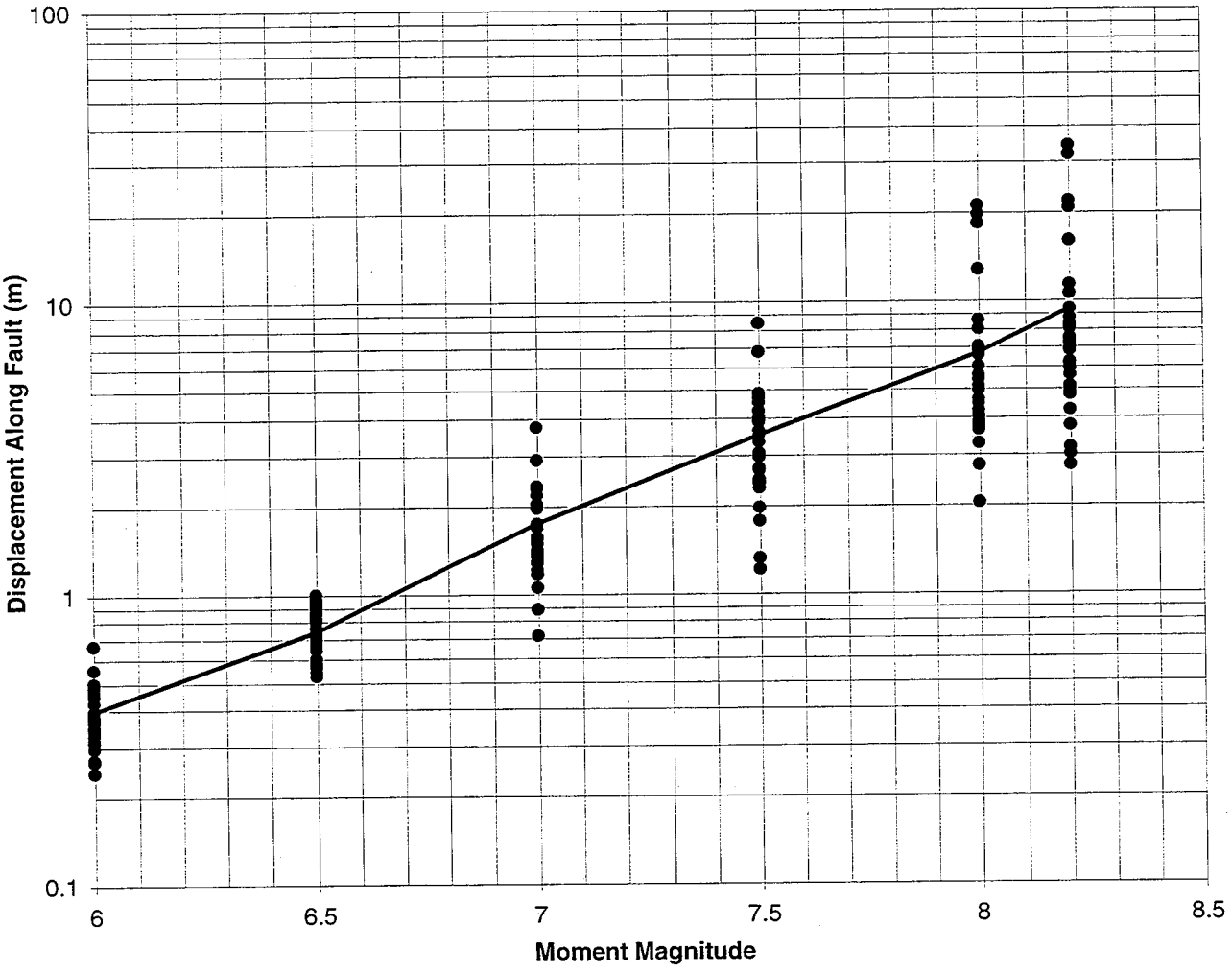


FIGURE **4-10**
**MONTE CARLO ASSIGNMENT OF FAULT SLIPPAGE**

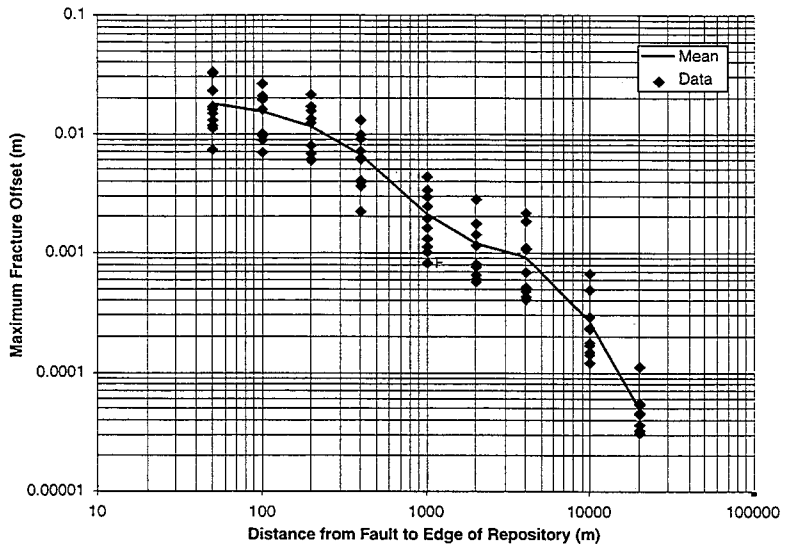


a) Magnitude 6.0

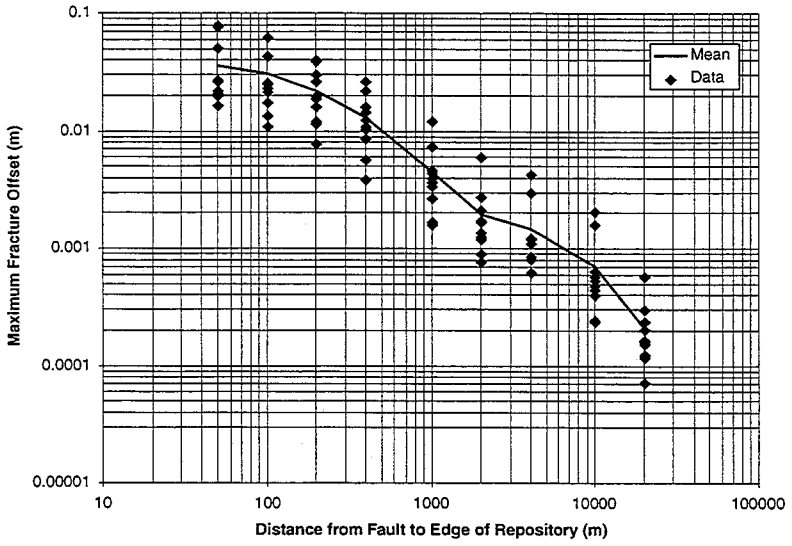


b) Magnitude 6.5

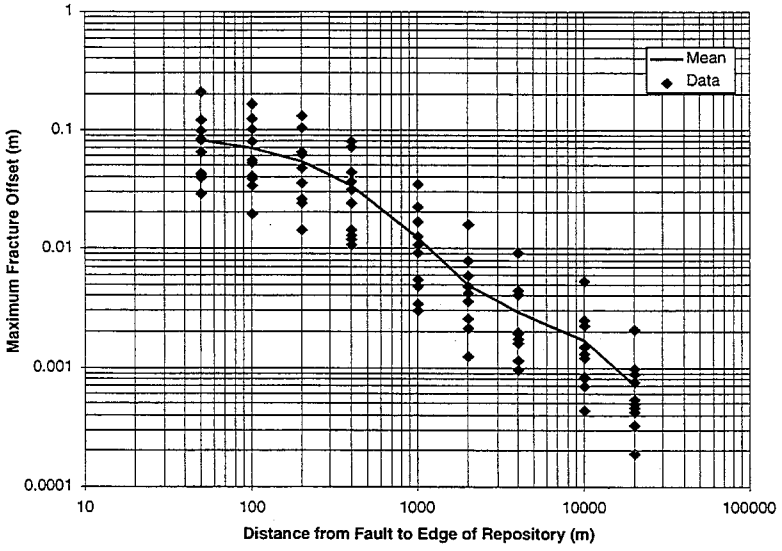


c) Magnitude 7.0

FIGURE **4-11**

**MAXIMUM INDUCED DISPLACEMENTS AS A FUNCTION OF DISTANCE TO REPOSITORY EDGE**

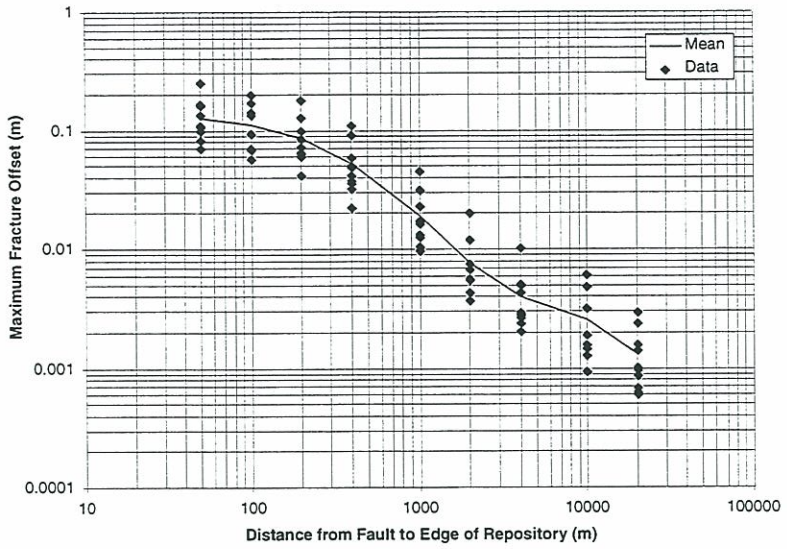


d) Magnitude 7.5

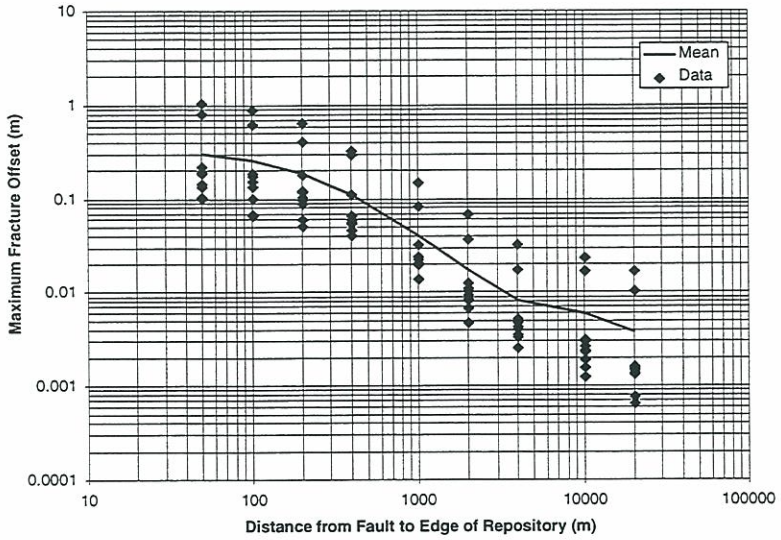


b) Magnitude 8.0

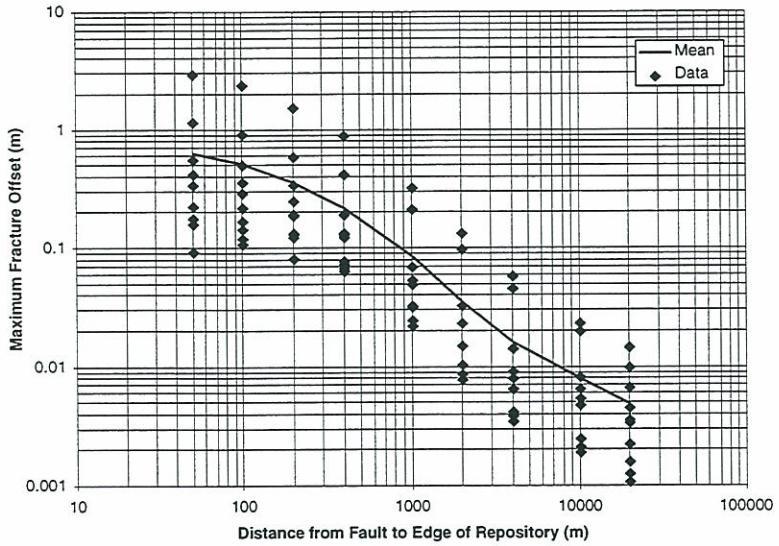


c) Magnitude 8.2

FIGURE **4-11** (cont.)
**MAXIMUM INDUCED DISPLACEMENTS AS A FUNCTION OF DISTANCE TO REPOSITORY EDGE**

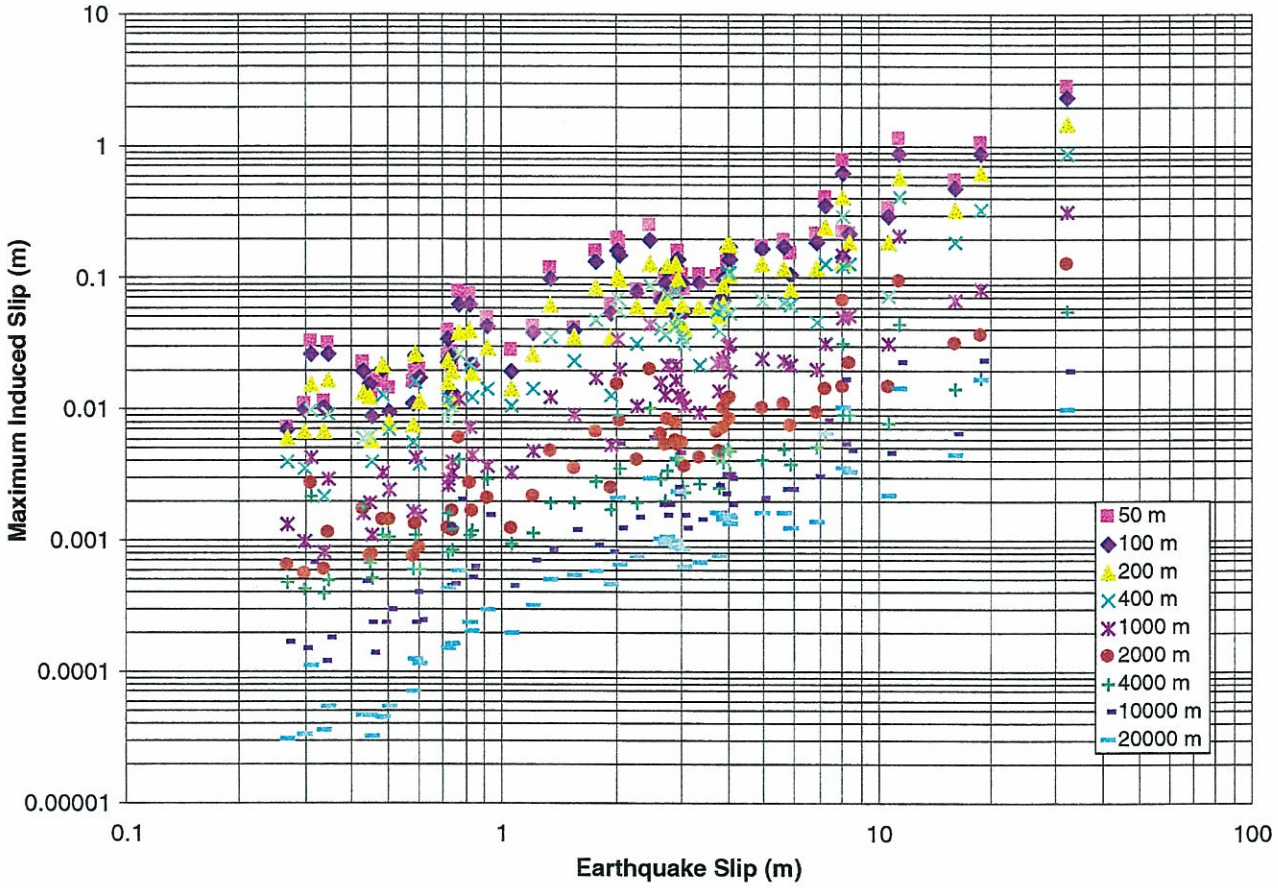


FIGURE **4-12**
**MAXIMUM REPOSITORY FRACTURE OFFSETS RESULTING FOM OFFSETS ON FAULTS 50 TO 20,000 M FROM THE EDGE OF THE REPOSITORY**

# 5. CONCLUSIONS AND DISCUSSION

1. **Development of Methodology:** A conservative method has been devised and applied to a generic site based on Äspö and the seismology of Sweden. The study demonstrates how the method could be applied to a selected site. It also shows how probabilistic information on displacements along fractures intersecting canister holes induced by an earthquake can be calculated for performance assessment or decision analysis calculations.

2. **Conservativeness of Modeling Approach:** This study demonstrates a method that can be applied to reconnaissance of potential sites for high level nuclear waste repositories in Sweden. It provides conservative information on the shear displacements due to earthquake-related fault movements.

3. **Potential Damages to Underground Openings:** There are two scenarios for earthquake disruption of canisters in a repository after repository closure: direct fault movement due to an earthquake along a seismogenic fault that intersects a repository; and displacements induced on fractures due to a direct earthquake. Published studies of earthquake damage to subsurface openings substantiate the numerical results, and imply that damage to a repository or its components should be negligible unless the earthquake takes place along a fault that directly intersects or is very close to a repository.

4. **Scaling Behavior:** Published literature concludes that for earthquakes smaller than about magnitude 6, data collection for some key earthquake parameters is problematic, making it difficult to determine how shear displacement or stress scales with fault size or other fault parameters. Analysis of larger earthquakes establishes log-log and log-linear regression relations which may not be appropriate for extrapolation to smaller earthquakes. Linearly elastic fracture mechanics produces results consistent with the regression relations to the extent that the smaller the fracture, the smaller the expected shear displacement due to a distant earthquake. The analysis does not clarify how primary earthquakes scale with size parameters for earthquakes much smaller than magnitude 6.

5. **Recurrence Rate Issues:** Published studies that have examined the relation between fault length (or size) and total displacement cannot be used for assessing maximum displacements within the repository without knowing the time period or recurrence rates over which the total measured displacements have occurred, and whether the observed net slip approximates the cumulative slip.

6. **Modeling Results - Äspö Generic Example:** Results for an individual earthquake that is greater than substantiated by the historical record in Sweden suggest that shear displacements affecting a canister or its immediate environment should be on the order of millimeters, due to a distant earthquake. The mean displacement of something less than 1 mm implies that at least 100 such magnitude 6.1 ruptures would be required over the regulatory period to produce 0.1 m of total slip. Without knowing the recurrence rate for earthquakes of this size in the vicinity of a proposed repository, it is not possible to assess performance.

7. **Modeling Results - Distance/Magnitude Simulations:** Simulations of re-activated, near-vertical faults show that maximum displacements induced on existing joints and faults is on the order of millimeters to tenths of meters for earthquakes ranging in magnitude from 6.0 to 8.2 for distances of 50 m to 20 km.

8. **Simplifying Assumptions:** The current study has made several simplifying assumptions. The calculated displacements assume that the rock mass behaves as a linearly elastic, brittle material. Secondary faults are frictionless. These are considered to be conservative assumptions. Likewise, stress concentration effects around the canister holes or repository were neglected. The maximum credible earthquake was based upon fault traces inferred from lineament maps for southern Sweden. The study did not consider more distant, larger earthquakes outside the boundaries of Sweden (Camelbeeck and Meghraoui, 1996). However, literature describing subsurface effects of great (> 8) earthquakes, such as in Alaska, suggest that these distant events would have little impact on a subsurface facility hundreds of kilometers away.

9. **Limitations:** There are several limitations in the use of the results from this study. First, the study did not address hydrological effects of earthquakes on the repository performance, nor did it consider damage to the drifts or shafts. More importantly, the calculated displacements were for a single rupture event, not a series of ruptures that could take place over the regulatory time frame for the repository. The study did not address a seismic creep due to glacial rebound.

Acknowledgments:

Ian Kluckow and Donald West contributed to the literature review and made contact with seismic hazard experts to obtain information included in this report. Don West also provided critical review of the content of this report. This project was carried out under the direction of Lars O. Ericsson, SKB, whose support is gratefully acknowledged.

# 6. REFERENCES

Arvidsson, R. (1996). Fennoscandian earthquakes: whole crustal rupturing related to postglacial rebound. Science, Vol. 274, 744-746.

Barton, N. (1990). Scale effects or sampling bias? 1st Workshop on Scale Effects in Rock Masses, Loen, Norway, Balkems, Rotterdam, pp. 31-55.

Barton, N. and H. Hansteen. (1979). Very large span openings at shallow depth: deformation magnitudes from jointed models and finite element analysis. Proceedings of the 4th Rapid Excavation and Tunneling Conference, Atlanta, Georgia. 1979. 1331-1353.

Camelbeeck, T. and M. Meghraoui. (1996). Large earthquakes in Northern Europe more likely than once thought. *Eos*, 77(42), 405,409.

Comninou, M. A. and J. Dunders (1975). The angular dislocation in a half-space. J. Elasticity, Vol. 5, 203-216.

Coppersmith, K. J. 1991. Seismic source characterization for engineering seismic hazard analysis, in proc. 4th International Conference on Seismic Zonation, Vol. I, Earthquake Engineering Research Institute, Oakland, California, 3-60.

Coppersmith, K. J. and R. R. Youngs. (1992). Modeling fault rupture hazard for the proposed repository at Yucca Mountain, Nevada. High Level Radioactive Waste Management, Las Vegas, Nevada. April, 1992, 1142-1150.

Crouch, S. L. and A. M. Starfield. (1983). Boundary Element Methods in Solid Mechanics. George Allen & Unwin, Ltd. London. 322p.

Darragh, R. B. and B. A. Bolt. (1987). A comment on the statistical regression relation between earthquake magnitude and fault rupture length. Bulletin of the Seismic Society of America, vol. 77, 1479-1484.

de Palo, et al. (1991). Historical surface faulting in the Basin and Range province, western North America: implications for fault segmentation, J. Struct. Geol. 18, 123-136.

Dershowitz, W. S. and others. (1996). Canister and Far-Field Demonstration of the Discrete Fracture Analysis Approach for Performance Assessment. Report to SKB from Golder Associates, October 1996.

Dowding, C. H., M. ASCE and A. Rozen. (1978). Damage to rock tunnels from earthquake shaking. *Journal of the Geotechnical Engineering Division.* 175-191.

Follin, S. and J. Hermansson. (1996). A discrete fracture network model of the Äspö TBM tunnel rock mass. Report to SKB from Golder Associates AB, Stockholm. June 1996.

Hanks, T. C. and H. Kanamori (1979). A moment-magnitude scale. J. Geophys. Res., Vol. 84, 2348-2350.

Islam, Q., P. La Pointe & M. Withjack. (1991). Experimental and numerical models of basement-detached normal faults [abstr.]: AAPG Bulletin, Vol. 75, p. 600.

Jeyakumaran, M., J. W. Rudnicki and L. M. Keer (1992). Modeling slip zones with triangular dislocation elements. Seismological Soc. America Bull., Vol. 82, 2153-2169.

Johnston, A. C. (1996). A wave in the earth. Science, Vol. 274, p. 735.

Kana, D. D. and others. (1991). Critical assessment of seismic and geomechanics literature related to a high-level nuclear waste underground repository, *U. S. Nuclear Regulatory Commission technical report*, June 1991.

Knuepfer, P. L. K. (1989). Implications of the characteristics of end-points of historical surface fault ruptures for the nature of fault segmentation. Fault Segmentation and Controls of Rupture Initiation and Termination, Palm Springs, California. 1989, 193-228.

La Pointe, P. R., P. C. Wallmann and S. Follin. (1995). Estimation of effective block conductivities based on discrete network analyses using data from the Äspö site. *SKB Technical Report 95-15*, September 1995.

Leijon, B. (1993). Mechanical properties of fracture zones, SKB TR 93-19, Swedish Nuclear Fuel and Waste Management Company, Stockholm.

Lenhardt, W. A. (1988). Damage studies at a deep level African gold mine. Proceedings of the 2nd International Symposium on Rockbursts and Seismicity in Mines, Minneapolis, Minnesota. 1988. 391-393.

McClure, C. R. (1981). Damage to underground structures during earthquakes. Proceedings on Seismic Performance of Underground Structures, Augusta, Georgia. 1981.

McGarr, A., S. M. Spottiswoode and N. C. Gay. (1979). Observations relevant to seismic driving stress, stress drop and efficiency. Journal of Geophysical Research, 84(B5), 2251-2261.

McGarr, A., R. W. E. Green, S. M. Spottiswoode. (1981). Strong ground motion of mine tremors; some implications for near-source ground motion parameters. Bulletin of the Seismological Society of America, vol. 71, no. 1, 295-319. 1981.

Muir-Wood, R. (1993). A review of the seismotectonics of Sweden. *SKB Technical Report 93-13*, April, 1993.

Nisca, D. H. & C.-A. Triumf. (1989). Detailed geomagnetic and geoelectric mapping of Äspö, SKB HRL PR 25-89-01.

Nur, A. (1974). Tectonophysics: The study of relations between deformation and forces in the Earth, 3rd Int. Congr. Int. Soc. Rock Mech., Denver, Vol. 1A, pp. 243-317.

Pollard, D. D. and P. Segall. (1987). Theoretical displacements and stresses near fractures in rock: with applications to faults, joints, veins, dikes, and solution surfaces, *Fracture Mechanics of Rock.* Academic Press Inc. Ltd., London, 1987.

Pratt, H. R., W. A. Hustrulid and D. E. Stephenson. (1978). Earthquake damage to underground facilities, *U. S. Department of Energy report* DP-1513, UC-13, November 1978.

Pusch, R. (1996). JADE, Jämförelse av bergmekaniska funktionssätt hos KBS3-V, KBS3-H och MLH, draft report.

Raney, R. G. (1988). Reported effects of selected earthquakes in the western North American intermontane region, 1852-1983, on underground workings and local and regional hydrology: a summary, *U. S. Dept. of Interior, Bureau of Mines, Division of Waste Management report*, April 1988.

Rhén, I., G. Gustafson, R. Stanfors and P. Wikberg (1996). Geoscientific evaluation 1996/5 - Models based on site characterization 1986-1995. *SKB Report,* October 1996, in press.

Robertson, E.C. (1987). Fault breccia, displacement, and rock type, Proc. 28th US Symp. Rock Mech., Tucson, Arizona, 29 June - 1 July, Balkema, Roterdam, pp. 65-72.

Schwartz, D.P. and K.J. Coppersmith. (1986). Seismic hazards--new trends in analysis using geologic data, in Active Tectonics, National Academy Press, Washington, D.C., 215-230.

SKBF/KBS. (1983). Final Storage of Spent Nuclear Fuel - KBS-3, Volume 2, Geology, Swedish Nuclear Fuel and Waste Management Company, Stockholm.

Slunga, R.S. (1991). The Baltic Shield Earthquakes Tectonophysics, vol. 89, 323-331.

Slunga, R. and L. Nordgren (1987). Earthquake Measurements in Southern Sweden, Oct 1, 1986 - Mar 31, 1987. SKB Technical Report 87-27, December, 1987.

Slemmons, D. B., P. Bodin and X. Zang. (1989). Determination of earthquake size from surface faulting events. Proceedings of the International Seminar on Seismic Zonation, Guangzhou, China, State Seismological Bureau, Beijing, 13.

Stanfors, R. and L. O. Ericsson (1993). Post-glacial faulting in the Lansjärv area, northern Sweden. Comments from the expert group on a field visit at the Molberget post-glacial fault area, 1991. *SKB Technical Report 93-11*, May, 1993.

Stephansson, O. and others. (1978). Deformation of a jointed rock mass. *Geologiska Föreningens; Stockholm Fördandlingar*, vol. 100, 287-294.

Tannant, D.T. (1990). Hydraulic response of a fracture zone to excavation-induced shear, Doctoral thesis, Dept. of Civ. Eng., University of Alberta, Alberta, Canada, 189 pp.

Thomas, A. L. (1993). Poly3D: A three-dimensional polygonal element displacement discontinuity boundary element computer program with applications to fractures, faults and cavities in the earth's crust. M. S. thesis, Stanford University, Stanford, CA, 221p.

Thomas, A. L. & D. D. Pollard. (1993). The geometry of echelon fractures in rock: implications from laboratory and numerical experiments. J. Structural Geol., Vol. 15, Nos. 3-5, 323-334.

Thorson, R.M. (1996). Earthquake Recurrence and Glacial Loading in Western Washington. Bull. Geol. Soc. America, 108(9), 1182-1191.

Tirén, S. A. & M. Beckholmen. (1988). Structural analysis of contoured maps Äspö, Ävrö and Simpevarv area, *SKB HRL PR 25-87-22*, January 1988.

Tirén, S. A., M. Beckholme and H. Isaksson. (1987). Structural analysis of digital terrain models, Simpevarv area, South-eastern Sweden, SKB HRL PR 25-87-21.

Turcotte, D. L. (1992). Fractals and chaos in geology and geophysics. Cambridge University Press, Great Britain, 1992.

Voegele, M. D. (1993). Photogeologic reconnaissance of X-tunnel at Little Skull Mountain. High Level Radioactive Waste Management, Las Vegas, Nevada. April, 1993, 182-187.

Wagner, H. (1984). Support requirements for rockburst conditions. Rockbursts and Seismcity in Mines. South African Institute of Mining and Metallurgy, Johannesburg, South Africa, 1984, 209-218.

Walsh, J. J. and J. Watterson. (1987). Distributions of cumulative displacement and seismic slip on a single normal fault surface. *Journal of Structural Geology*, 9(8), 1039-1046.

Walsh, J. J. and J. Watterson. (1989). Displacement gradients on fault surfaces. *Journal of Structural Geology*, 11(3), 307-316.

Walsh, J. J. and J. Watterson. (1992). Populations of faults and fault displacements and their effects on estimates of fault-related regional extension. *Journal of Structural Geology*, 14(6), 701-712.

Watterson, J. (1986). Fault dimensions, displacements and growth. Pure & Appl. Geophys. 124, 365-373.

Wells, D. L. and K. J. Coppersmith. (1994). New empirical relationships among magnitude, rupture length, rupture width, rupture area, and surface displacement. *Bulletin of the Seismological Society of America*, 84(4), 974-1002.

Withjack, M. O., Q. T. Islam & P. R. La Pointe. (1995). Normal faults and their hanging-wall deformation: an experimental study. AAPG Bulletin, Vol. 79, No. 1, 1-18.

# APPENDIX A
# VERIFICATION

*Verification Test Case 1*

Test Case 1 is a comparison of the POLY3D results to an analytical solution for a two-dimensional line displacement in an infinite medium, as given in Crouch and Starfield (1983). The parameters for this solution are:

- Line segment: Length, 2
- Opening displacement = 0.1 ($D_y$ = -0.1)
- $D_x$ = 0.0
- Poisson's ratio = 0.25
- *POLY3D* dislocation element extends from -50 to +50 out of plane ("z" direction in figure) so that a plane strain assumption is valid at the element centroid.

[NOTE: The lengths used in these are unitless. If the length is 1 meter then the opening displacement and the resulting displacement are fractions of a meter. However, the results are scale independent and could equally as well be kilometers or microns. This only applies to displacements. For stresses, the length scale units must be consistent with the shear modulus.]

Figures A-1a-d show the comparison between the results obtained from POLY3D and the analytical solutions. The lines in the figures show different observation lines where displacements were calculated and compared to analytic solutions. In these plots, the analytical solutions are shown as lines, while the POLY3D calculations are shown by symbols. The following four comparisons were made:

- Displacement in x for the constant Y observation lines (Figure A-1a)
- Displacement in y for the constant Y observation lines (Figure A-1b)
- Displacement in x for the constant X observation lines (Figure A-1c)
- Displacement in y for the constant X observation lines (Figure A-1d)

In all of the four test cases, the displacement calculated by POLY3D plot almost exactly on the corresponding line for the analytical solution. This demonstrates excellent agreement between POLY3D and an analytical test case.

*Verification Test Case 2*

The second test case consists of two fractures, one horizontal and one vertical, that intersect in an infinite medium. The boundary conditions used are:

- Dislocations: Vertical fracture vertices: (0, -1, -1), (0, 1, -1), (0, 1, -2), & (0, -1, -2)
- Horizontal fracture vertices: (-1, -1, -1.25), (-1, 1, -1.25), (1, 1, -1.25), & (1, -1, -1.25)

- Additional vertices for "Meshed" case: (0, -1, -1.25), & (0, 1, -1.25)

This test case does not have an analytical solution. However, it verifies that POLY3D computes the displacements correctly for two intersecting fractures. The verification consists of comparing the displacements for the two fractures with the displacements obtained by superimposing solutions for reach fracture separately. In addition, a case was run in which each of the fractures was subdivided or "meshed" to see whether treating fractures as single elements produces numerical error.

There were four simulations carried out:

1. No Meshing – Two elements with no common vertices; fractures intersect without an edge defining the intersection in the simulation.
2. Meshing – Four elements; each element shares the two "additional" vertices with the other three elements. The line of fracture intersection is an edge in each element.
3. Vertical – Only the Vertical fracture
4. Horizontal – Only the Horizontal fracture

Results from Cases 3 and 4 are combined to compare with Cases 1 and 2 for verification. Successful verification consists of demonstrating that the summed displacements for Cases 3 and 4 match Case 1 and Case 2.

Figure A-2 shows x and z displacements for an observation line located along the x-axis from x=-10 to x=10:

- x displacement ($u_x$) for each case (Figure A-2a)
- z displacement ($u_z$) for each case (Figure A-2b)

Figures A-2a, b show that the POLY3D results compare very well. Cases 1, 2, and (3+4) are all essentially equal. The individual horizontal and vertical components are also plotted.

These simple test cases show that POLY3D correctly calculates the displacements on fractures in 3D.

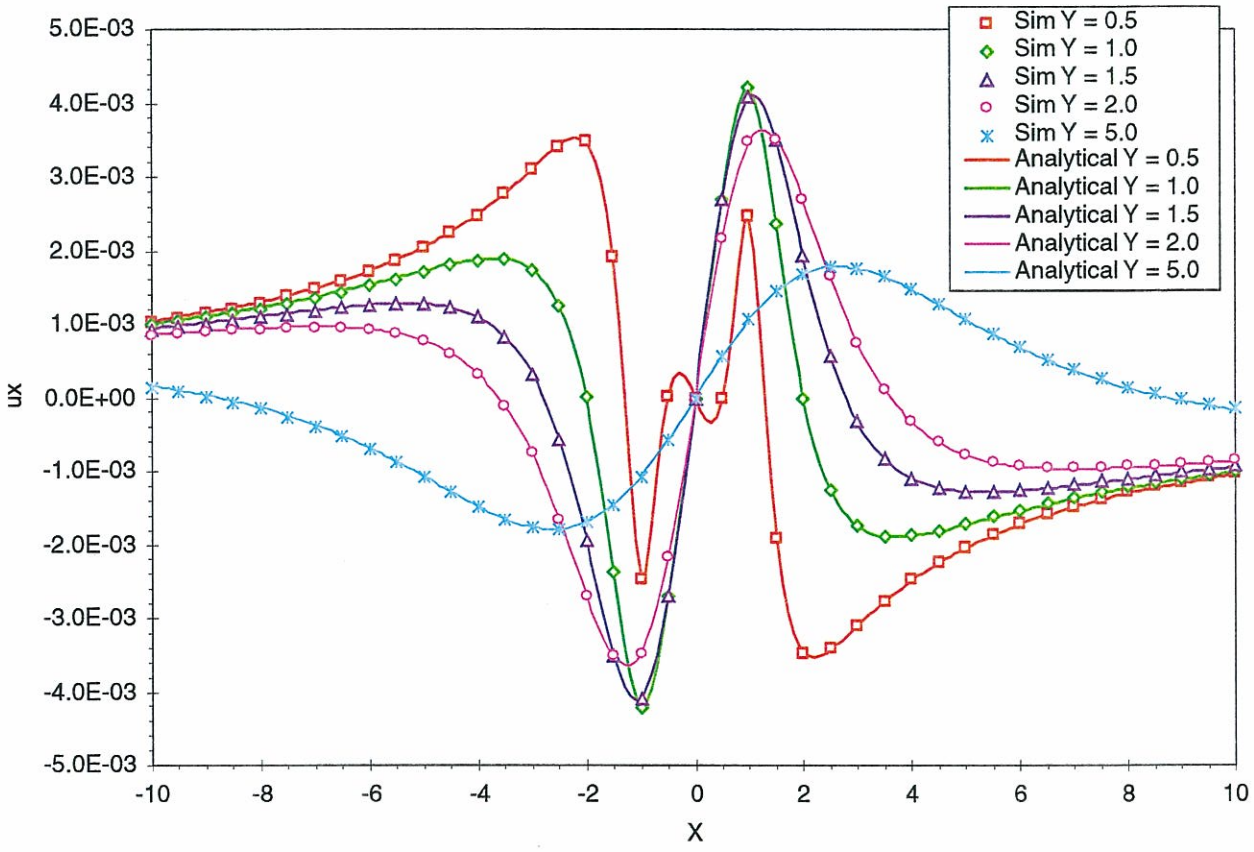


FIGURE **A-1a**
**COMPARISON - Ux(Y)**

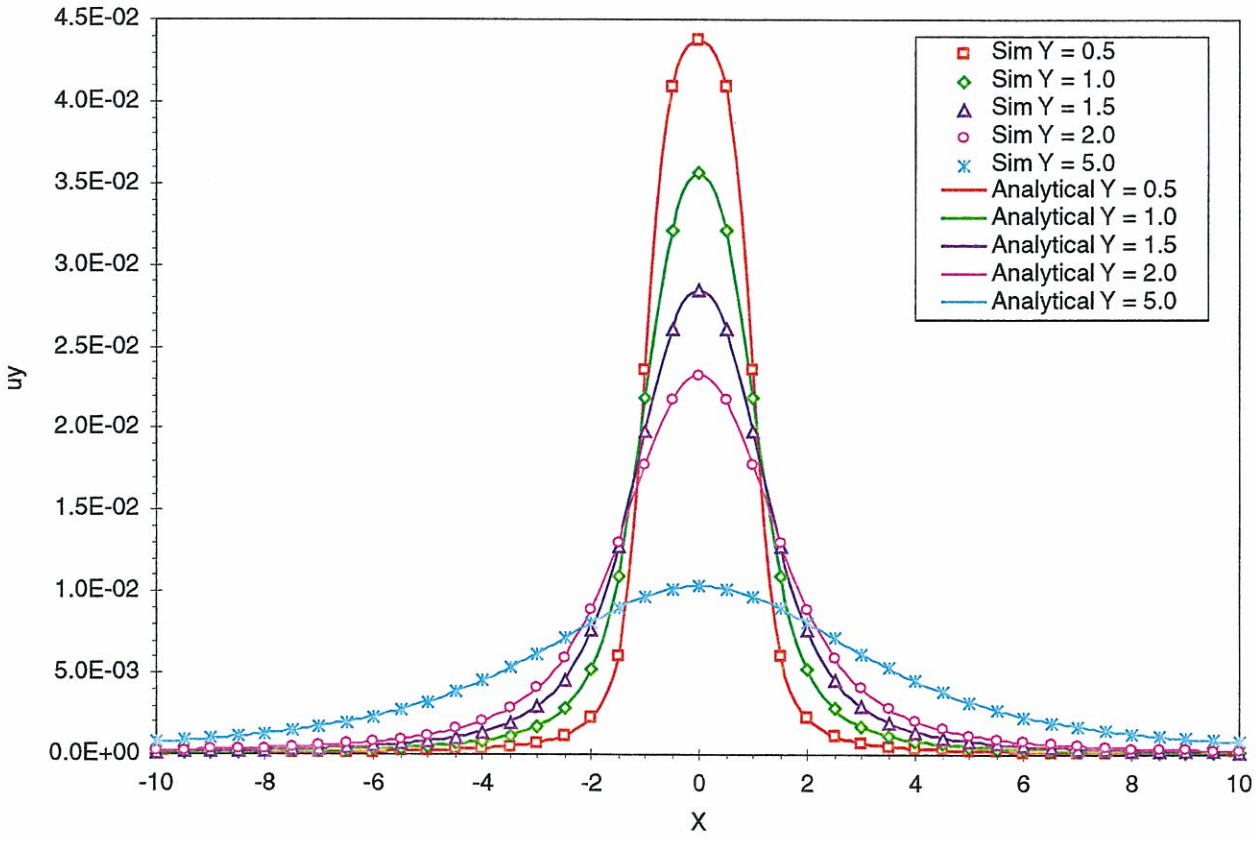


FIGURE **A-1b**
**COMPARISON - Uy(Y)**

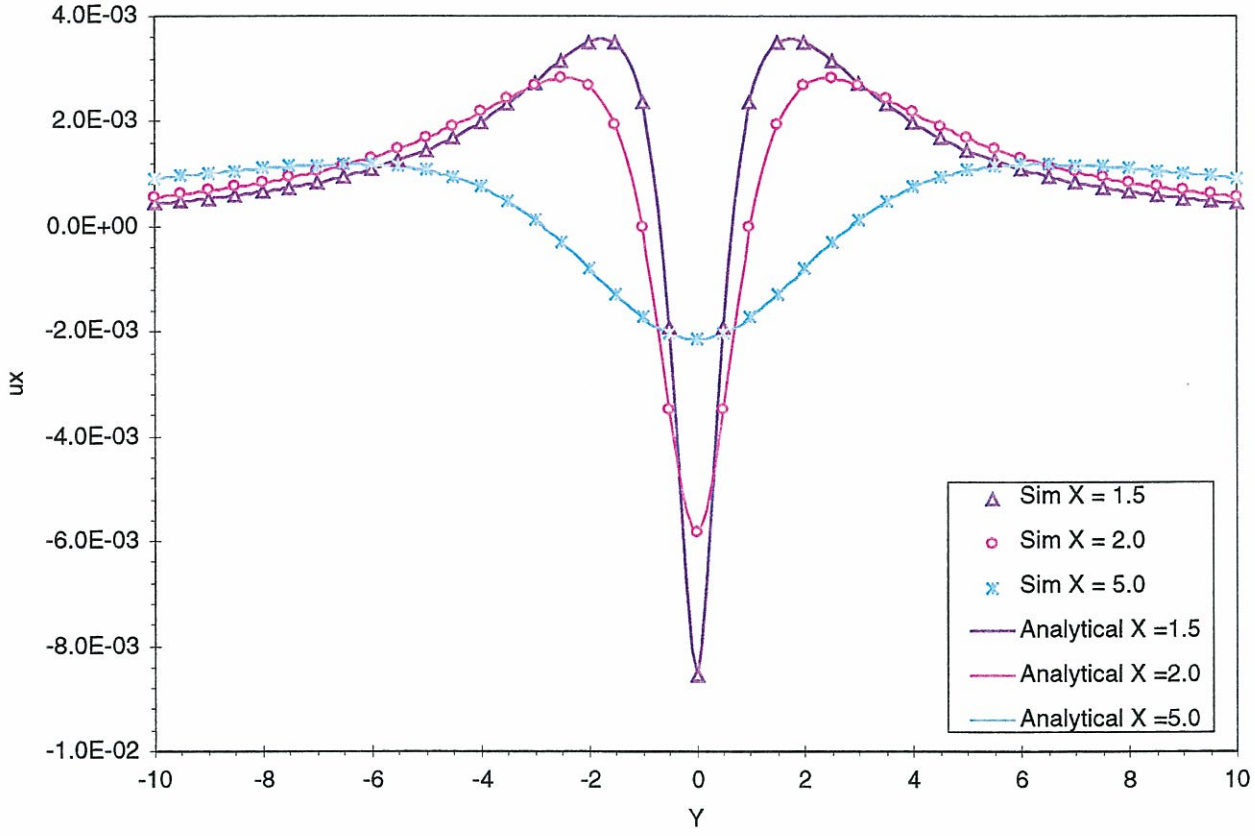


FIGURE **A-1c**
**COMPARISON - Ux(X)**

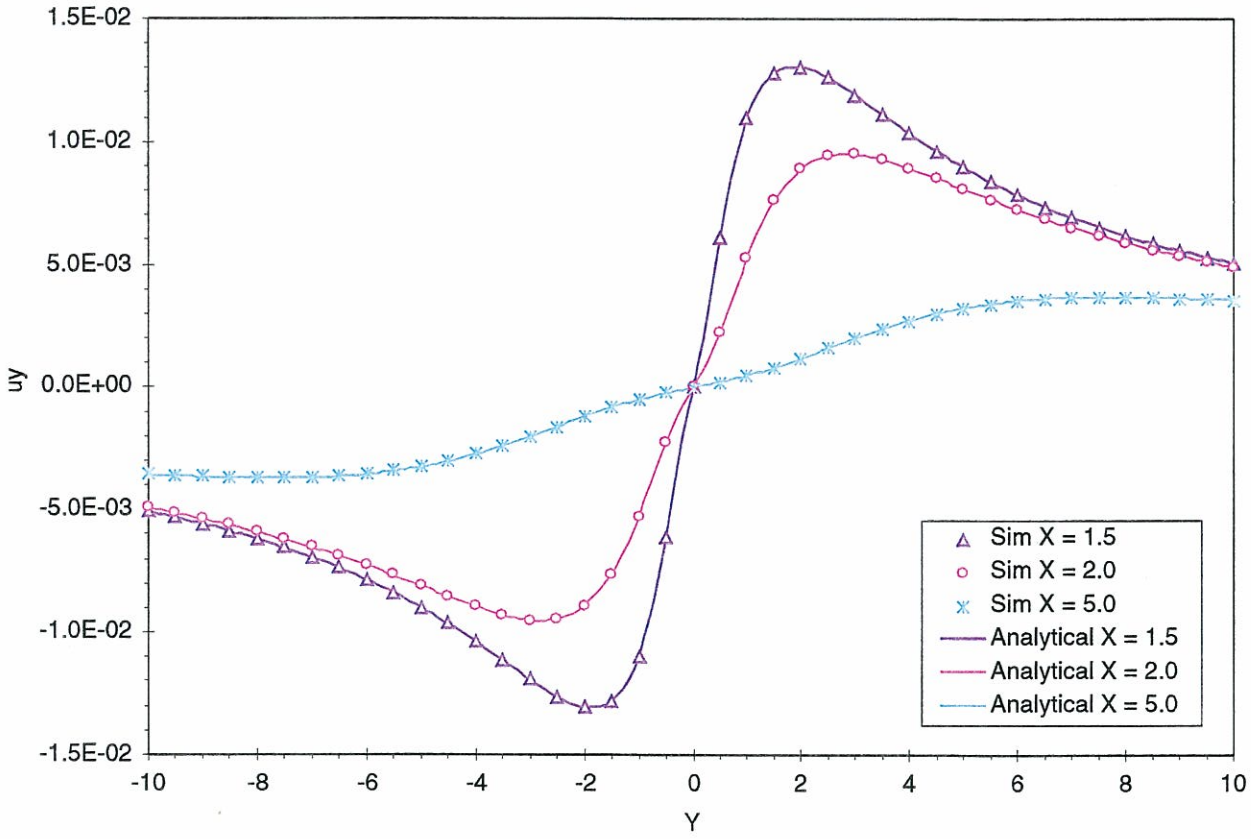


FIGURE **A-1d**
**COMPARISON - Uy(X)**

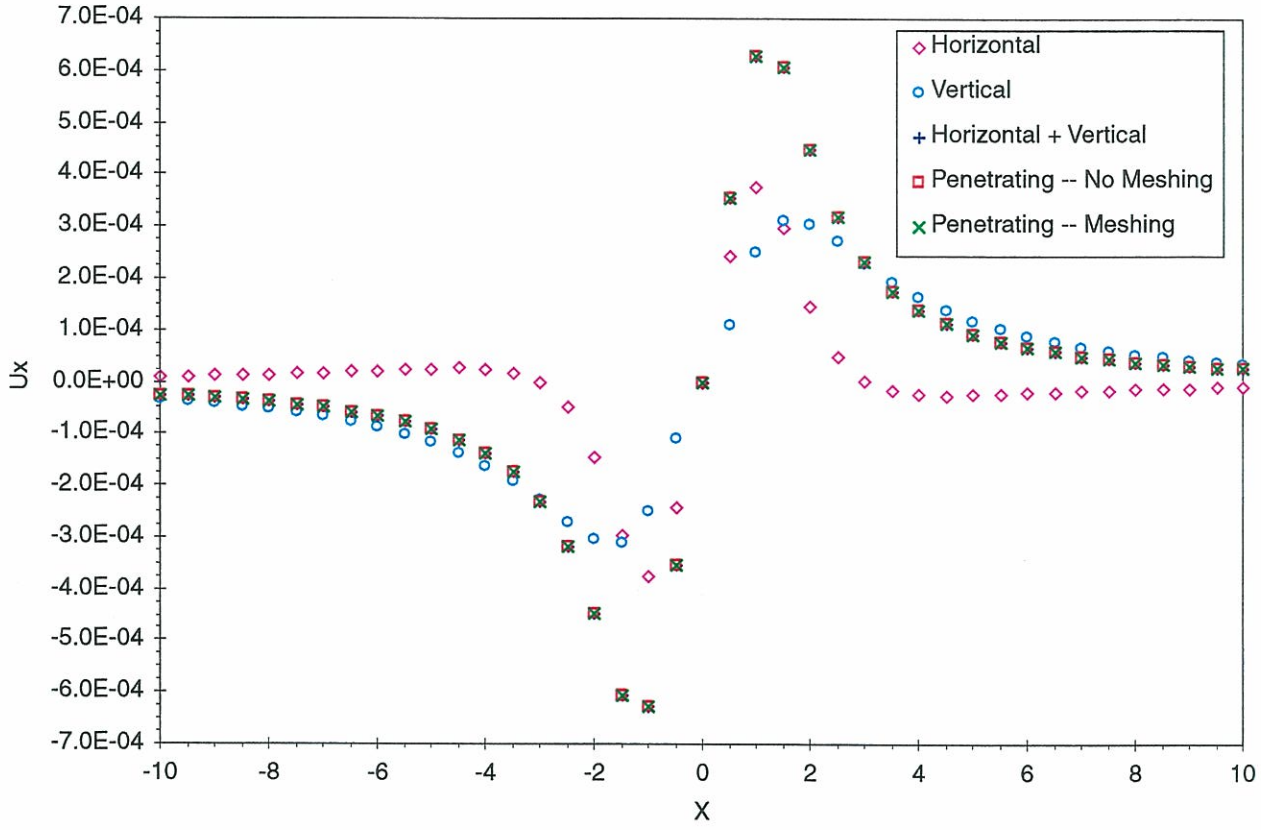


FIGURE **A-2a**
**PENETRATING - UX**

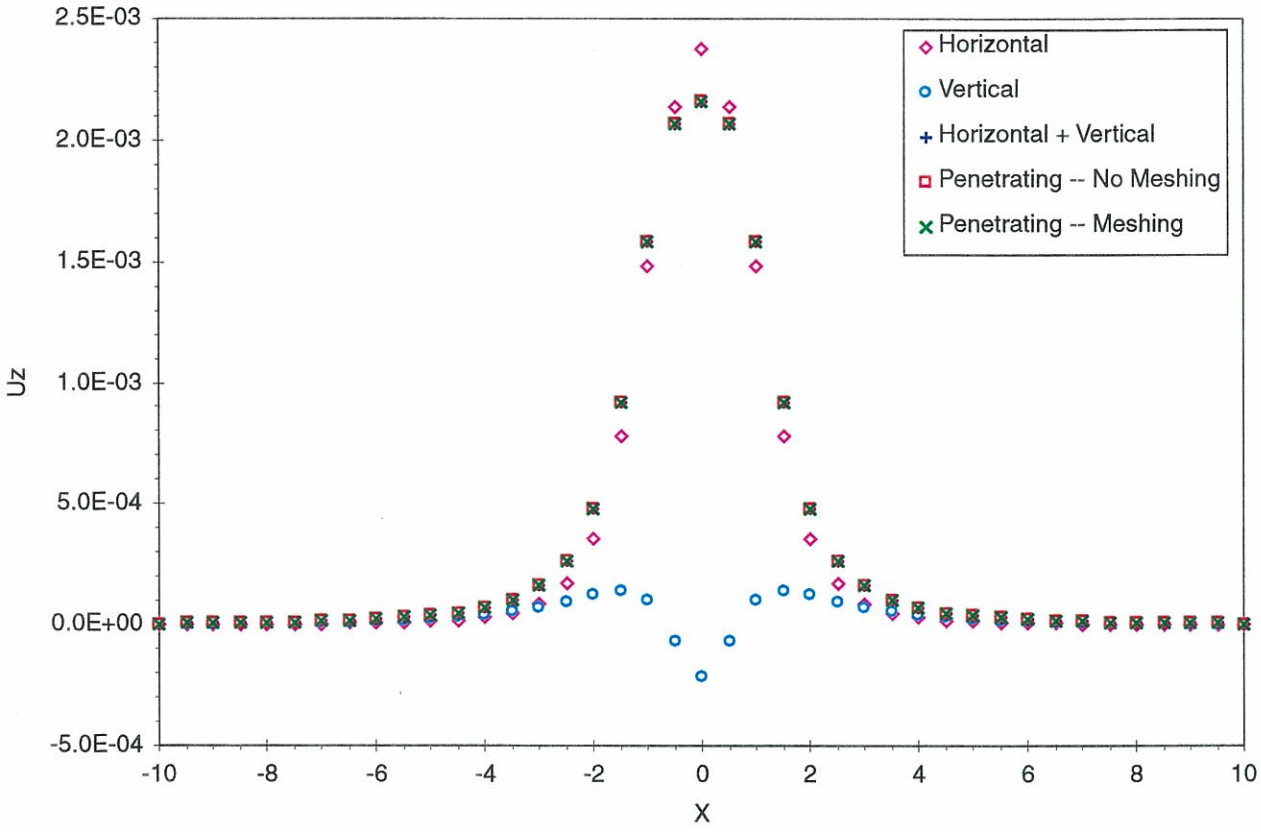


FIGURE **A-2b**
**PENETRATING - UZ**

# APPENDIX B

# CITATIONS FOR LITERATURE REVIEW

**Citations for Literature Review**

Ahmed, M. and B. Stimpson (1989). An experimental study of fracturing in a thick rock beam and its application to potash mining-induced seimicity, Saskatchewan. *42nd Canadian Geotechnical Conference, Winnipeg, Manitoba.* October, 1989 177-183.

Anderson, O. L. and P. C. Grew (1977). Stress corrosion theory of crack propagation with applications to geophysics. *Reviews of Geophysics and Space Physics*, 15(1), 77-104.

Asakura, T. and Y. Sato. (1996). Damage to mountain tunnels in hazard area. *Soils and Foundations Special Issue*, 301-310.

Atkinson, B. K. (1982). Subcritical crack propagation in rocks: theory, experimental results and applications. *Journal of Structural Geology*, 4(1), 41-56.

Bard, P-Y. and B. E. Tucker (1995). Underground and ridge site effects: a comparison of observation and theory. *Bulletin of the Seismological Society of America*, 75(4), 905-919.

Barnett, J. A. M. and others. (1987). Displacement geometry in the volume containing a single normal fault. *The American Association of Petroleum Geologists Bulletin*, 71(8) 925-937.

Ben-Zion, Y. and J. R. Rice (1993). Quasi-static simulations of earthquakes and slip complexity along a 2D fault in a 3D elastic solid. Workshop LXIII, USGS Red-Book Conference on the Mechanical Involvement of Fluids in Faulting. June 1993. 406-435.

Bonilla, M. G. (1970) Surface faulting and related effects. Earthquake Engineering, Prentice-Hall, Inc., Englewood Cliffs, NJ, 1970.

Bonilla, M. G., R. K. Mark and J. J. Lienkaemper. (1984). Statistical relations among earthquake magnitude, surface rupture length and surface fault displacement. *Bulletin of the Seismological Society of America*, vol. 74, 2379-2411.

Caine, J. S., J. P. Evans and C. B. Forster. (1996). Fault zone architecture and permeability structure. *Geology*, vol. 24, 1025-1028.

Camelbeeck, T. and M. Meghraoui. (1996). Large earthquakes in Northern Europe more likely than once thought. *Eos*, 77(42), 405,409.

Cane, Braxy, Vanzant and Nair. (1991). Critical assessment of seismic & geomechanics literature related to a high-level nuclear waste repository. NUREG/CR-5440, NRC, Washington, D.C., 1991.

Chowdhury, A. H., S-M Hsiung and M. P. Ahola. (1992). Options for dynamic analyses of underground facilities. High Level Nuclear Waste Repositories, San Francisco, California. August, 1992, 286-301.

Chunan, T. and X. Xiaohe. (1990). A new method for measuring dynamic fracture toughness of rock. *Engineering Fracture Mechanics*, 35(4/5), 783-791.

Chunan, T. and X. Xiaohe. (1990). Stiffness machine characteristics and its application in an earthquake model. *Engineering Fracture Mechanics*, 35(4/5), 801-805.

Cladouhos, T. T. and R. Marrett. (1996). Are fault growth and linkage models consistent with power-law distributions of fault lengths? *Journal of Structural Geology*, 18(2/3), 281-293.

Coppersmith, K. J. and R. R. Youngs. (1992). Modeling fault rupture hazard for the proposed repository at Yucca Mountain, Nevada. High Level Radioactive Waste Management, Las Vegas, Nevada. April, 1992, 1142-1150.

Cowie, P. A., R. J. Knipe and I. G. Main. (1996). Introduction to the special issue. *Journal of Structural Geology*, 18(2/3), v-xi.

Dowding, C. H., M. ASCE and A. Rozen. (1978). Damage to rock tunnels from earthquake shaking. *Journal of the Geotechnical Engineering Division*. 175-191.

Ericsson, L. O. and B. Ronge. (1987). Localizing of caverns according to permeability of tectonic elements. Proceedings of the International Symposium on Large Rock Caverns, Helsinki, Finland. August, 1987, 951-960.

Flint, A. L., L. E. Flint and J. A. Hevesi. (1993). The influence of long term climate change on net infiltration at Yucca Mountain, Nevada. High Level Radioactive Waste Management, Las Vegas, Nevada. April, 1993, 152-159.

Focus '95, Proceedings, American Nuclear Society, Methods of seismic hazards evaluation. Las Vegas, Nevada. September 18-20, 1995.

Follin, S. and J. Hermanson. (1996). A discrete fracture network model of the Äspö TBM tunnel rock mass, *Power Nuclear Commission model report*, June 1996.

Foltz, S. D. and others. (1993). Investigation of fracture-matrix interaction: preliminary experiments in a simple system. High Level Radioactive Waste Management, Las Vegas, Nevada. April, 1993, 328-335.

Freund, L. B. (1979). The mechanics of dynamic shear crack propagation. *Journal of Geophysical Research,* 84(B5), 173-211.

Germanovich, L. N. and others. (1994). Mechanisms of brittle fracture of rock with pre-existing cracks in compression. *Pure and Applied Geophysics*, 143(1/2/3), 117-149.

Ghosh, A., S. M. Hsiung and A. H. Chowdhury. (1996). Seismic response of rock joints and jointed rock mass, *U. S. Nuclear Regulatory Commission technical report*, NUREG/CR-6388 & CNNRA 95-013, June 1996.

Gibson, J. D. (1992). Preclosure seismic hazards and their impact on site suitability of Yucca Mountain, Nevada. High Level Radioactive Waste Management, Las Vegas, Nevada. April, 1992, 1151-1158.

Gillespie, P. A. and others. (1993). Measurement and characterization of spatial distributions of fractures. *Tectonophysic*, vol. 226, 113-141.

Gillespie, P. A., J. J. Walsh and J. Watterson. (1992). Limitations of dimension and displacement data from single faults and the consequences for data analysis and interpretation. *Journal of Structural Geology*, 14(10), 1157-1172.

Golder Associates Inc. (1994). Application of RIP (Repository Integration Program) to the Potential Repository at Yucca Mountain: Conceptual Model and Input Data Set, *Office of Civilian Radioactive Waste Management (OCRWM) final report*, June 1994.

Gupta, D. C. and others. (1992). NRC's geotechnical engineering research needs for the high-level waste repository program. High Level Radioactive Waste Management, Las Vegas, Nevada. April, 1992, 212-219.

Hakami, H. and O. Stephansson. (1990). Shear fracture energy of stripa granite--results of controlled triaxial testing. *Engineering Fracture Mechanics*, 35(4/5), 855-865.

Hickman, S., R. Sibson and R. Bruhn. (1993). The mechanical involvement of fluids in faulting. *Proceedings, USGS National Earthquake Hazards Reduction Program open file report 94-228*, June 1993.

Hsiung, S. M. and others. (1991). Field investigations for seismic effects on mechanical and geohydrologic response of underground structures in jointed rock. High Level Radioactive Waste Management, Las Vegas, Nevada. April, 1991, 822-829.

Hsiung, S. M. and others. (1993). Field investigation of mining-induced seismicity on local geohydrology. High Level Radioactive Waste Management, Las Vegas, Nevada. April, 1993, 913-920.

Hsuing, S. M. and others. (1992). Effects of mining-induced seismic events on a deep underground mine. *Pageoph*, 139(3/4), 741-759.

Kana, D. D., D. J. Fox and S. M. Hsuing. (1996). Interlock/friction model for dynamic shear response in natural jointed rock. *Int. J. Rock Mech. Min. Sci. & Geomech. Abstr.*, 33(4), 371-386.

Kana, D. D., S. M. Hsuing and A. H. Chowdhury. (1995). A scale model study of seismic response of an underground opening in jointed rock. 35th U. S. Symposium on Rock Mechanics, Reno, Nevada. June, 1995, 503-509.

Kana, D. D. and others. (1991). Critical assessment of seismic and geomechanics literature related to a high-level nuclear waste underground repository, *U. S. Nuclear Regulatory Commission technical report*, June 1991.

Kneupfer, P. L. K. (1989). Implications of the characteristics of end-points of historical surface fault ruptures for the nature of fault segmentation. Fault Segmentation and Controls of Rupture Initiation and Termination, Palm Springs, California. 1989, 193-228.

Komada, H. Study on earthquake resistance of large underground caverns.

Manteufel, R. D. and others. (1993). An assessment of coupled thermal-hydrologic-mechanical-chemical processes. High Level Radioactive Waste Management, Las Vegas, Nevada. April, 1993, 576-583.

Marine, I. W. (1982). Workshop on seismic performance of underground facilities, *U. S. Department of Energy technical report DP--1623, DE 82009181*, January 1982.

McGarr, A., R. W. E. Green, S. M. Spottiswoode. (1981). Strong ground motion of mine tremors; some implications for near-source ground motion parameters. Bulletin of the Seismological Society of America, vol. 71, no. 1, 295-319. 1981.

McGuire, R. K. and others. (1992). Perspectives on seismic design basis deterministic and probabilistic approaches. High Level Radioactive Waste Management, Las Vegas, Nevada. April, 1992, 1137-1141.

McGuire, R. K. and others. (1990). Demonstration of a risk-based approach to high-level waste repository evaluation, *Electric Power Research Institute final report*, October 1990.

McGuire, R. K. and others. (1992). Demonstration of a risk-based approach to high-level waste repository evaluation, *Electric Power Research Institute final report*, May 1992.

Mohanty, B. (1990). Explosion generated fractures in rock and rock-like materials. *Engineering Fracture Mechanics*, 35(4/5), 889-898.

Nicholl, M. J., R. J. Glass and H. A. Nguyen. (1992). Gravity-driven fingering in unsaturated fractures. High Level Radioactive Waste Management, Las Vegas, Nevada. April, 1992, 321-331.

Nisca, D. H. and C-A. Triumf. (1989). Detailed geomagnetic and geoelectric mapping of Äspö, *SKB Progress Report 25-89-01*, January 1989.

Öncel, A. O. and others. (1996). Spatial variations of the fractal properties of seismicity in the Anatolian fault zones. *Tectonophysics*, vol. 257, 189-202.

Öncel, A. O. and others. (1996). Temporal variations in the fractal properties of seismicity in the North Anatolian fault zone between 31°E and 41°E. *Pageoph*, 147(1), 147-159.

Patrick, S. M. (1993). Earthquakes and nuclear waste: a lesson in media relations. High Level Radioactive Waste Management, Las Vegas, Nevada. April, 1993, 1014-1022.

Pollard, D. D. and P. Segall. (1987). Theoretical displacements and stresses near fractures in rock: with applications to faults, joints, veins, dikes, and solution surfaces, *Fracture Mechanics of Rock.* Academic Press Inc. Ltd., London, 1987.

Pratt, H. R., W. A. Hustrulid and D. E. Stephenson. (1978). Earthquake damage to underground facilities, *U. S. Department of Energy report* DP-1513, UC-13, November 1978.

Pratt, H. R., G. Zandt and M. Bouchon. (1979). Earthquake related displacement fields near underground facilities, *U. S. Department of Energy technical report*, April 1979.

Qunli, Z. (1987). Compression shear fracture analysis of dam bedrock and reservoir earthquake. Proceedings, SEM/RILEM International Conference on Fracture of Concrete and Rock, Houston, Texas. June, 1987, 558-560.

Raney, R. G. (1988). Reported effects of selected earthquakes in the western North American intermontane region, 1852-1983, on underground workings and local and regional hydrology: a summary, *U. S. Dept. of Interior, Bureau of Mines, Division of Waste Management report*, April 1988.

Rautman, C. A. and others. (1993). Influence of deterministic geologic trends on spatial variability of hydrologic properties in volcanic tuff. High Level Radioactive Waste Management, Las Vegas, Nevada. April, 1993, 921-929.

Schwartz, D. P. and K. J. Coppersmith. (1986). Seismic hazards: new trends in analysis using geologic data, *Studies in Geophysics: Active Tectonics*. National Academy Press, Washington, D. C., 1986, 215-230.

Shimizu, I. and others. (1995). Earthquake related ground motion and groundwater pressure change at the Kamaishi Mine.

Slemmons, D. B. and R. McKinney. (1977). Definition of "Active Fault", *U. S. Army Corps of Engineers final report*, May 1977.

Spetzler, H., H. Mizutani and F. Rummel. (1982). A model for time-dependent rock failure. *High-Pressure Researches in Geoscience*, 85-93.

Stephansson, O. and others. (1979). Deformation of a jointed rock mass. *Geologiska Föreningens; Stockholm Fördandlingar*, vol. 100, 287-294.

Stevens, P. R. (1977). A review of the effects of earthquakes on underground mines, *U.S. Geological Survey open-file report 77-313*, April 1977.

Tidwell, V. C., J. D. VonDoemming and K. Martinez. (1993). Scale dependence of effective media properties. High Level Radioactive Waste Management, Las Vegas, Nevada. April, 1993, 1059-1065.

Tirén, S. A., M. Beckholmen and H. Isaksson. (1987). Structural analysis of digital terrain models, Simpevarp area, southeastern Sweden, *SKB Progress Report 25-87-21*, November 1987.

Tirén, S. A. and M. Beckholmen. (1988). Structural analysis of contoured maps Äspö and Ävrö, Simpevarp area, southeastern Sweden, *SKB Progress Report 25-87-22*, January 1988.

Tirén, S. A. and M. Beckholmen. (1990). Influence of regional shear zones on the lithological pattern in central Sweden. *Geologiska Föreningens; Stockholm Fördandlingar*, vol. 112, 197-199.

Tirén, S. A. and M. Beckholmen. (1990). Rock block configuration in southern Sweden and crustal deformation. *Geologiska Föreningens; Stockholm Fördandlingar*, vol. 112, 361-364.

Tirén, S. A. and M. Beckholmen. (1992). Rock block map analysis of southern Sweden. *Geologiska Föreningens; Stockholm Fördandlingar*, vol. 114, 253-269.

Tirén, S. A. (1993). Planning of infrastructures and the role of remote analysis of structural elements in the bedrock. *GFF*, vol. 115, 275-277.

Turcotte, D. L. (1992). Fractals and chaos in geology and geophysics. Cambridge University Press, Great Britain, 1992.

Vere-Jones, D. (1976). A branching model for crack propagation. *Pure and Applied Geophysics*, 114(4), 711-726.

Voegele, M. D. (1993). Photogeologic reconnaissance of X-tunnel at Little Skull Mountain. High Level Radioactive Waste Management, Las Vegas, Nevada. April, 1993, 182-187.

Wagner, H. (1984). Support requirements for rockburst conditions. Rockbursts and Seismcity in Mines. South African Institute of Mining and Metallurgy, Johannesburg, South Africa, 1984, 209-218.

Walsh, J. J. and J. Watterson. (1987). Distributions of cumulative displacement and seismic slip on a single normal fault surface. *Journal of Structural Geology*, 9(8), 1039-1046.

Walsh, J. J. and J. Watterson. (1989). Displacement gradients on fault surfaces. *Journal of Structural Geology*, 11(3), 307-316.

Walsh, J. J. and J. Watterson. (1992). Populations of faults and fault displacements and their effects on estimates of fault-related regional extension. *Journal of Structural Geology*, 14(6), 701-712.

Walsh, J. J., J. Watterson and G. Yielding. (1991). The importance of small-scale faulting in regional extension. *Nature*, vol. 351, 391-393.

Walsh, J. J. and J. Watterson. (1993). Fractal analysis of fracture patterns using the standard box-counting technique: valid and invalid methodologies. *Journal of Structural Geology*, 15(12), 1509-1512.

Walsh, J. J. and J. Watterson. (1988). Analysis of the relationship between displacements and dimensions of faults. *Journal of Structural Geology*, vol. 10, 329-347.

Wells, D. L. and K. J. Coppersmith. (1994). New empirical relationships among magnitude, rupture length, rupture width, rupture area, and surface displacement. *Bulletin of the Seismological Society of America*, 84(4), 974-1002.

Wood, R. M. and G. C. P. King. (1991). An empirical data base for the investigation of earthquake-related changes in crustal hydrology. High Level Radioactive Waste Management, Las Vegas, Nevada. April, 1991, 1284-1290.

Xiao-he, X. and Z. Yi. (1990). Determination for the critical damage factor of a perfect brittle rock. *Engineering Fracture Mechanics*, 35(4/5), 647-650.

# APPENDIX C

# SOME COMMENTS AND CONCLUSIONS REGARDING MATERIAL PROPERTIES OF FRACTURE ZONES IN FRACTURED CRYSTALLINE ROCK

## Some Comments and Conclusions Regarding Material Properties of Fracture Zones in Fractured Crystalline Rock

The concept of *shear strength* is meaningful when the *scale* of the problem at hand and the fracture zone is such that the fracture zone can be treated as a single discontinuity. When this approach is valid, concerns are with the strength of fractures forming constituents of the fracture zones, rather than the strength of a zone as a whole. Figure C-1 shows that the relative shear displacement, $\delta_p/L$, at peak shear strength is dependent on the length L of the block sheared. The data fall in two distinct groups; one contains results from experiments on a meter-scale or less at low normal stress levels, whereas the other is data from surface observations of fault displacements in connection with major earthquakes, thus representing high normal stress levels. The figure clearly demonstrates the almost complete absence of data referring to the scale interval in between these two groups, i.e. roughly the interval 10 m to 10 km. In Figure C-1, the experimental data (upper left) refers to peak shear displacement during loading. Earthquake fault displacements refer to unloading. It should be noted that these mechanisms may not be comparable.

Leijon (1993) has compiled a report on this subject and an excerpt of the author's comments and conclusions are summarized in the next section.

### *Friction Angle and Cohesion*

The shear strength of fracture zones is mainly controlled by frictional resistance and the cohesive contribution is generally insignificant. Figure C-2 attempts to summarize friction angles inferred from various studies. The figure suggests that there is an apparent increase of friction angles for common filling materials. As expected, these are somewhat lower then those for fracture zones.

Leijon (1993) concludes that friction angle is *not* a material property in a conventional sense, but rather a parameter that conveniently quantifies the net effect of a process that has not yet been fully understood. Furthermore, the author draws the conclusion that friction angle is *not* inherently scale dependent and that misconceptions in these respects are common.

As regards friction angles of fault zones, Leijon (1993) points out that an indirect size dependency may exist because of differences in displacement magnitudes and morphology. Geological investigations of fault zones have not revealed clear correlations between: 1) fault zone extension and displacement magnitude (Watterson, 1986), and 2) displacement magnitude and thickness of gouge material formed by the shearing process (Robertson, 1987). Since the friction of fault gouge, and probably also of other wear

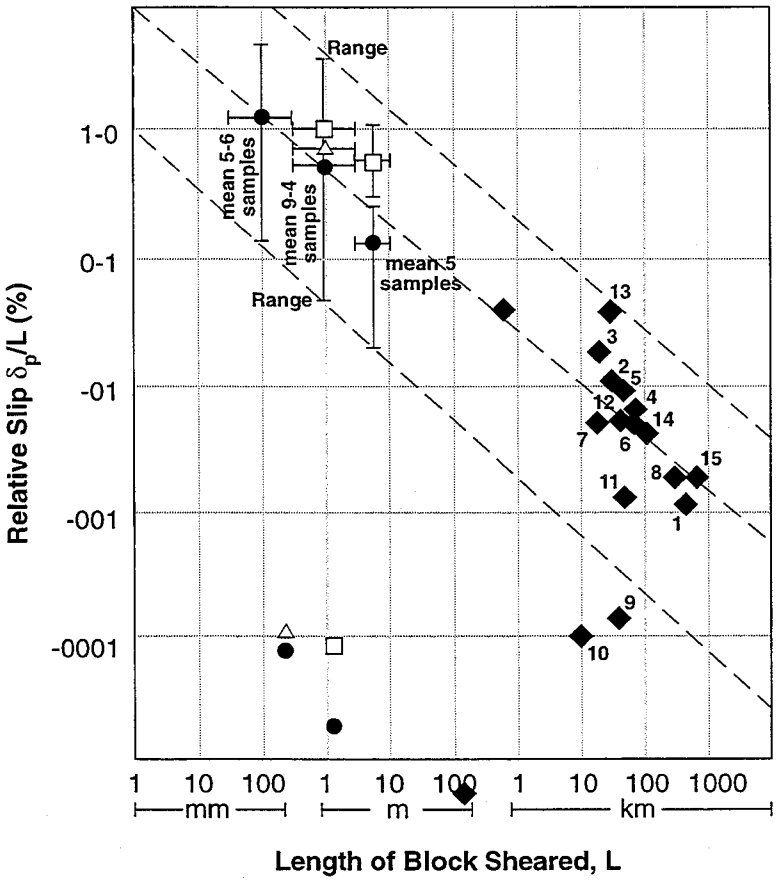


- ● Clay Bearing Discontintuities
- △ Rock Joints
- □ Model Joints
- ◆ Earthquake Faults

FIGURE **C-1**
**RELATIVE SHEAR DISPACEMENT LENGTH OF BLOCK SHEARED**

Data from Barton (1990) and Nur (1974)

**Golder Associates**

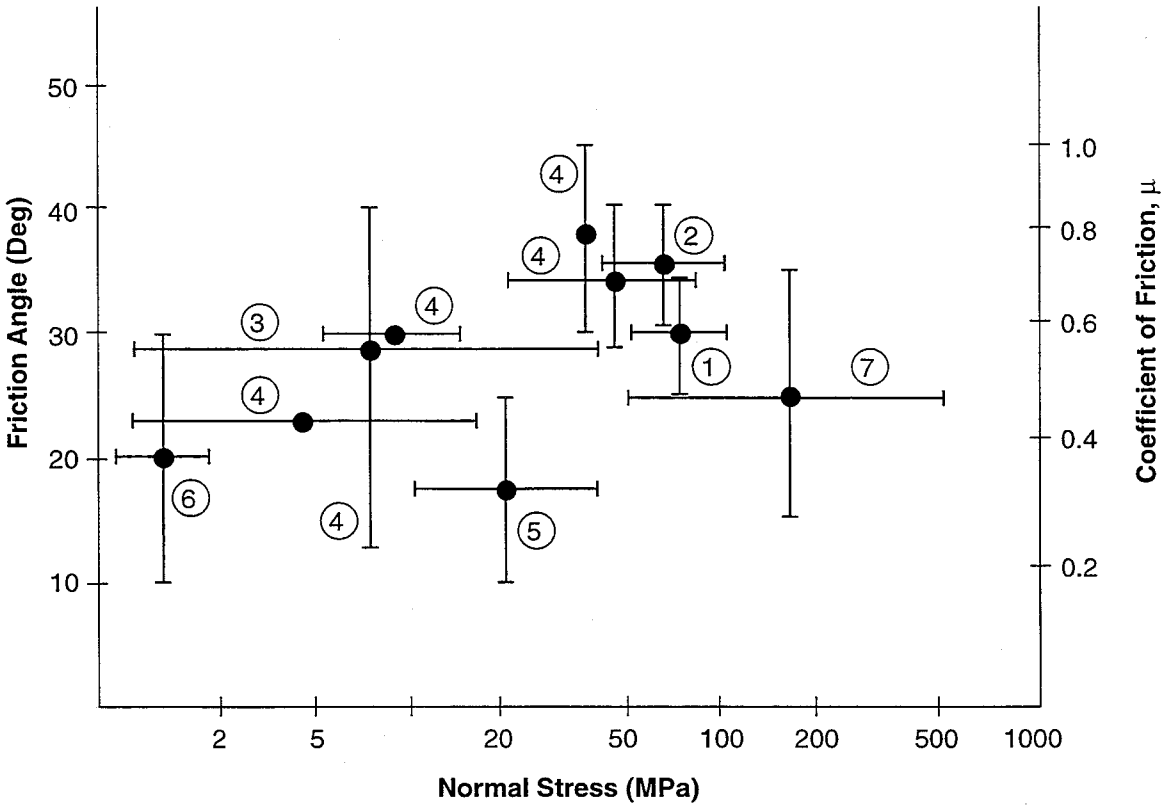


1 Faults in South African gold mines, modelling and field observation

2 Strathcona mine, modelling and field observation

3 Back-Calculation from stress measurements - general data

4 Back-Calculation from stress measurements in areas of active faulting

5 Weak contact zones in Swedish mines, modelling and field observation

6 Common discontinuity filling materials, laboratory and field testing

7 Fault gorge material, laboratory testing

FIGURE **C-2**
**FRICTION ANGLE AND FRICTION COEFFICIENT OF FRICTION AS A FUNCTION OF NORMAL STRESS**

products, is lower than for clean rock surfaces, friction angles would be expected to decrease somewhat with increased scale of the fault zone. According to Leijon (1993), however, this hypothesis cannot be supported by any observational evidence whatsoever.

In contrast to the conclusions presented above, Pusch (1996) suggests a quite detailed classification of discontinuities in respect to the friction angle and cohesion, see Table C-1 and Table C-2.

**Table C-1 Friction Angles of Discontinuities in Crystalline Rock**

| Order | Size | Friction angle, $\phi$ |
|---|---|---|
| 1 | Length > $10^4$ m, Spacing > $10^3$ m | <20 |
| 2 | Length $10^3$ - $10^4$ m, Spacing $10^2$ - $10^3$ m | 20 - 25 |
| 3 | Length $10^2$ - $10^3$ m, Spacing 10 - $10^2$ m | 20 - 30 |
| 4 | 10 m < Length < $10^2$ m | 20 - 30 |
| 5 | $10^{-1}$ m < Length < 10 m | 35 - 50 |
| 6 | $10^{-2}$ m < Length < $10^{-1}$ m | 45 - 60 |
| 7 | Length < $10^{-2}$ m | |

**Table C-2 Approximate Material Properties of Crystalline Rock with Discontinuities (valid for vertical 2D cases)**

| Volume $m^3$ | Cohesion, C Mpa | Friction Angle, $\phi$ | Order |
|---|---|---|---|
| <0.001 | 10 - 50 | 45 - 60 | 7 |
| 0.001 - 0.1 | 1 - 10 | 45 - 50 | 6 - 7 |
| .01 - 10 | 1 - 5 | 35 - 45 | 5 - 7 |
| 10 - 100 | 0.1 - 1 | 25 - 35 | 4 - 7 |
| 100 - 10,000 | 0.01 - 0.1 | 20 - 30 | 3 - 7 |
| > 10,000 | < 0.1 | < 20 | 1 - 7 |

*Modulus of Deformation*

The modulus of deformation, modulus of rigidity, bulk modulus and Poisson's ratio (all related to each other) are all material properties that may be used to describe the deformability of the rock mass composing the zone. Consequently, these parameters can be defined only if the zone has a finite width and they are applicable in cases when fracture zones can be represented by equivalent rock masses.

The modulus of deformation of fracture zones have been studied in the field in Sweden at Finnsjön, Fjällveden and Kamlunge. It was found that commonly used empirical methods are applicable to slightly disturbed zones with moderate fracturing, but not too intensely shared zones displaying heavy fracturing and abundance of poor-quality material. The result suggests that 10 - 25 GPa are reasonable estimates for the modulus of deformation of the former category of fracture zones, and thus provide an upper bound estimates for the latter. Lower bound estimates cannot be obtained form borehole data.

*Normal and Shear Stiffness*

Shear deformation properties become meaningful only if defined for some discontinuity area that is considerably larger than the surface irregularities responsible for the shear resistance. Normal deformation properties, however, can be defined for specific locations (or for some larger area). This means that borehole information is much more useful for assessing normal deformation characteristics than for estimating shear properties of fracture zones.

The normal and shear stiffness, $K_n$ and $K_s$, are functions of the modulus of deformation, modulus of rigidity, bulk modulus, Poisson's ratio and of the geometry of the fracture zone. $K_n$ and $K_s$ are "global parameters" in that they describe the stiffness of the entire zone at a particular location. These parameters can be defined irrespective of whether the zone is assigned a finite width or not. Hence, they are not material constants, but rather describe the characteristics of the fracture zone as a system component. This does not preclude the spatial variability of stiffness parameters over the plane of the fracture zone.

There are no large-scale fracture zone measurements of normal stiffness made in Sweden. However, geometrical data and the modulus values suggest an effective stiffness of 0.1 - 10 GPa. Measurements exist in two fracture zones at the URL; for a 20 m wide zone the normal stiffness is approximately 2 - 5 GPa, whereas for a 0.4 m wide zone the normal stiffness is about 50 - 160 GPa. In conclusion, available normal stiffness data for fracture zones are meaningful, although they are scattered over three orders of magnitudes. For a particular fracture zone, the parameter can show large local variations contributed by: 1) variations in width, and 2) variations in internal characteristics of the zone.

Field-scale observations of the shear stiffness of fracture zones are completely absent according to Leijon (1993). Data from laboratory experiments combined with empirical scaling laws provide the only means at present for estimating this parameter. In addition, all these data refer to single discontinuities and it is not clear how they relate to the stiffness of the system of fractures comprising a fracture zone. For a given discontinuity, however, shear stiffness is mostly found to be lower than the normal stiffness. Ratios between 5 and 50 are typically encountered (Tannant, 1990). As a first approximation, it is reasonable to assume that these ratios hold also for fracture zones.

# *List of SKB reports*

## Annual Reports

*1977-78*
TR 121
**KBS Technical Reports 1 – 120**
Summaries
Stockholm, May 1979

*1979*
TR 79-28
**The KBS Annual Report 1979**
KBS Technical Reports 79-01 – 79-27
Summaries
Stockholm, March 1980

*1980*
TR 80-26
**The KBS Annual Report 1980**
KBS Technical Reports 80-01 – 80-25
Summaries
Stockholm, March 1981

*1981*
TR 81-17
**The KBS Annual Report 1981**
KBS Technical Reports 81-01 – 81-16
Summaries
Stockholm, April 1982

*1982*
TR 82-28
**The KBS Annual Report 1982**
KBS Technical Reports 82-01 – 82-27
Summaries
Stockholm, July 1983

*1983*
TR 83-77
**The KBS Annual Report 1983**
KBS Technical Reports 83-01 – 83-76
Summaries
Stockholm, June 1984

*1984*
TR 85-01
**Annual Research and Development Report 1984**
Including Summaries of Technical Reports Issued during 1984. (Technical Reports 84-01 – 84-19)
Stockholm, June 1985

*1985*
TR 85-20
**Annual Research and Development Report 1985**
Including Summaries of Technical Reports Issued during 1985. (Technical Reports 85-01 – 85-19)
Stockholm, May 1986

*1986*
TR 86-31
**SKB Annual Report 1986**
Including Summaries of Technical Reports Issued during 1986
Stockholm, May 1987

*1987*
TR 87-33
**SKB Annual Report 1987**
Including Summaries of Technical Reports Issued during 1987
Stockholm, May 1988

*1988*
TR 88-32
**SKB Annual Report 1988**
Including Summaries of Technical Reports Issued during 1988
Stockholm, May 1989

*1989*
TR 89-40
**SKB Annual Report 1989**
Including Summaries of Technical Reports Issued during 1989
Stockholm, May 1990

*1990*
TR 90-46
**SKB Annual Report 1990**
Including Summaries of Technical Reports Issued during 1990
Stockholm, May 1991

*1991*
TR 91-64
**SKB Annual Report 1991**
Including Summaries of Technical Reports Issued during 1991
Stockholm, April 1992

*1992*
TR 92-46
**SKB Annual Report 1992**
Including Summaries of Technical Reports Issued during 1992
Stockholm, May 1993

*1993*
TR 93-34
**SKB Annual Report 1993**
Including Summaries of Technical Reports Issued during 1993
Stockholm, May 1994

*1994*

TR 94-33

**SKB Annual Report 1994**

Including Summaries of Technical Reports Issued during 1994
Stockholm, May 1995

*1995*

TR 95-37

**SKB Annual Report 1995**

Including Summaries of Technical Reports Issued during 1995
Stockholm, May 1996

*1996*

TR 96-25

**SKB Annual Report 1996**

Including Summaries of Technical Reports Issued during 1996
Stockholm, May 1997

## List of SKB Technical Reports 1997

TR 97-01

**Retention mechanisms and the flow wetted surface – implications for safety analysis**

Mark Elert
Kemakta Konsult AB
February 1997

TR 97-02

**Äspö HRL – Geoscientific evaluation 1997/1. Overview of site characterization 1986–1995**

Roy Stanfors[1], Mikael Erlström[2], Ingemar Markström[3]
[1] RS Consulting, Lund
[2] SGU, Lund
[3] Sydkraft Konsult, Malmö
March 1997

TR 97-03

**Äspö HRL – Geoscientific evaluation 1997/2. Results from pre-investigations and detailed site characterization. Summary report**

Ingvar Rhén (ed.)[1], Göran Bäckblom (ed.)[2], Gunnar Gustafson[3], Roy Stanfors[4], Peter Wikberg[2]
[1] VBB Viak, Göteborg
[2] SKB, Stockholm
[3] VBB Viak/CTH, Göteborg
[4] RS Consulting, Lund
April 1997

TR 97-04

**Äspö HRL – Geoscientific evaluation 1997/3. Results from pre-investigations and detailed site characterization. Comparison of predictions and observations. Geology and mechanical stability**

Roy Stanfors[1], Pär Olsson[2], Håkan Stille[3]
[1] RS Consulting, Lund
[2] Skanska, Stockholm
[3] KTH, Stockholm
May 1997

TR 97-05

**Äspö HRL – Geoscientific evaluation 1997/4. Results from pre-investigations and detailed site characterization. Comparison of predictions and observations. Geohydrology, groundwater chemistry and transport of solutes**

Ingvar Rhén[1], Gunnar Gustafson[2], Peter Wikberg[3]
[1] VBB Viak, Göteborg
[2] VBB Viak/CTH, Göteborg
[3] SKB, Stockholm
April 1997

TR 97-06

**Äspö HRL – Geoscientific evaluation 1997/5. Models based on site characterization 1986–1995**

Ingvar Rhén (ed.)[1], Gunnar Gustafson[2], Roy Stanfors[4], Peter Wikberg[4]
[1] VBB Viak, Göteborg
[2] VBB Viak/CTH, Göteborg
[3] RS Consulting, Lund
[4] SKB, Stockholm
May 1997